

COMPUTER MODELING OF CORONA DISCHARGE PHENOMENA

BY

Cha-Mei Tang Hui

S.B., Massachusetts Institute of Technology
(1971)

SUBMITTED IN PARTIAL FULFILLMENT OF THE
REQUIREMENTS FOR THE DEGREE OF
MASTER OF SCIENCE

and

ELECTRICAL ENGINEER

at the

MASSACHUSETTS INSTITUTE OF TECHNOLOGY

June, 1973

Signature of Author

Department of Electrical Engineering, May 11, 1973

Certified by -

Thesis Supervisor

Accepted by

Chairman, Departmental Committee on Graduate Students



COMPUTER MODELING OF CORONA DISCHARGE PHENOMENA

BY

Cha-Mei Tang Hui

Submitted to the Department of Electrical Engineering
on May 11, 1973 in partial fulfillment of
the requirements for the Degree of Master of Science
and Electrical Engineer

ABSTRACT

This work is a numerical study of the parameters that effect the behavior of corona on coaxial lines in the steady state. The important primary processes are creation of electrons by electron neutral collision, and attachment of electrons to neutrals forming slow moving negative ions. The secondary process that this work concentrated on is photoionization in the bulk of the gas.

An iterative method is used to solve the self consistant problem involving space charges and its effect on the electric field. The current densities as well as total current are also calculated.

For both positive and negative corona, the total current per unit length below onset is very small. Within a narrow range of applied voltage at onset, the current jumps by 5 or 6 orders of magnitude. Above onset, the current increase slowly again as the voltage is raised. This type of current versus voltage curves is very similar to experimentally measured curves.

An increase in attachment or decrease in ionization coefficient raises the corona onset. An increase in photon absorption rate decreases the onset. Changes in mobility of ions only effect the current above onset.

The onset of corona for many different inner conductor radii are also calculated and plotted against Peek's formula. The onset of negative corona is always above that of positive corona.

THESIS SUPERVISOR: Gerald L Wilson

TITLE: Associate Professor of Electrical Engineering

ACKNOWLEDGEMENT

I would like to say my sincere thanks to Professor Gerald L Wilson for his constant guidance and suggestions. I am also indebted to Dr. Don Bosack for his help, and especially for introducing me to the details of the subject during the start of this work.

I am also grateful to American Electric Power Service Corporation for sponsoring this research.

Table of Contents

	<u>Page</u>
1. Introduction.	13
2. Corona Characteristics.	14
2.1 Positive (Anode) Corona.	14
2.2 Negative (Cathode) Corona.	18
2.3 Critical Corona Gradient	21
3. Physical Processes.	23
3.1 Drift Velocity and Mobility.	23
3.2 Cosmic Radiation	26
3.3 Alpha Ionization Process	26
3.4 Attachment of Electrons to Neutrals.	28
3.5 Measurements of Ionization and Attachment Coefficients	29
3.6 Recombination.	32
3.7 Diffusion.	32
3.8 Secondary Mechanism and Their Physical Characteristics.	33
3.9 Photoelectric Emission	35
3.10 Emission of Electrons from Metal due to Ion Impact.	35
3.11 Photoionization	39
4. Model for Positive Corona without Feedback Process	42
4.1 Assumptions.	42

	<u>Page</u>
4.2 Equation with Just Ionization and Attachment Processes.	42
4.3 An Exact Expression of Current for Unperturbed Electric Field.	46
4.4 Some Numerical Results.	48
4.5 Space Charges	50
4.6 Cosmic Radiation.	51
5. Positive Corona with Photoionization	55
5.1 Justification for Photoionization.	55
5.2 Assumptions	55
5.3 Derivation of the Photoionization term.	57
5.4 Analytical Prediction of Corona Onset	60
5.5 The Full Set of Equations Used.	63
5.6 Numerical Method.	65
5.7 Method Used in the Calculation of the Electric Field.	66
6. Results for Anode Corona	69
6.1 A Detailed Analysis of One Special Case	69
6.2 Electron Current Density Boundary Condition	
6.3 Numerical Accuracy.	79
6.4 Rate of Convergence and Stability	82
6.5 Effect of R_0	86
6.6 Modifying Alpha	89
6.7 Modifying η	90

	<u>Page</u>
6.8 Modifying μ_p and Q	90
6.9 Mobility.	92
6.10 Recombination.	94
6.11 Diffusion.	94
6.12 Variations on Anode Size and Comparison of Results to Peek's Formula.	96
7. Model for Negative Corona.	103
7.1 Derivation of Equation without Feedback Processes	103
7.2 The Exact Solution.	106
7.3 With Cosmic Radiation	107
7.4 Photoionization Term.	109
8. Results for Negative Corona.	113
8.1 A Detailed Analysis of the Standard Case.	113
8.2 Sensitivity Tests	117
8.3 Variations on the Size of the Outer Conductor	123
8.4 Ion Bombardment and Photoelectric Emission.	125
8.5 Variations on Cathode Size and Comparison of Results to Peek's Formula.	127
9. Conclusions	130
 Appendices	
1. Derivation of Geometric Factor for Positive Corona	132

	<u>Page</u>
2. Derivation of Geometric Factor for Negative Corona	139
3. Calculating an Approximate Value for μ_{eff}	143
4. Program Listing for Positive Corona	145
5. Program Listing for Negative Corona	164
References	181

Table of Figures

	<u>Page</u>
2.1 Geometry of set up.	15
2.2 Miller's Data for positive corona	17
2.3 Miller's data for negative corona	19
3.1 Electron drift velocity in dry air, humid air and water vapor	24
3.2 Drift velocity of positive ions in dry air, humid air, and water vapor	25
3.3 Ionization and attachment coefficients.	30
3.4 Schematic diagram illustrating Auger neutralization of an ion at a metal surface.. . . .	37
3.5 The rate of photon absorption,	40
4.1 Derivation for the electron continuity equation for positive corona	44
4.2 Total current as a function of the applied voltage with $J_{e0} = 1 \times 10^{-15}$ amp/cm.	49
4.3 Total current as a function of the applied voltage with cosmic radiation.	54
5.1 Illustration of photon travel for positive corona	56
5.2 Analytic calculation of critical corona onset gradient and comparison against Peek's formula	62
6.1 Sensitivity tests for 1.5 cm inner conductor with positive polarity	70
6.2 Current densities for $E_0 = 37$ kv/cm standard case	73
6.3 Particle densities for $E_0 = 37$ kv/cm standard case. . . .	74

6.4	Values of α and η as a function of position for two different applied voltages.	76
6.5	Current densities for $E_0 = 38$ kv/cm standard case	77
6.6	Particle densities for $E_0 = 38$ kv/cm standard case. . . .	78
6.7	Deviation of the electric field from the K/r field as a function of position for different applied voltages . . .	80
6.8	With the transformation, $r = f(x)$, equal spacing in x will give variable spacing for r	83
6.9	Rate of convergence illustrated by the total current at the end of each iteration for the standard case	84
6.10	Current density when the radius of the outer cylinder is changed to 7.5 cm	87
6.11	The effect of the dimension of the outer cylinder on the electric field	88
6.12	The effect of increasing the attachment coefficient for all E/p by 10% on the current densities.	91
6.13	The photoionization term as a function of position . . .	93
6.14	Comparing the recombination term to other terms. . . .	95
6.15	Current as a function of the applied voltage when the radius of the inner conductor is .2 cm	97
6.16	Current as a function of the applied voltage when the radius of the inner conductor is .5 cm	98
6.17	Current as a function of the applied voltage when the radius of the inner conductor is 1.0 cm.	99
6.18	Current as a function of the applied voltage when the	

radius of the inner conductor is 2.0 cm.	100
6.19 Comparison of results to Peek's formula.	101
7.1 Derivation for the electron continuity equation for negative corona	104
7.2 Approximating a term of the geometric factor by a linear function of r/r'	112
8.1 Sensitivity tests when the applied voltage on the 1.5 cm inner conductor is negative	114
8.2 Current densities for $E_0 = 39$ kv/cm standard case	116
8.3 Current densities for $E_0 = 40$ kv/cm standard case , . . .	118
8.4 Particle densities for $E_0 = 39$ kv/cm standard case. . . .	119
8.5 Particle densities for $E_0 = 40$ kv/cm standard case. . . .	120
8.6 Deviation of the electric field from the K/r field as a function of position for different applied voltages . . .	121
8.7 Values of α and η as a function of position for two different applied voltages.	122
8.8 The photoionization term as a function of position. . . .	124
8.9 The effect of the dimension of the outer cylinder on the electric field.	126
8.10 Current densities when $\gamma_1 = .0001$ and photoionization term set to 0	128
A1.1 Two different view points for the derivation of geometric factor of positive corona.	133
A1.2 Definition of variables used in the derivation	135

A2.1	Two different view points for the derivation of geometric factor of negative corona.	140
A2.2	Definition of variables used in the derivation.	141

List of Tables

	<u>Page</u>
6.1 Explanation for the Figure 6.1.	71
8.1 Explanation for the Figure 8.1.	115

1. Introduction

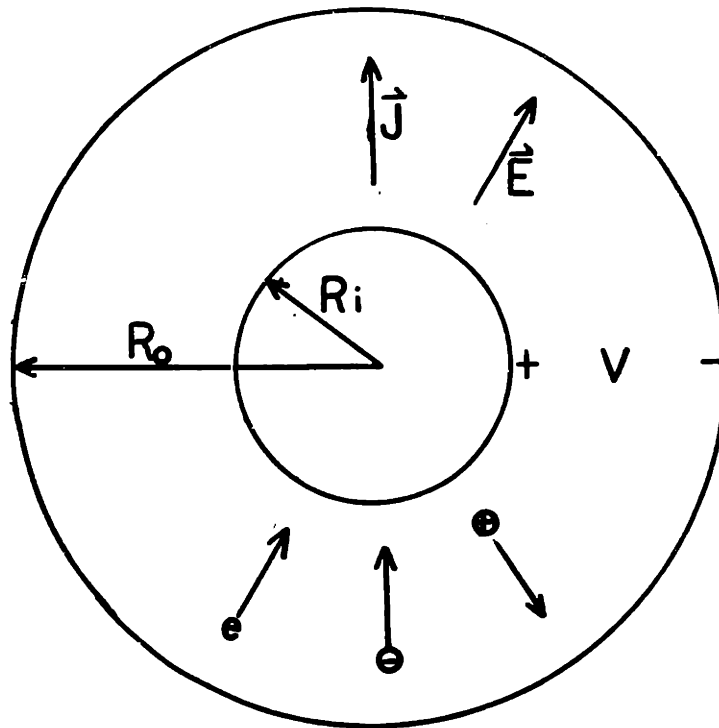
Transmission line voltages are designed at an electric field value on the surface of the conductor below the corona breakdown threshold field in dry air. When there is rain, snow or fog on the conductor, the electric field is locally increased resulting in local breakdown. Corona not only results in heavy losses for the transmission line, but also creates a disturbance both both acoustically and on a wide range of radio and television broadcast bands. To be able to increase the onset voltage and or reduce the noise, the physical processes involved must be well understood. Many experiments have been done to study corona. However it is very hard to separate one process from another. If the problem can be modelled mathematically, than it can be solved by the use of computers. If the model is correct, the results of computer programs should be in agreement with some known experimental data. Then not only may each known processes be studied independently or concurrently with other processes, but also running the program becomes an easy way to perform an actual experiment. It can give useful data that is hard to measure.

2. Corona Characteristics

To be able to model corona, it is essential to know its characteristics. Air is a pretty good insulator in electric fields much below 30 kv/cm. Near or above that range, air becomes conductive, causing breakdown. When a voltage is applied to a curved surface, the electric field is large near the surface and decays with distance. The smaller the radius of curvature, the faster the decay. As a consequence, a voltage can be applied such that the electric field near the curved surface is high enough for breakdown and yet not high enough at increasing distances to cause complete flashover. The partial breakdown near such a highly stressed surface is called corona. Since the main interest is in understanding the problems associated with transmission lines, coronas on coaxial geometry are considered. The first trace of breakdown can be associated with a large increase in current measured and appearance of visible light near the stressed surface.

2.1 Positive (Anode) Corona

Positive corona is a name given to the type of corona that exists on the surface with higher curvature when it is charged positively with respect to ground. For the geometry of interest, consider the inner cylinder or wire as the anode. Electrons and negative ions travel toward



a) Positive corona case

V - applied voltage
 \vec{E} - electric field
J - current density

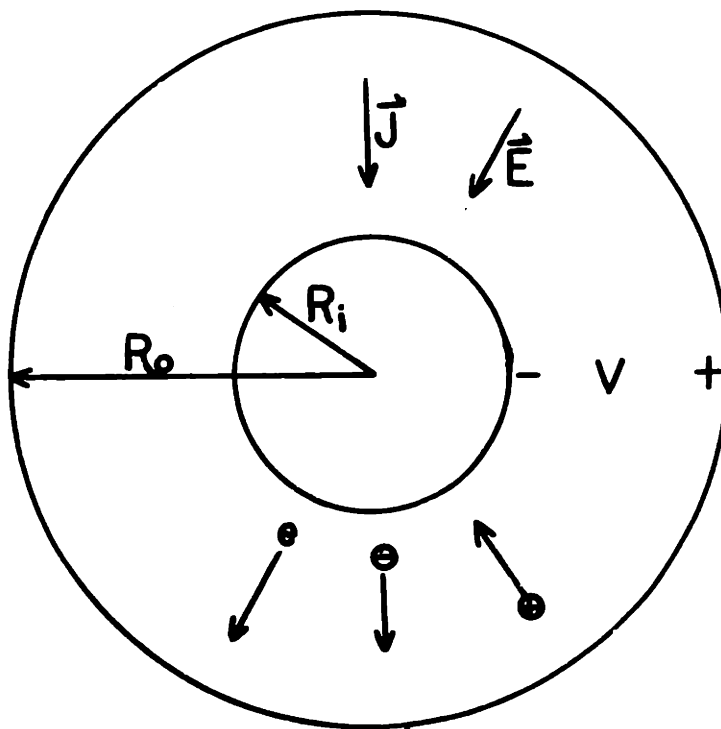
R_i - radius of inner cylinder

R_o - radius of outer cylinder

e - electron

⊖ - negative ion

⊕ - positive ion



b) Negative corona case

Figure 2.1 Geometry of set up

the center into stronger fields while positive ions move into weaker fields. See Figure 2.1.a.

Assuming that a positive voltage is applied to the wire for an "indefinitely" long period of time in air, three distinct modes of corona can be differentiated above threshold as a function of the applied voltage. When the voltage applied is below the threshold, no visible activity can be seen. As the voltage is raised slowly to the threshold, luminous light with the shape of a slightly branched filamentary thread can be seen in a well-darkened room. It is usually given the name burst pulses. The burst pulses become more frequent as voltage is raised and they tend to spread laterally. The burst pulses exist only in a narrow band of voltages at the threshold.^{15,16}

As the voltage is raised further, the streamers tend to be self-sustaining and more frequent until the discharge becomes continuous. A steady thin glow appears very close to the surface. As the voltage raises, the glow becomes more luminous.

At even higher voltages, streamers reappear. They are more vigorous, very bright, reaching further than the burst pulses, and quite noisy acoustically. These types of streamers are called breakdown streamers. They exist along with the glow. As voltage is raised higher and higher, eventually a spark occurs resulting in a complete

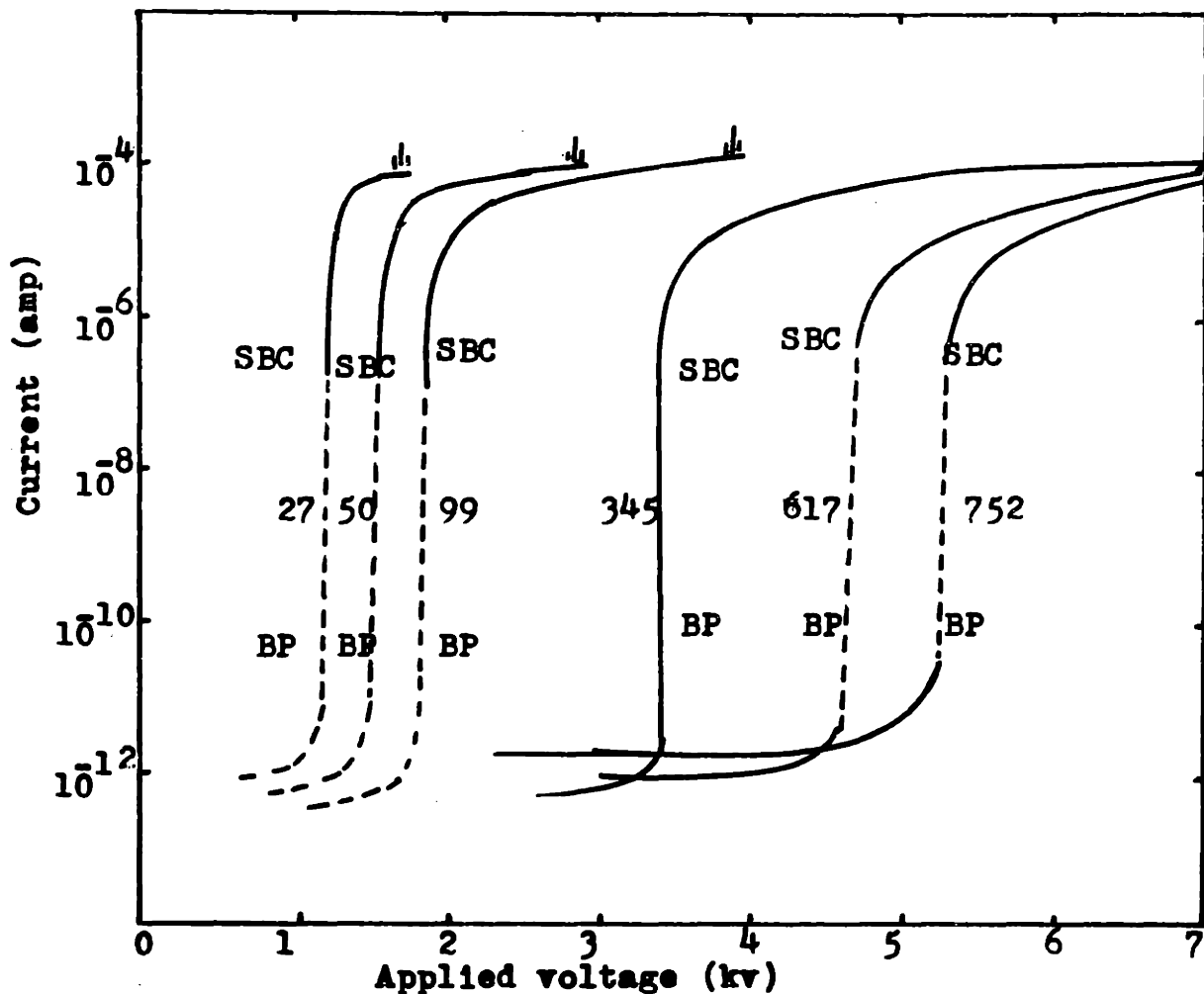


Figure 2.2 This is the current-potential curves in clean dry air with coaxial cylindrical geometry measured by Miller. The numbers indicate the pressure in mm Hg. Note the abrupt current jump to a burst pulse corona, marked by BP, and onset of steady corona, SBC. Breakdown streamers, indicated by vertical lines above the curve, could only be observed below 99 mm Hg as the potential source was not adequate. Dashed lines indicate none reproducible data.

breakdown.

The onset of corona can also be detected by the average current measured. Below the threshold the conduction current is very small generally on the order of 10^{-11} amp/cm or smaller,¹² and is due to charged pairs created by cosmic radiation and earth radioactivity. Around a small band of voltage at the threshold, the current suddenly increases by many orders of magnitude. After the onset of corona, the current increases gradually until complete breakdown. Miller measured corona onset values for a P_t wire of .174 mm diameter mounted coaxially in a 28.5 mm diameter nickel cylinder. Figure 2.2 shows a set of voltage versus current curves for air at different pressures. Note that glow is the most important mode of discharge.

2.2 Negative (Cathode) Corona

When a steady voltage applied to the central wire is negative as in Figure 2.1.b, the type of corona discharge is quite different. Because of the secondary processes involved on the cathode such as emission of electrons by positive ion impact or photoelectric emission, the resulting behaviors depend highly on the type and condition of the negative wire.

Miller used the same set up for negative corona measurements. The polished P_t wire is allowed to rest

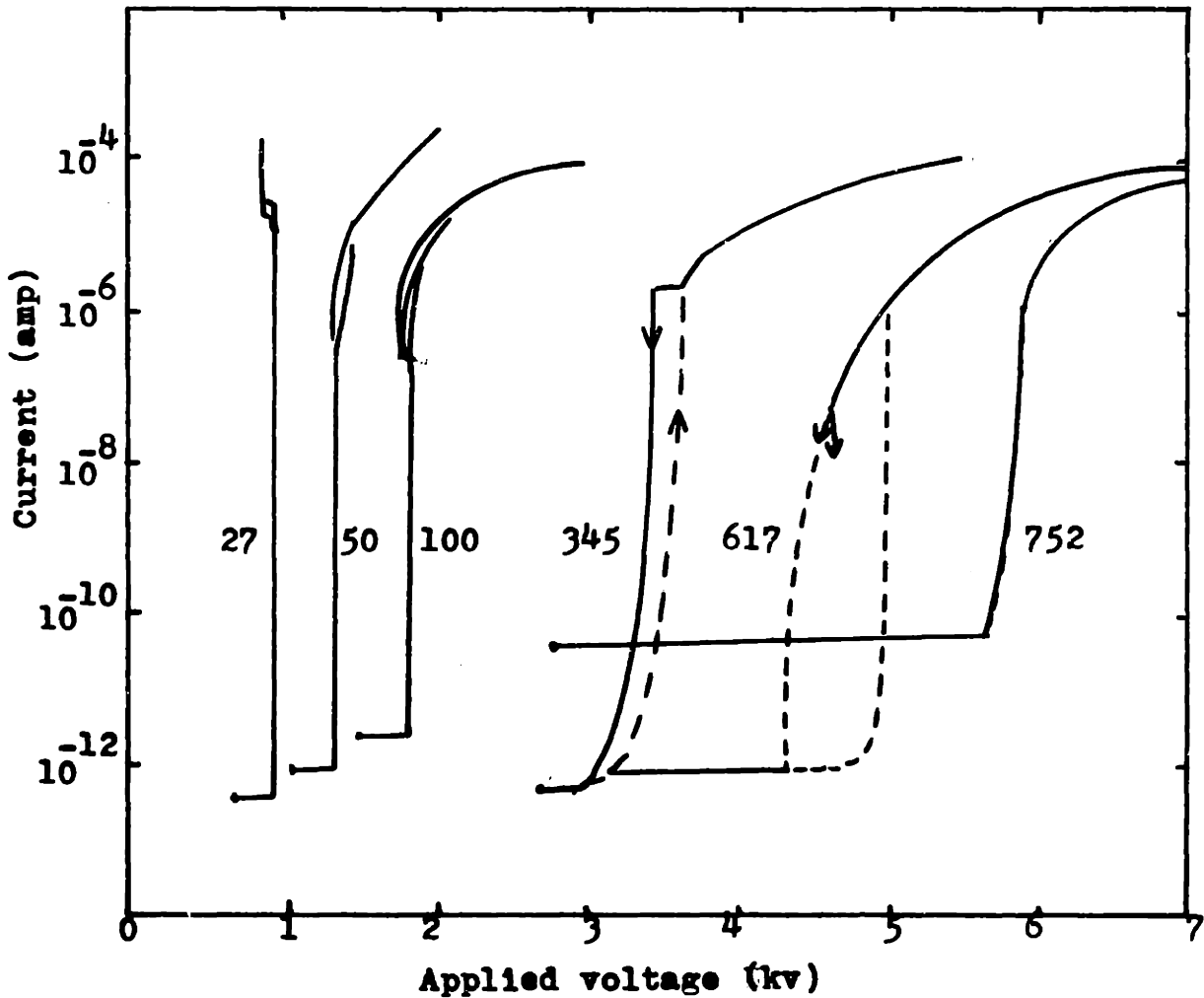


Figure 2.3 This is the current-potential curves in air with negative wire in coaxial cylindrical geometry measured by Miller. The numbers indicates the pressure in mm Hg. The curve at 752 mm Hg was made with a freshly outgassed filament. Note the varied levels of the pre-threshold currents and sharp irregular thresholds. The curves at 617 mm Hg and below represent the altered system after those at 752. Note the onset at 752 mm Hg is higher for the negative wire than that of the positive wire.

in air with no voltage. The voltage is then increased until the visual manifestation of threshold is observed as a glow along the whole length of wire. At the same time the current jumps to about 10^{-5} amp. See Figure 2.3. The uniform glow is explained by the fact that the surface oxidizes in air so that the number of electrons created per ion impact, γ_i , is low. Photoelectric emission at the cathode or photoionization in air could become the dominant secondary processes. If the glow is left standing for 10 to 12 hours, then the discharge will contract to spots. This is because positive ion impact on the cathode cleaned off some oxide on the surface and effectively increased γ_i at the spot.^{18,14,17}

Trichel pulses began with the appearance of spots. The frequency of the pulses increases with increasing potential at the start. However, Trichel pulses in coaxial geometry never reach a frequency of 10^6 cycles per sec as in point-to-plane geometry.

However if the wire is initially oxidized, and before the glow contracts to spots, a potential can be reached so that no spots can form at all. This can be explained by the fact that oxides form on the surface faster than can be cleared by ion impact. If spots did form, then no further uniform glow regions are experienced for voltages above this level.

2.3 Critical Corona Gradient

There are two phenomenon associated with onset of corona: a jump in current and appearance of visible light at the surface of the inner conductor. Peek collected data for corona onset by the visual method. He found that the onset for alternating current is the same as the direct current positive and direct current negative corona cases. Others such as Whitehead, Brown and Farwel found that negative corona onset occurred above the positive corona onset, and alternating current corona onset is close to the onset of negative corona.¹⁸ Miller also found the negative corona onset above positive corona onset. All the experiments mentioned above were done on very small inner conductors.

Because the voltage applied to create identical fields depends on the dimensions of the configuration, the onset can be more easily defined in terms of the electric field needed at the surface of the inner conductor. This electric field is called the critical corona gradient, E_c . It is unique for a given corona, independent of the outer radius, because below onset the space charge is so low that the electric field still maintains the K/r form. Peek fitted a formula to his data.

$$E_c = 31m \delta \left(1 + \frac{308}{\delta a}\right) \text{ kv/cm} \quad (1)$$

The radius of the inner conductor is 'a' in centimeters.

Pressure, p , in cm Hg and temperature, T , in C° are also important. Their effect are incorporated into the variable δ .

$$\delta = \frac{3.92p}{273 + T} . \quad (2)$$

For standard temperature and pressure $\delta = 1$. For polished wire, but oxidized, the start of the visual corona is sharp and the irregularity factor m is unity. If the wire developed spots or is soiled, then m can be as low as .72.

3. Physical Processes

Breakdown is a term used when the current suddenly increases by many orders of magnitude even though the voltage is changed only slightly. Currents come about as results of movement of charged particles. Therefore, the first question that should be asked is where did the charged particles come from and where do they go. The primary processes that occur in air consist of ionization by cosmic radiation, ionization by electron-neutral collision, attachment of electrons to neutrals, recombination, and diffusion. However, a discharge cannot be self-sustaining unless there is at least one secondary feedback mechanism. One of the most acknowledged mechanism is emission of electrons from the cathode due to ion impact. Other important feedback processes are photoelectric emission from metal and photoionization in the bulk of the air.

3.1 Drift Velocity and Mobility

When a charged particle is placed in an electric field, it accelerates. In a gas, this charged particle will lose its kinetic energy gained during collision with the gas molecules. The average velocity travelled along the electric field lines is called the drift velocity, v . Mobility, μ , is defined as v/E , where

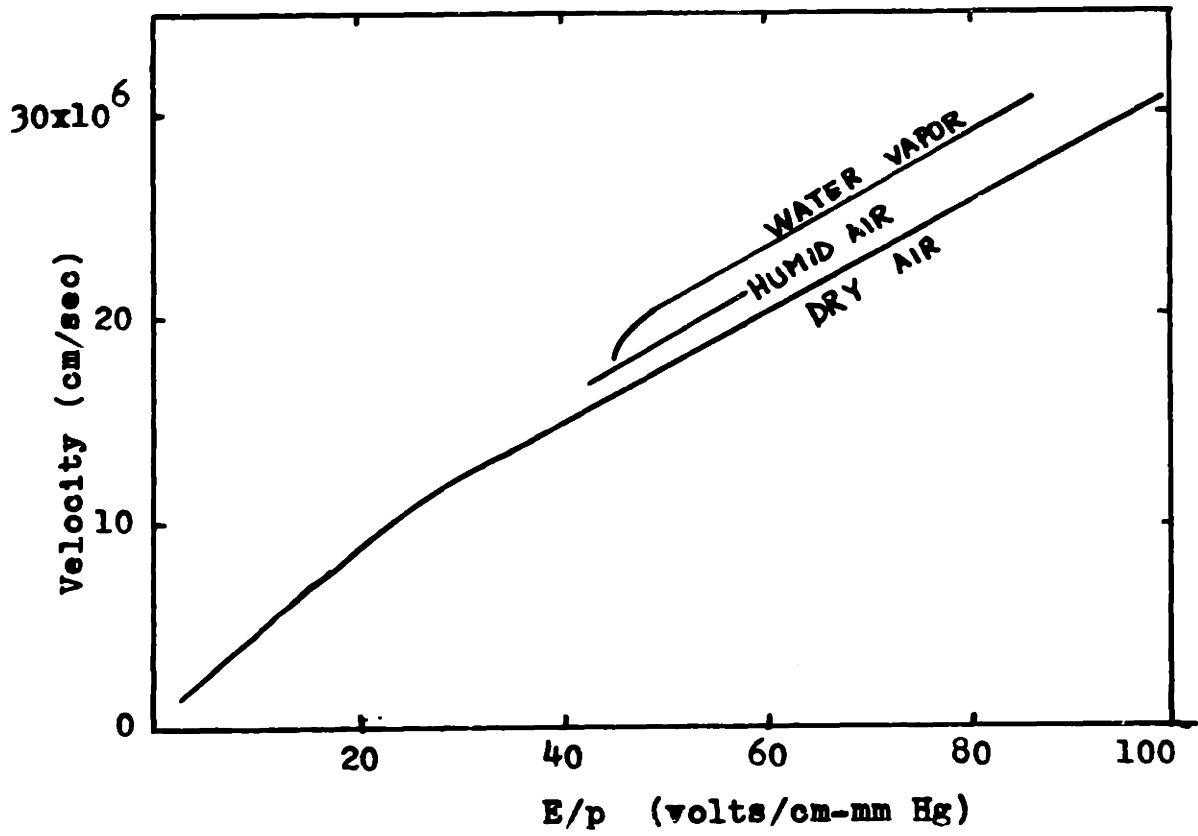


Figure 3.1 Electron drift velocity in dry air, humid air and, water vapor.

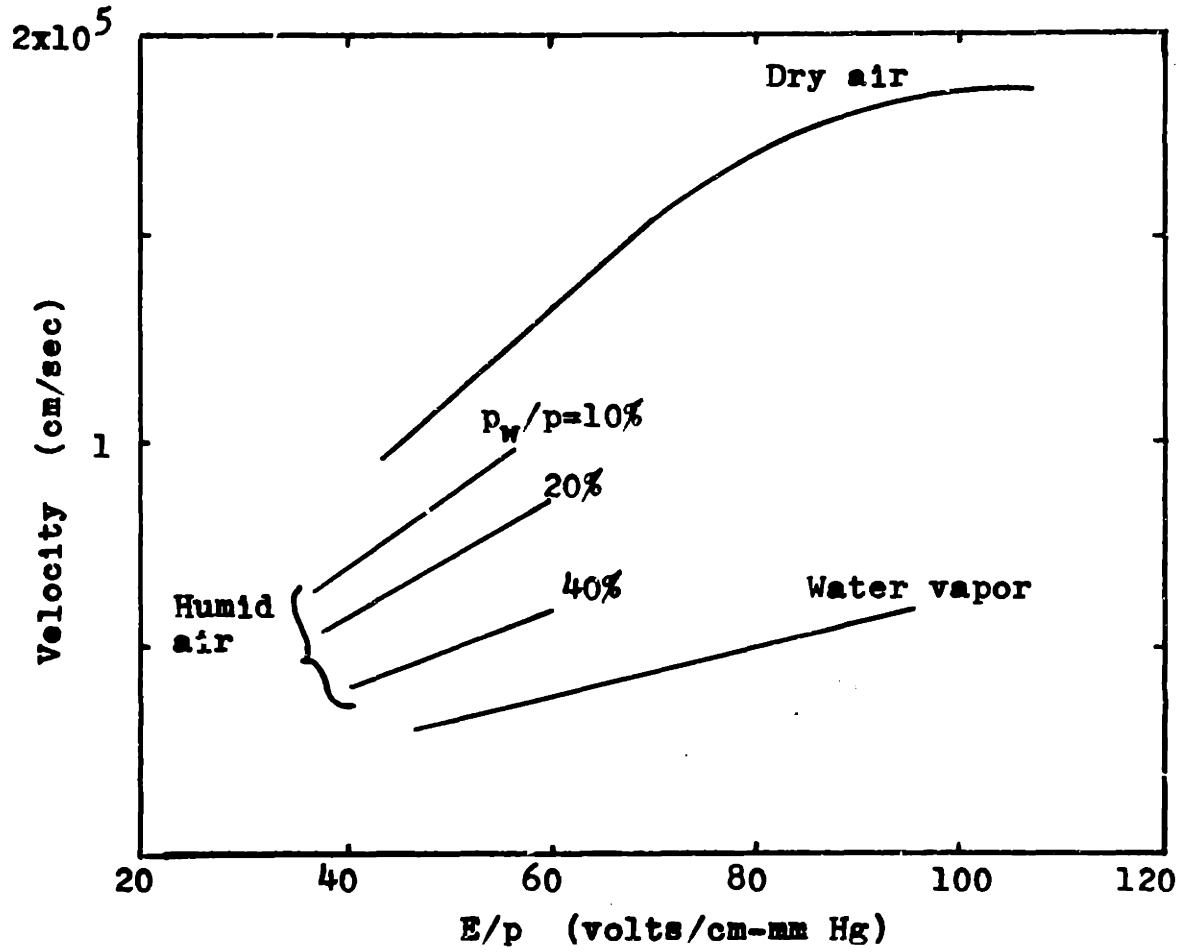


Figure 3.2 Drift velocity of positive ions in dry air, humid air, and water vapor.

E is the electric field strength. In a certain range of interest, μ can be approximated by a constant. Figure 3.1 and 3.2 respectively have plots of electron drift velocity and positive ion drift velocity in air as function of E/p , where p is the pressure.²⁰ The drift velocity of negative ions is assumed to be not too different from that of the positive ions.

3.2 Cosmic Radiation

Cosmic rays, usually very high energy protons, are capable of stripping an electron from a gas molecule, resulting in an electron and a heavy positively charged ion. Because cosmic rays are capable of penetrating most conventional materials, free electrons are created everywhere continuously. From sea level to a few thousand feet, the number of electron-ion pairs created ranges from about 4 to 10 per cm^3/sec .²⁴ The current produced by cosmic radiation alone is insignificantly small. But it is important as a source of free electrons that can start other processes.

3.3 Alpha Ionization Process

One of the most important processes is ionization by electron neutral collisions. During such a collision the electron can lose all or part of its kinetic energy to the neutral. If the kinetic energy of the electron is

greater than the ionization energy, it can ionize the neutral directly producing an electron/ion pair. If the energy of the electron is less than the ionization energy but larger than required for the next allowable atomic transition, then the atom could be excited.

Before the atom emits one or more photons in the process of returning to lower states and eventually the ground state, the excited atom could collide with another electron. The atom has another chance to be ionized or move up to an even higher excited state. This is called "step ionization". When the average kinetic energy of electrons are small, "step ionization" is the predominant method of ionization.

It is possible that an atom is left in a metastable state so that the atom could not return to a lower state without violating the selection rules. The average lifetime of metastable states is on the order of 10^{-3} second, much longer than that of the normal excited states, which is only on the order of 10^{-8} seconds. Because of its long lifetime, metastable states play an important role in gaseous ionization.

Positive ions are not efficient ionizers for E/p less than 100 volts/cm-mm Hg. They are effective ionizers when their velocities are as great as those of electrons which have fallen through the minimum ionization potential.

They are unable to gain such high velocity because their mass prevents them from having accelerations as high as electrons.

3.4 Attachment of Electrons to Neutrals

Not all electrons freed remain free to ionize. Electrons can be captured by atoms lacking one or two electrons in their outer shell forming heavy slow moving negative ions. All gases that have this property are known as electro-negative gases. They are composed of atoms in the groups VII A and VI A family. In air, the attached molecules are mainly O_2^- and O^- . The reaction



is called dissociative attachment and is predominant in molecular gases, in this case oxygen.⁷ Electron energies required are of the order of 3.1 to 3.6 ev.¹² For a negative ion to be stable, so that it can exist for sometime, its total energy must be lower than its neutral ground state. Attachment is an important process because it reduces the number of electrons available as efficient ionizing agents. Also the negative ion's slow drift velocity results in accumulation of negative space charges, which can alter the local electric field to a great extent.

Negative ions can be lost through many processes

such as recombination, detachment or collision into walls. No reliable data on detachment of negative ions in air as a function of E/p has been measured due to experimental difficulties. However, it is known that the following processes

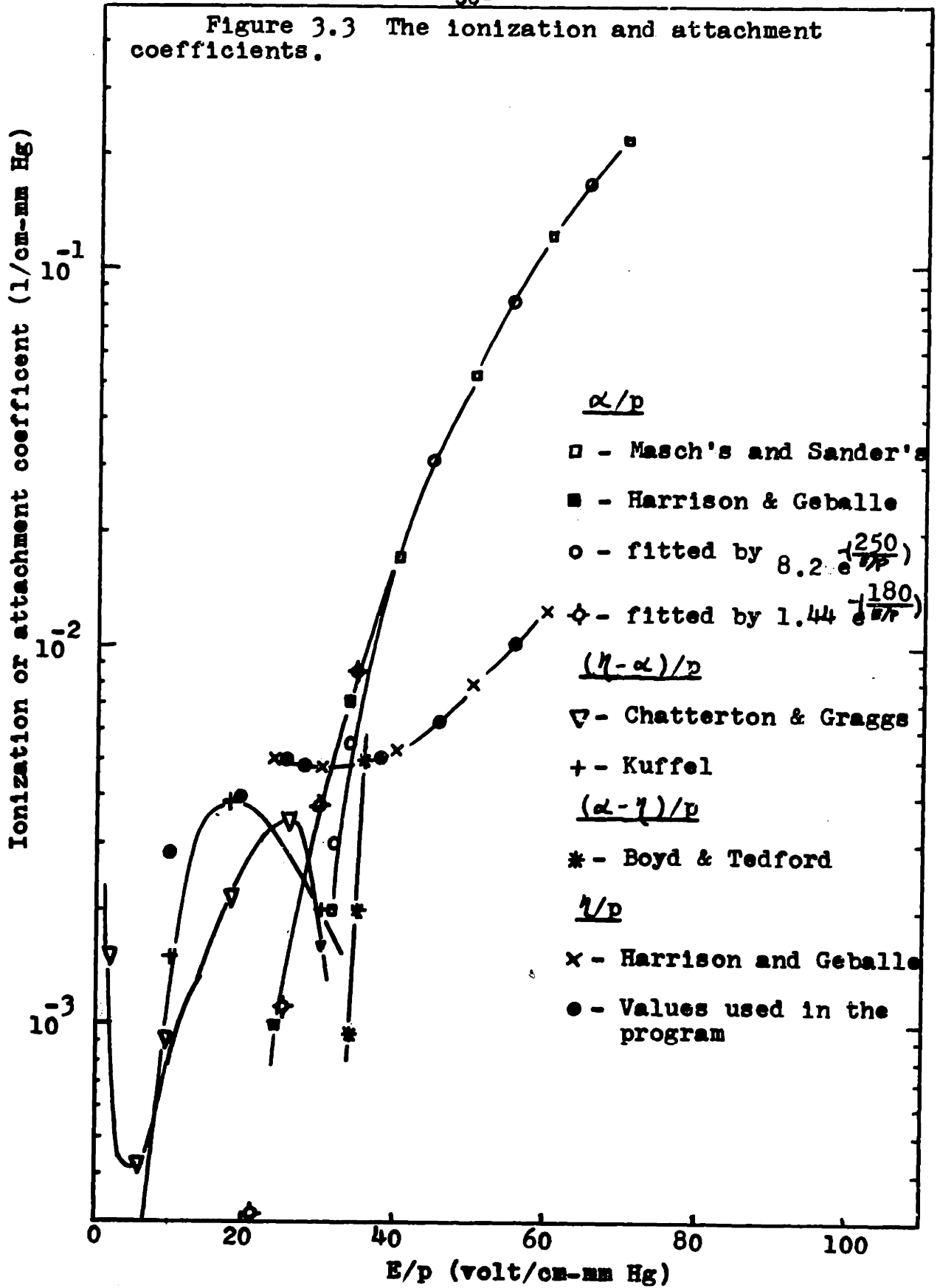


occur in air. In both cases, approximately 1 ev is needed for the reaction to occur.¹⁹ This process is probably included in the measurement of α/p since the experiments could not isolate them. However it is known that in the higher field region of E/p greater than 90 volts/cm-mm Hg, electrons detach and remain free.¹²

3.5 Measurements of Ionization and Attachment Coefficients

Because the growth of the electron density in a constant electric field is an exponential function of space, it is vital to know exactly how many electrons are produced per unit length in the field direction by one electron. This data is usually known as the ionization coefficient by electron collision, Townsend's first ionization coefficient or simply as alpha, α . The effectiveness of electrons to ionize depends directly on the energy an electron can pick up in an electric

Figure 3.3 The ionization and attachment coefficients.



field between two collisions. However, alpha is not a function of the electric field alone. Pressure is proportional to the particle density and inversely proportional to the mean free path and hence inversely proportional to a power of the energy gained between successive collisions. Figure 3.3 gives a few plots of α/p versus E/p as measured by different people for air in the region of interest. Both Masch's and Sander's data differs from Harrison and Geballe's data at low values of E/p . This can be explained by the fact that Masch and Sanders both did not separate out the effect of attachment of electrons to neutrals. Otherwise their data are in fair close agreement. Boyd and Tedfor also measured the apparent primary ionization coefficient, $(\alpha - \eta)/p$, about $E/p = 35$ volts/cm-mm Hg when dissociation is assumed to be negligible. Their values are the smallest.

The number of electrons attached per centimeter per electron is usually called η . Figure 3.3 contains one measured curve for η/p and two curves for $\eta/p - \alpha/p$ as function of E/p . They are not in close agreement with each other. However, there is general concent that below E/p vales of about 32 volts/cm-mm Hg, η/p is greater than α/p . That means almost all of the electrons produced become attached, forming negative ions in the low E/p region.

3.6 Recombination

Recombination is a loss mechanism for all charged particles of opposite sign namely electrons with positive ions, and negative ions with positive ions. The number of recombinations per unit time must be directly proportional to the positive ion density, n^+ , as well as the negative ion density, n^- . So one can write

$$dn^+ = dn^- = - \beta n^+ n^- dt \quad (3)$$

where β is called the recombination coefficient. For air at normal temperature and pressure the ion-ion recombination coefficient is about $2.3 \times 10^{-6} \text{ cm}^3/\text{sec.}^2$. The electron-ion recombination would be smaller because electrons have much larger velocities than ions; leaving the ion after an elastic collision as fast as it approaches. The interaction time is so short that an electron is hard to be captured.

3.7 Diffusion

Collisions of gas molecules and charged particles result in semi-random motion in an applied electric field, so that the net result is that particles tend to smooth out concentration gradients. This phenomenon is known as diffusion. This effect can be measured in terms of current

$$\vec{J} = (D_e \nabla n_e + D_- \nabla n_- - D_+ \nabla n_+)e \quad (4)$$

where D_e , D_+ , D_- are respectively the diffusion coefficients of electrons, positive ions and negative ions. The diffusion coefficients are functions of concentration, average velocity and mean free path of particles of gas type 1 and gas type 2. Measurements by various experimentalists gave an approximate value of $.03 \text{ cm}^2/\text{sec}$ for D_+ and $.043 \text{ cm}^2/\text{sec}$ for D_- in dry air under normal temperature and pressure. The diffusion coefficient for electrons are much higher. For a rough estimate of D_e one can use a simple relation

$$D_e = \mu^{2/3} u_{av}. \quad (5)$$

The quantity u_{av} is called the average energy. μ is the mobility. For an electron with 1 ev, D_e is on the order of $400 \text{ cm}^2/\text{sec}$.

3.8 Secondary Mechanisms and Their Physical Characteristics

To understand all the processes, it is instructive to visualize them in time. The clearest experiment is to use the inner conductor as the anode, and with no space charges between conductors initially. A pulse of n_0 electrons are released at the cathode. As the electrons travel across the gap more electrons are created by electron neutral collision. Photons too are released when

excited atoms return to lower energy states. The total number of electrons created is

$$\exp \int_{R_1}^{R_0} (\alpha(r) - \eta(r)) dr \quad (6)$$

Most of the electron-ion pairs, and as well as photons are created in the neighborhood of the anode. A large pulse is measured due to the creation of electrons within the electron transit time across the gap, τ_e . If no secondary mechanisms present, a small residual current remains for the length of ion transit time, τ_i , due to the movement of positive and negative ions. Because of their slow mobility, the current measured is a few hundred magnitude smaller and τ_i is a few hundred times longer than that of electrons.

The avalanche of electrons, and resulting ions and photons enables three possible secondary mechanisms.

- 1) On arrival of positive ions at the cathode, on the average γ_i electrons can be released per positive ion. This results in one or more pulses spaced about $\tau_e + \tau_i$ apart in time.
- 2) If photons have energy larger than the cathode work function, γ_p electrons can be released per photon arrived. This process is characterized by one or more pulses separated τ_e apart in time.
- 3)

Photons with enough energy can ionize gas molecules also.

This process results in current of much larger magnitude and duration. For onset streamers, the delay time is independent of triggering. For heavy ionizing streamers, the current is regular and very short.

3.9 Photoelectric Emission

Electron can be emitted from the metal surface due to an incident photon when the energy of the photon is greater than the work function of the metal. However, Huber found that with a cathode made of nickel placed in air, photoelectric emission is insignificant; it is not the mechanism responsible for breakdown. In general either photoionization in air or ion bombardment become more important than photoelectric emission.

3.10 Emission of Electrons from Metal due to Ion Impact

The phenomenon of secondary liberation of electrons from the cathode by positive ion bombardment is important in "most" corona discharges. In fact it is the predominant cause of Trichel pulses with period of the pulse roughly on the order of the ion transit time. However, it will be shown that for air, with smooth coaxial cylinders, and low E/p values at atmospheric pressure, the ion bombardment coefficient is not the cause of breakdown.

The established principle behind electron emission

by positive ion bombardment is called Auger neutralization.^{5,6} When a positive ion is close to the surface of the metal, the energy level of the ion is much lower than the highest conduction bands in the metal. An electron can tunnel through to the ground state of the atom at the same time releasing the energy difference between the electron and the ground state of the atom to a second electron in the metal, which with the excess energy could overcome the work function and be detected outside. See Figure 3.4. The kinetic energy of the electron, E_k , is dependent on the ionization energy of the atom, E_1 , minus the energy levels ζ and ω of the two responsible electrons below the vacuum level in the metal.

$$E_k = E_1 - \zeta - \omega . \quad (7)$$

Therefore, the necessary condition for Auger neutralization is $E_1 > 2\phi$, where ϕ is the work function of the metal. (Actually E_1 should be replaced by the effective ionization energy because ionization energy is a function of distance s from the surface.)

Measurements of electron yield, γ_1 , per ion created between the cathode and anode, is usually called the Townsend second coefficient. It has been found that indeed γ_1 is dependent on the ionization energy of the gas but independent of the kinetic energy of the ion, if

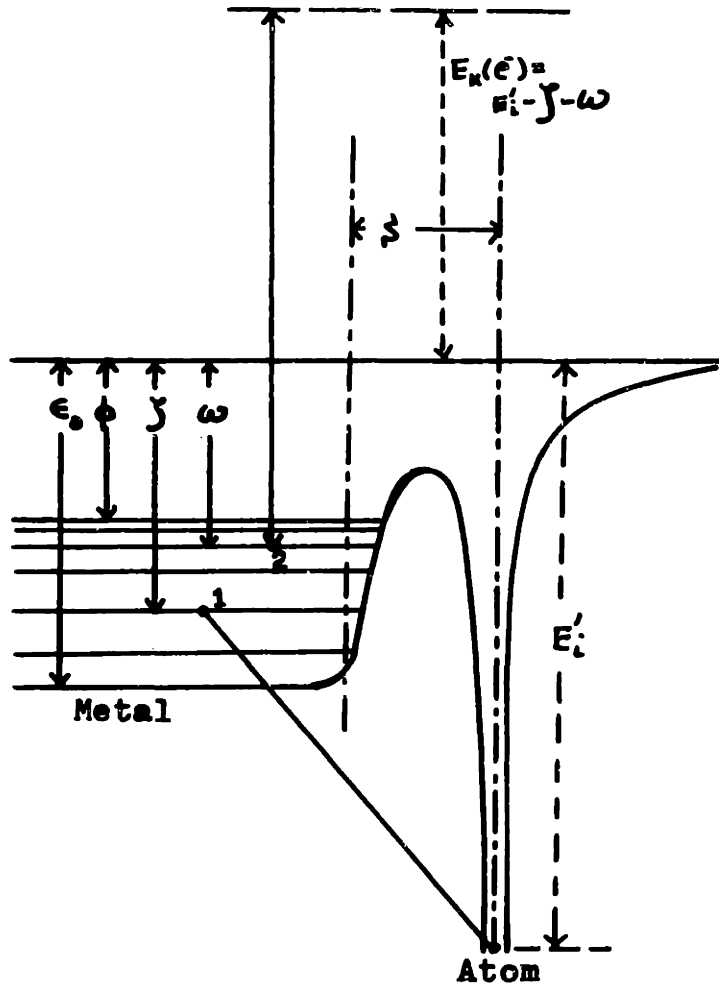


Figure 3.4 Schematic diagram illustrating Auger neutralization of an ion at a metal surface.

the metal is clean.^{5,17,22} However, the γ_1 of interest has to be for air. The predominant components of air are nitrogen and oxygen. Huber studied γ_1 from a nickel cathode with different concentrations of oxygen in nitrogen. She did the experiment with positive coaxial geometry. Based on the theory of Auger neutralization that γ_1 is independent of ion kinetic energy, the same result can be applied to negative corona as well.

Huber found the following results. With pure nitrogen the average γ_1 is about .025, relatively independent of pressure and applied field when back diffusion is taken into account. Back diffusion is caused by reflection of electrons in their first few encounters with gas atoms or molecules. It is more important when pressure is high and electric field is weak; or equivalently E/p values below 100 volts/cm-mm Hg.²⁶ The actual measurements of γ_1 varied as a function of pressure. At 600 mm Hg the measured γ_1 is only .0006, much smaller than the adjusted value. With 5% oxygen, the value of γ_1 decreased approximately by a factor of 5. Increasing the oxygen concentration up to 20%, Huber found that the cathode indicated no secondary mechanism at all. At the same time the onset voltage is actually lowered due to another feedback mechanism, photoionization in the gas.

The effect of oxygen on nickel, as well as other metals,¹⁷ can be associated with an increase of the work function. This is the first reason why χ will decrease. Another reason is that oxygen decreases the population density of higher energy levels in the range of levels the electrons could occupy inside the metal. This results in the emission of more slow electrons. Back diffusion has a greater effect on slow electrons. Again χ_1 is decreased.

3.11 Photoionization

In Huber's experiment, photoionization in the gas is a more important secondary mechanism than ion bombardment, or photoelectric emission. Gas can be ionized not only by electron neutral collisions, but also by photons of high enough energy. Experiments show that photons of 3.87 ev can ionize some gases while photons of 9.9 ev can ionize almost all gases; even though most gases have ionization energies greater than 9.9 ev. This can be explained by the process of step ionization and photo emission from dust and moisture.

Photons are emitted when an excited gas molecule returns to a lower energy state or during the process of ion-ion recombination. The same photon may be absorbed by another atom and leave it in an excited state. If $h\nu$ of the photon is greater than the excitation energy

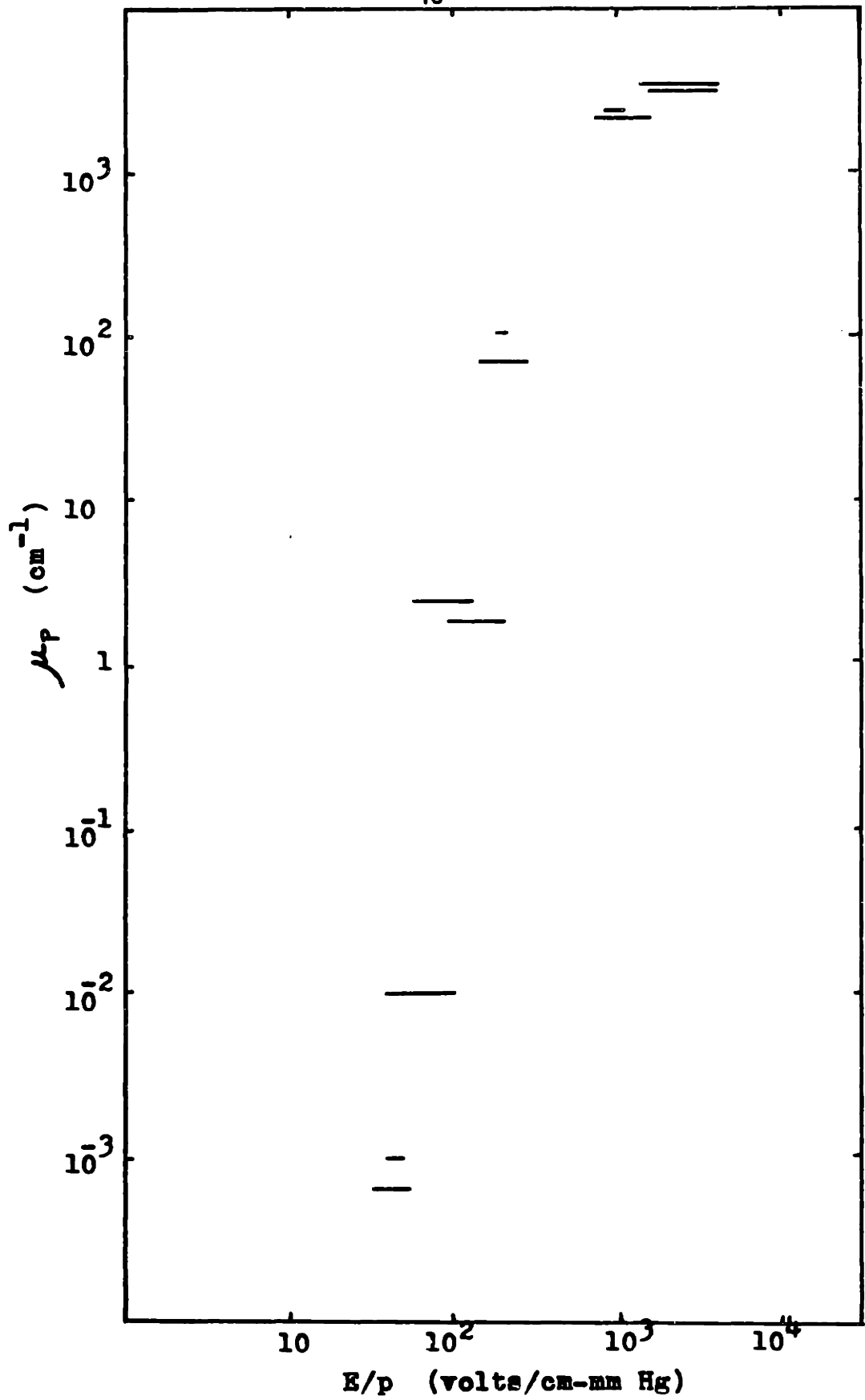


Figure 3.5 The rate of photon absorption, μ_p .

of the atom, the excess energy may be emitted as a photon.



is a reversible process. The effect in the presence of oxygen is shorter ionization steps and greater number of total steps.

Let δ be the number of photons of frequency of interest produced by one electron moving for one centimeter. One can define photon efficiency per ionizing collision, Q , as

$$Q = \delta/\alpha = \text{photons/electron created.} \quad (9)$$

Q is found to vary only from 10^{-2} to 10^{-3} for corona discharge in air.¹⁹ The rate of photon absorption, μ_p , in air in an interval Δx is proportional to Δx and the photon intensity, I .

$$dI = -\mu_p I dx \quad (10)$$

Figure 3.5 gives some measurements of μ_p as function of E/p . Both Q and μ_p are averaged values of many frequencies and different transitions that take place in air.

4. Model for Positive Corona without Feedback Process

4.1 Assumptions

In forming a mathematical model, it is necessary to isolate the problem and make appropriate assumptions. As mentioned before, coaxial geometry is picked for analysis. For this set up, experimental results showed that a glow is the dominant mode of discharge for positive corona, and it could be the dominant mode of negative corona discharge as well if the surface condition is right. This leads to two simplifying assumptions, which will be very good for glow discharge but poor for streamers and Trichel pulses. First, space charge distributions can be made independent of angle and position along the axis, so that all other variables too are independent of the angle and position along the length of the wire. Second, all processes are in the steady state. The net result is that all variables become a function of radius alone. The vector quantities E and J have the form

$$\vec{E} = E(r)\hat{i}_r \quad (1)$$

and

$$\vec{J} = J(r)\hat{i}_r.$$

4.2 Equation with Just Ionization and Attachment Processes

A rather simple model to start with involves only two processes: the production of electron/ion pairs by electron-neutral collisions denoted by α , and attach-

ment of electrons to neutrals forming heavy negative ions denoted by η . The equations involved are:

$$\vec{J}_e = - \rho_e \mu_e \vec{E} \quad (2)$$

$$\vec{J}_- = - \rho_- \mu_- \vec{E} \quad (3)$$

$$\vec{J}_+ = + \rho_+ \mu_+ \vec{E} \quad (4)$$

$$\nabla \cdot \epsilon_0 \vec{E} = \rho_+ + \rho_- + \rho_e \quad (5)$$

$$\vec{E} = -\nabla V \quad (6)$$

$$\nabla \cdot \vec{J}_e = - (\alpha - \eta) J_e \quad (7)$$

$$\nabla \cdot \vec{J}_- = - \eta J_e \quad (8)$$

$$\nabla \cdot \vec{J}_+ = \alpha J_e \quad (9)$$

where the subscripts e, -, + stand for the species : electron, negative ion and positive ion respectively. Equations 2 through 4 express the fact that the current density, J, is related to the electric field E, the mobility, μ , and space charge density ρ . The sign of the charge is include in ρ . Equations 5 and 6 calculate the electric field in terms of the free charge density and in terms of the imposed voltage V. Equations 7 through 9 express the creation of charged particles by the ionization and attachment mechanisms.

A derivation for the electron continuity equation in coaxial cylindrical geometry is given below. See Figure 4.1 for reference. The net gain of electrons/sec-axial length in a gring of radius r to $r+\Delta r$ is

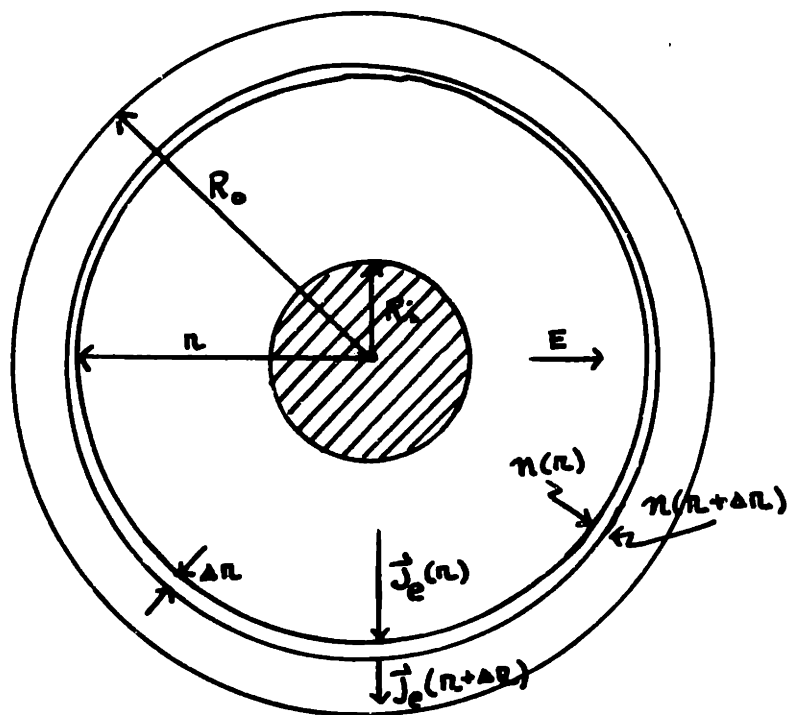


Figure 4.1 The diagram used in the explanation of the derivation for the electron continuity equation for positive corona.

$$(r+\Delta r) J_e(r+\Delta r) - r J_e(r) \quad (10)$$

This expression can be rewritten in the limit $\Delta r \rightarrow 0$ as

$$d(rJ_e) = (\nabla \cdot \vec{J}_e) r dr \quad (11)$$

using equation 1, equation 9 can also be rewritten as

$$-q \mu_e E \left[r n_e(r) - (r+\Delta r) n_e(r+\Delta r) \right] \quad (12)$$

using

$$J_e = -f_e \mu_e E = -(-q) n_e \mu_e E \quad (13)$$

where $(-q)$ is the charge of an electron and n_e is electron density. The difference in n_e is equal to the number of electrons created minus number of electrons attached. as

$$\begin{aligned} r n_e(r) - (r+\Delta r) n_e(r+\Delta r) & \quad (14) \\ & = r n_e(r+\Delta r) (\alpha - \eta) \Delta r \end{aligned}$$

which to first order becomes

$$\begin{aligned} r dr (\nabla \cdot \vec{J}_e) & = -q \mu_e E (\alpha - \eta) n_e r dr \quad (15) \\ & = \mu_e E f_e (\alpha - \eta) \end{aligned}$$

$$\nabla \cdot \vec{J}_e = -(\alpha - \eta) J_e. \quad (16)$$

By similar arguments one can get the rest of the continuity equations.

The boundary conditions are

$$J_e(R_0) = J_{ec}, \quad (17)$$

$$J_-(R_0) = J_{-0},$$

and $J_+(R_1) = 0,$

where R_1 is the radius of the inner cylinder and R_0 is the radius of the outer cylinder. Actually, the outer

cylinder is only an imaginary cylinder.

4.3 An Exact Expression of Current for Unperturbed Electric Field

An exact solution can be derived if space charges are assumed to be unimportant. The electric field will remain in a K/r form wher K can be related to the applied voltage by

$$V = K \ln(R_0/R_1). \quad (18)$$

The total current per centimeter in the z direction can be found.

Equation 6 to 8 can be rewritten in the following form

$$\frac{d}{dr}(rJ_e) = - (\alpha - \eta)(rJ_e) \quad (19)$$

$$\frac{d}{dr}(rJ_-) = - \eta (rJ_e) \quad (20)$$

$$\frac{d}{dr}(rJ_+) = \alpha (rJ_e) \quad (21)$$

with the equation 17 as boundary conditions.

Equation 19 can be solved independently. The solution is

$$J_e(r) = \frac{R_0}{r} J_{e0} \exp \int_r^{R_0} (\alpha(r') - \eta(r')) dr' \quad (22)$$

where $0 < R_1 < r < r' < R_0$

Substitute $J_e(r)$ into right handside of equation 20.

The negative ion current density can be integrated directly.

$$J_-(r) = \frac{R_0 J_{e0}}{r} \int_r^{R_0} \eta(r'') \exp \left[\int_{r''}^{R_0} (\alpha(r') - \eta(r')) dr' \right] dr'' + \frac{R_0}{r} J_{-0} \quad (23)$$

where $0 < R_1 < r < r'' < r' < R_0$

Similarly the current due to the movement of positive ions can be found.

$$J_+(r) = \frac{R_0 J_{e0}}{r} \int_{R_1}^r \alpha(r'') \exp \left[\int_{r''}^{R_0} (\alpha(r') - \eta(r')) dr' \right] dr'' \quad (24)$$

where $0 < R_1 < r'' < r' < r < R_0$

The total current, I, perunit length of z should be a constant independent of r because

$$\nabla \cdot \vec{J}_e + \nabla \cdot \vec{J}_- + \nabla \cdot \vec{J}_+ = 0. \quad (25)$$

I is defined as

$$I = 2\pi r (J_e + J_- + J_+) = \text{constant} \quad (26)$$

To derive I, $J_e(r)$ has to be rewritten in another form by substituting the original J_e as in equation 22 back into equation 19 One finds

$$J_e(r) = - \frac{R_0 J_{e0}}{r} \int_{R_0}^r (\alpha(r'') - \eta(r'')) \exp \left[\int_{r''}^{R_0} (\alpha(r') - \eta(r')) dr' \right] dr'' \quad (27)$$

now simply add J_e , J_- and J_+ . (28)

$$I = 2\pi R_0 \left\{ J_{-0} + J_{e0} \int_{R_1}^{R_0} \alpha(r'') \exp \left[\int_{r''}^{R_0} (\alpha(r') - \eta(r')) dr' \right] dr'' \right\}$$

I is found to be indeed independent of radius r.

4.4 Some Numerical Results

Equation 28 cannot be integrated directly without making more assumptions. It is reasonable to take R_0 as the position α and η cross and it is at

$$E/p = 32 \text{ volts/cm-mm Hg}, \quad (29)$$

since all experiments found that the radius of the outer cylinder is unimportant. Using

$$E = K/r, \quad (30)$$

$$R_0 = K/32p. \quad (31)$$

Letting

$$(\alpha - \eta)/p = A \exp(-\frac{B}{E/p}) \quad (32)$$

with $A = 8.2 \quad 1/\text{cm-mm Hg} \quad (33)$

and $B = 250 \quad \text{volts/cm-mm Hg}$

I can be integrated. See plot of the equation 32 in

Figure 3.3 .

$$I = \frac{2\pi K}{p} \left\{ J_{-0} + J_{e0} \int_{R_1}^{R_0} A p \exp(-\frac{B p r''}{K}) \exp \int_{r_1}^{R_0} A p \exp(-\frac{B p r'}{K}) dr' dr'' \right\} \quad (34)$$

$$= \frac{\pi K}{p} \left\{ J_{-0} + J_{e0} \left[\exp\left(\frac{AK}{B} \left(\exp(-\frac{B p R_1}{K}) - \exp(-\frac{B}{32}) \right) - 1 \right) \right] \right\} \quad (35)$$

A plot of current as a function of the electric field

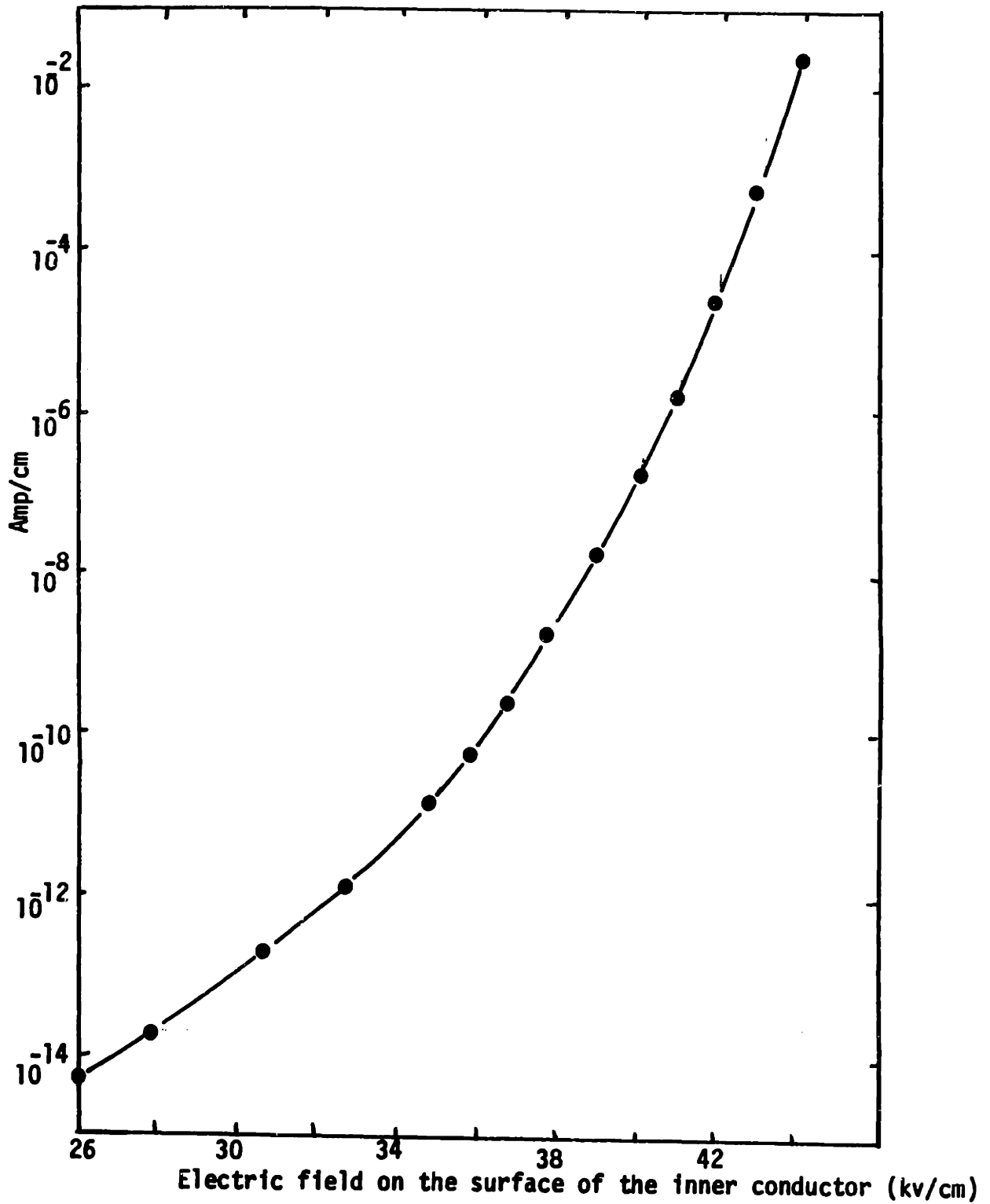


Figure 4.2 Total current as a function of the applied voltage with $J_{e0} = 1 \times 10^{-15}$ amp/cm.

at the surface of a 1.5 cm radius inner cylinder is shown in Figure 4.2 . J_{-0} is taken to be zero for simplicity. J_{e0} is arbitrarily taken to be 1×10^{-15} amp/cm since on log scale, the effect of multiplying J_{e0} to the whole equation is simply achieved by scaling the whole curve. At this point, we are really interested in its shape and not its absolute value.

The current as a function of electric field is simply the result of Townsend's electron avalanche. The Peek's value of electric field for breakdown on a 1.5 cm radius inner conductor is 38.8 kv/cm. The curve include the case of 38.8 kv/cm electric field. However, it does not look like typical current versus voltage graphs near the threshold of breakdown.

4.5 Space Charges

The space charges can be estimated. For simplicity, η is assumed to be identically zero. and

$$\alpha/p = (\alpha - \eta)/p. \quad (35)$$

So the total current I now is due to movement of electrons and positive ions only.

$$f_e(r) = - \frac{R_0 J_{e0}}{K e} \exp (AK/B (\exp(-Bpr/K) - \exp(-BpR_0/K)) \quad (36)$$

$$f_+(r) = \frac{R_0 J_{e0}}{K +} \exp (AK/B (\exp(-BpR_1/K) - \exp(-Bpr/K)) \quad (37)$$

The electron charge density, $f_e(r)$, is large near the surface of the inner conductor and the positive ion charge

density, $\rho_+(r)$, is larger further away from center. However, $\rho_e(r)$ and $\rho_+(r)$ are of equal magnitude very close to the surface of the inner conductor because

$$\mu_+ \ll \mu_e. \quad (38)$$

Their effect on the electric field for a fixed voltage is to lower the electric field on the surface of the inner conductor and raise it further away.

4.6 Cosmic Radiation

The boundary conditions now control the magnitude of the total current. The true source of initial free electrons comes from cosmic radiation. The effect of cosmic radiation can be included very easily. Assume cosmic rays create on the order of 10 charged pairs/cm³/sec, then the continuity equations look like

$$\nabla \cdot \vec{J}_e = - (\alpha - \eta) J_e - 10q \quad (39)$$

$$\nabla \cdot \vec{J}_- = - \eta J_e \quad (40)$$

$$\nabla \cdot \vec{J}_+ = \alpha J_e + 10q \quad (41)$$

The solution of equation 39 looks like

$$J_e(r) = - \frac{10q}{rS(r)} \int_{R_0}^r r' S(r') dr' + \frac{R_0 J_{e0} S(R_0)}{rS(r)} \quad (42)$$

$$\text{where } S(r) = \exp\left(\int (\alpha(r'') - \eta(r'')) dr''\right). \quad (43)$$

The second term on the right handside is the same as without cosmic radiation. The negative ion and positive ion current densities both have one additional term also.

$$J_-(r) = \frac{10q}{r} \int_{R_0}^r \frac{\eta(r'')}{S(r'')} \int_{R_0}^{r''} r' S(r') dr' dr'' \quad (44)$$

$$- \frac{R_0 J_{e0} S(R_0)}{r} \int_{R_0}^r \frac{(r'')}{S(r'')} dr'' + \frac{R_0 J_{-0}}{r} .$$

$$J_+(r) = - \frac{10q}{r} \int_{R_1}^r \frac{\alpha(r'')}{S(r'')} \int_{R_0}^{r''} r' S(r') dr' \quad (45)$$

$$+ \frac{R_0 J_{e0} S(R_0)}{r} \int_{R_1}^r \frac{(r'')}{S(r'')} dr'' + \frac{10q}{r} \int_{R_1}^r r'' dr''$$

$$I = 2\pi(10q) \int_{R_1}^{R_0} r'' dr'' \quad (46)$$

$$+ 2\pi(10q) \int_{R_1}^{R_0} \frac{(r'')}{S(r'')} \int_{r''}^{R_0} r' S(r') dr' dr''$$

$$+ 2\pi R_0 J_{e0} S(R_0) \int_{R_1}^{R_0} \frac{(r'')}{S(r'')} dr'' + 2\pi R_0 J_{e0} .$$

The first term on the right handside of the expression for total current expresses the current produced by cosmic radiation without multiplication, and it is insignificant compared to the following terms. The second term gives the current produced due to Twonsend avalanche but with electrons initially produced by cosmic radiation. The third and fourth terms are the same as without cosmic radiation.

If the same assumptions are made here as in section 4.4,

$$I = \pi(10q) (R^2 - R_1^2) \quad (47)$$

$$+ 2\pi(10q) \int_{R_1}^{R_0} A_p \exp\left(-\frac{Bpr''}{K}\right) \exp\left(\frac{AK}{B} \exp\left(-\frac{Bpr''}{K}\right)\right) \times$$

$$\left[\int_{r''}^{R_0} r' \exp\left(-\frac{AK}{B} \exp\left(-\frac{Bpr'}{K}\right)\right) dr' \right] dr''$$

$$+ 2\pi R_0 J_{e0} \left(\exp\left(\frac{AK}{B} \left(\exp\left(-\frac{BpR_1}{K}\right) - \exp\left(-\frac{B}{32}\right) - 1\right)\right) \right)$$

$$+ 2\pi R_0 J_{-0} .$$

The second term of equation 47 has to be integrated numerically. Figure 4.3 is a plot of the result- the total current as a function of electric field with just cosmic radiation and Townsend avalanche. This curve has the same shape as the curve given by the third term of equation 47 . If one defines J_{e0} as the current necessary to make the second term the same as the third term, J_{e0} is found to be fairly constant, ranging from 1.9×10^{-15} amp/cm at 27 kv/cm to 54×10^{-15} amp/cm at 45 kv/cm.

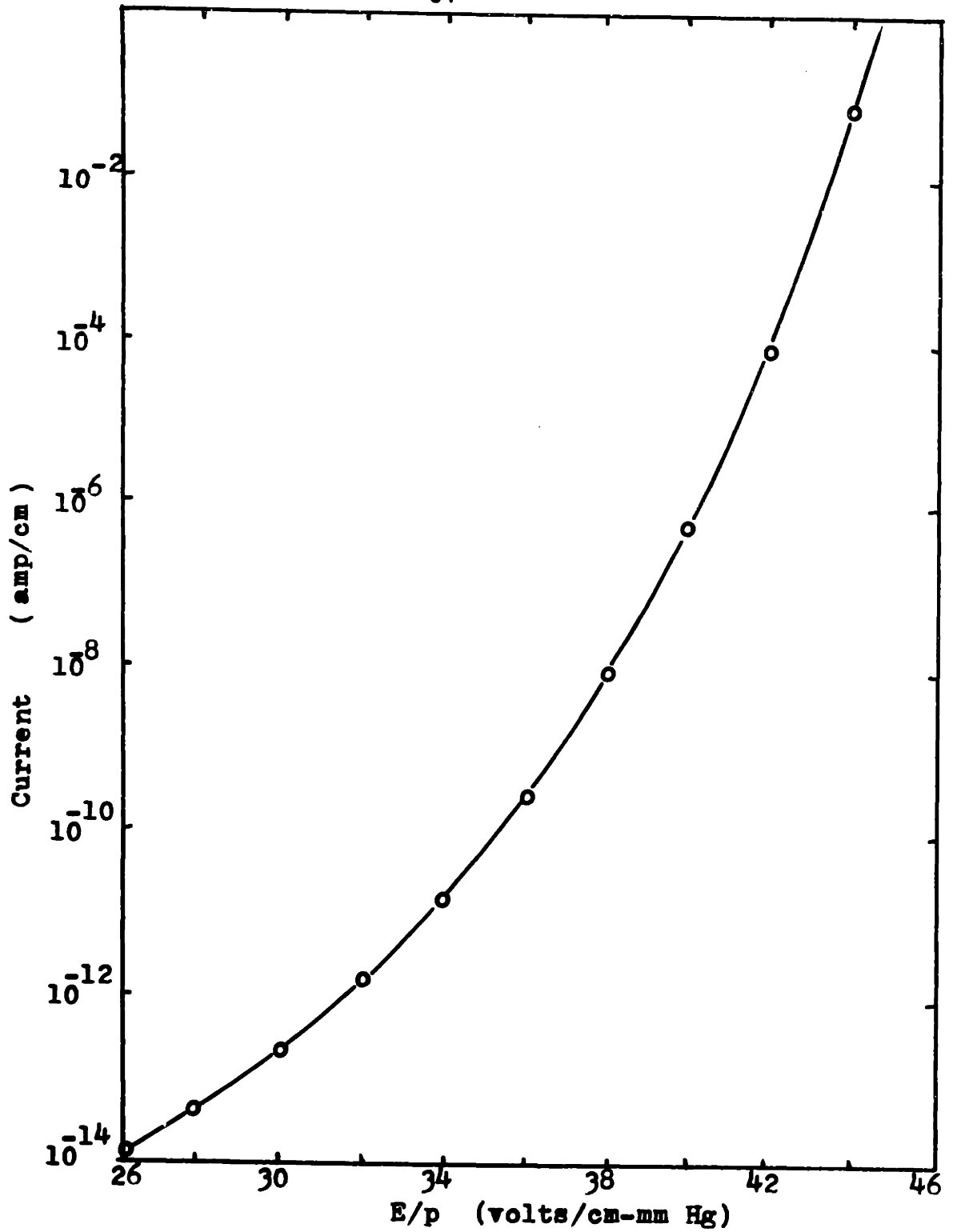


Figure 4.3 The total current per cm axial length as a function of the electric field at the surface of the inner conductor with cosmic radiation.

5. Positive Corona with Photoionization

5.1 Justification for Photoionization

A large change in current of many orders of magnitude within a small range of voltage was found to be unobtainable based simply on Townsend avalanche. A feedback mechanism is necessary. For now, consider only a smooth polished wire placed in air. Ion bombardment and photoelectric emission are not found to be the feedback mechanism, due to the difference in time delay and magnitude of current involved in breakdown; at the same time those facts support photoionization in air as the important process. Additional information can support this theory. First of all both visible and ultraviolet light are detected at and above the voltage that the current increases by many orders of magnitude.¹⁸ Secondly, the threshold for negative corona is the same or slightly higher than the critical electric field of positive corona.

5.2 Assumptions

A few assumptions are made in the process of making a mathematical model. Photons are assumed to have equal probability in travelling in any direction

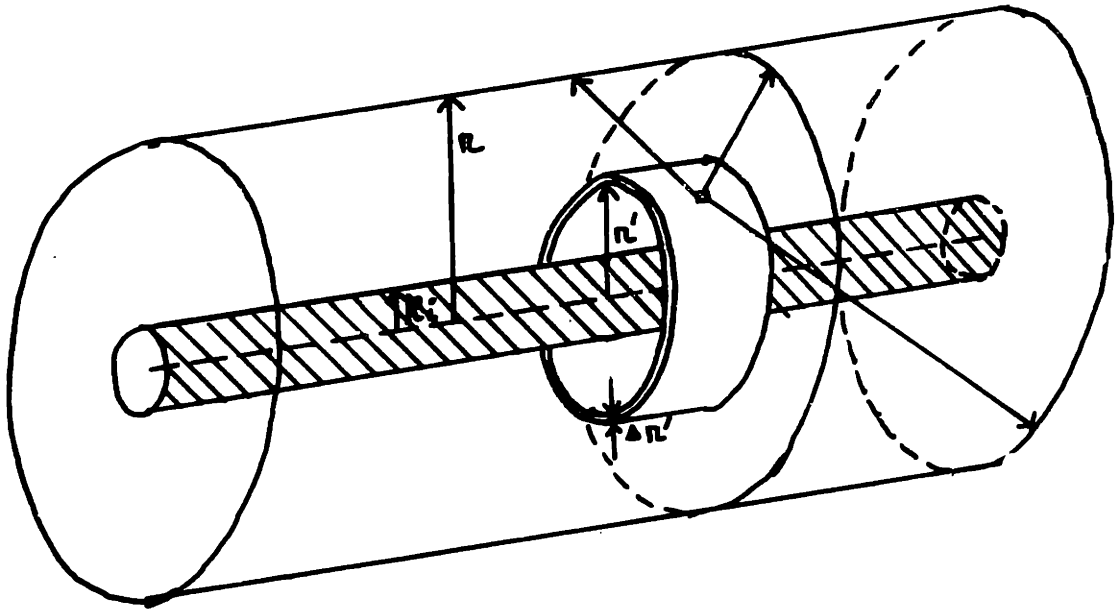


Figure 5.1 Illustration of some possible directions a ray emitted on the ring of radius r' could travel, and be absorbed on the cylinder of radius r , where $r > r'$.

in a straight line from the point of creation. Most of the Townsend electrons are created near the inner wire surface. For every electron created, Q photons are created. Consequently most of the photons are also created near the surface of inner wire. Visual observation confirms this fact.¹⁸ Therefore, one can assume that all photons that reach a ring of radius r come from within the ring of radius r' . See Figure 5.1. The assumption as a whole is good, even though the numbers will not be accurate very close to the surface of the inner conductor, because the electrons created further away are more important. They create more electrons on their way in due to Townsend avalanche, then electrons created near the inner cylinder surface.

5.3 Derivation of the Photoionization term

The contribution to the number of electrons created due to photons is formulated below. For references see Figure 5.1 and 5.2. The total number of electrons passing through a ring of unit length in the axial direction defined by radius r' per second is

$$2\pi r' J_e(r') \quad (1)$$

The number of photons created at r' per unit length in the axial direction is

$$2\pi Q \alpha(r') r' J_e(r') \quad (2)$$

Therefore for a ring $\Delta r'$ thick, the number of photons created is

$$2\pi Q \alpha(r') r' J_e(r') \Delta r'. \quad (3)$$

Not all the photons created in the ring of radius r' $\Delta r'$ thick can reach an infinitely long cylinder of radius r greater than r' . Part of the photons run into the inner wire; part are absorbed in the intermediate space. The ones that do reach the cylinder of radius r have to travel different distances to get there. Let K be the percentage of photons arriving at radius r per photon emitted from a point P on radius r' . Then the number of photons that actually reach the ring of radius r is

$$K 2\pi Q \alpha(r') r' J_e(r') \Delta r' \quad (4)$$

where
$$K = \frac{r}{\pi} \int_0^{\theta_{\max}} \int_0^{\infty} \frac{(r - r' \cos \theta) \exp(-\mu D)}{D^3} dz d\theta \quad (5)$$

$$|D| = (r^2 + r'^2 - 2rr' \cos \theta + z^2)^{\frac{1}{2}} \quad (6)$$

$$\theta_{\max} = \cos^{-1} \left[\frac{1}{rr'} (R_1^2 - ((r^2 - R_1^2)(r'^2 - R_1^2))^{\frac{1}{2}}) \right] \quad (7)$$

The derivation of K is in Appendix 1. This is too complicated an expression to evaluate. An approximate expression in the form

$$K \approx G \exp(-\mu_{\text{eff}}(r-r')) \quad (8)$$

is simple to understand and easy to use. G , the geometric

factor, is the number of electrons not blocked by the inner wire, under the assumption that nothing is absorbed by air. μ_{eff} is the effective μ_p when approximating a three dimensional system by a one dimensional system.

$$G = \frac{\theta_{\text{max}}}{2\pi} + \frac{1}{\pi} \tan^{-1} \left(\left(\frac{r+r'}{r-r'} \right) \tan \left(\frac{\theta_{\text{max}}}{2} \right) \right) \quad (9)$$

See Appendix 3 for calculation of μ_{eff} .

So the total number of photons produced in a ring of radius r' thickness $\Delta r'$ per unit axial length can result in

$$2\pi \mu_p G \alpha(r') r' J_e(r') \exp(-\mu_{\text{eff}}(r-r')) \Delta r' \Delta r \quad (10)$$

electrons produced at a cylinder of radius r and thickness Δr . Summing up the effect of all the photons created from within the cylinder of radius r , one gets

$$2\pi \mu_p \int_{R_1}^r G \alpha(r') r' J_e(r') \exp(-\mu_{\text{eff}}(r-r')) dr' \Delta r \quad (11)$$

as the number of electrons created in thickness Δr per unit length in z -direction.

$$\begin{aligned} & J_e(r + \Delta r) 2\pi(r + \Delta r) - J_e(r) 2\pi r \quad (12) \\ & = 2\pi r \Delta r (\nabla \cdot J_e) \\ & = -2\pi r (\alpha(r) - \eta(r)) J_e(r) \Delta r - 10q 2\pi r \Delta r \\ & \quad - 2\pi \mu_p \int_{R_1}^r G \alpha(r') r' J_e(r') \exp(-\mu_{\text{eff}}(r-r')) dr' \Delta r \end{aligned}$$

Now the continuity equations can be replaced by

$$\frac{d}{dr}(rJ_e) = - (\alpha(r) - \eta(r))(rJ_e) - 10qr - Ph \quad (13)$$

$$\frac{d}{dr}(rJ_-) = - \eta(r)(rJ_e) \quad (14)$$

$$\frac{d}{dr}(rJ_+) = \alpha(r)(rJ_e) + 10qr + Ph \quad (15)$$

where

$$Ph = \mu_p \int_{R_1}^r G \alpha(r') r' J_e(r') \exp(-\mu_{eff}(r-r')) dr' \quad (16)$$

5.4 Analytical Prediction of Corona Onset

A very much simplified picture might help to understand photoionization and give a rough estimate of critical electric field required for breakdown as a function of the radius of the inner conductor. One can assume that instead of photoionization occurring in the inter-electrode region in air, photons could only ionize at a ring of thickness Δr , radius R_0 , where E/p is 32 volts/cm-mm Hg. This particular radius R_0 is picked because if an electron is created by photon, it can produce the most number of new electrons in an avalanche, yet not in such a low field region that attachment is dominant. Further assume the geometric factor G to be a constant

and no decay in photon intensity between the place of emission and arrival at radius R_0 .

Then a self sustaining discharge requires

$$R_0 J_{e0} = G \mu_p Q \int_{R_1}^{R_0} \alpha(r') r' J_e(r') dr' \quad (17)$$

If one takes the expression for α as

$$\alpha/p = A \exp\left(-\frac{B}{E/p}\right) \quad (18)$$

Then the solution for $J_e(r)$ is equation 4.22. Substituting them into equation 18 above, then

$$1 = G \mu_p Q \left[\exp\left(\frac{AK}{B} \left(\exp\left(-\frac{BpR_1}{K}\right) - \exp\left(-\frac{B}{32}\right) - 1\right)\right] \quad (19)$$

For a given $G \mu_p Q$, a set of critical electric fields as a function of inner conductor radii can be calculated numerically. Pick $G \mu_p Q$ so that the critical electric field of a 1.5 cm radius conductor coincides with Peek's value. When

$$A = 8.2 \quad \text{l/cm-mm Hg} \quad (20)$$

$$B = 250 \quad \text{volts/cm-mm Hg}$$

then $G \mu_p Q$ is found to be 1.4×10^{-6} . Figure 5.2 shows plots of both curves. The agreement is not very good.

If instead,

$$A = 50 \quad \text{l/cm-mm Hg} \quad (21)$$

$$B = 335 \quad \text{volts/cm-mm Hg}$$

are used, the critical electric field curve is found to

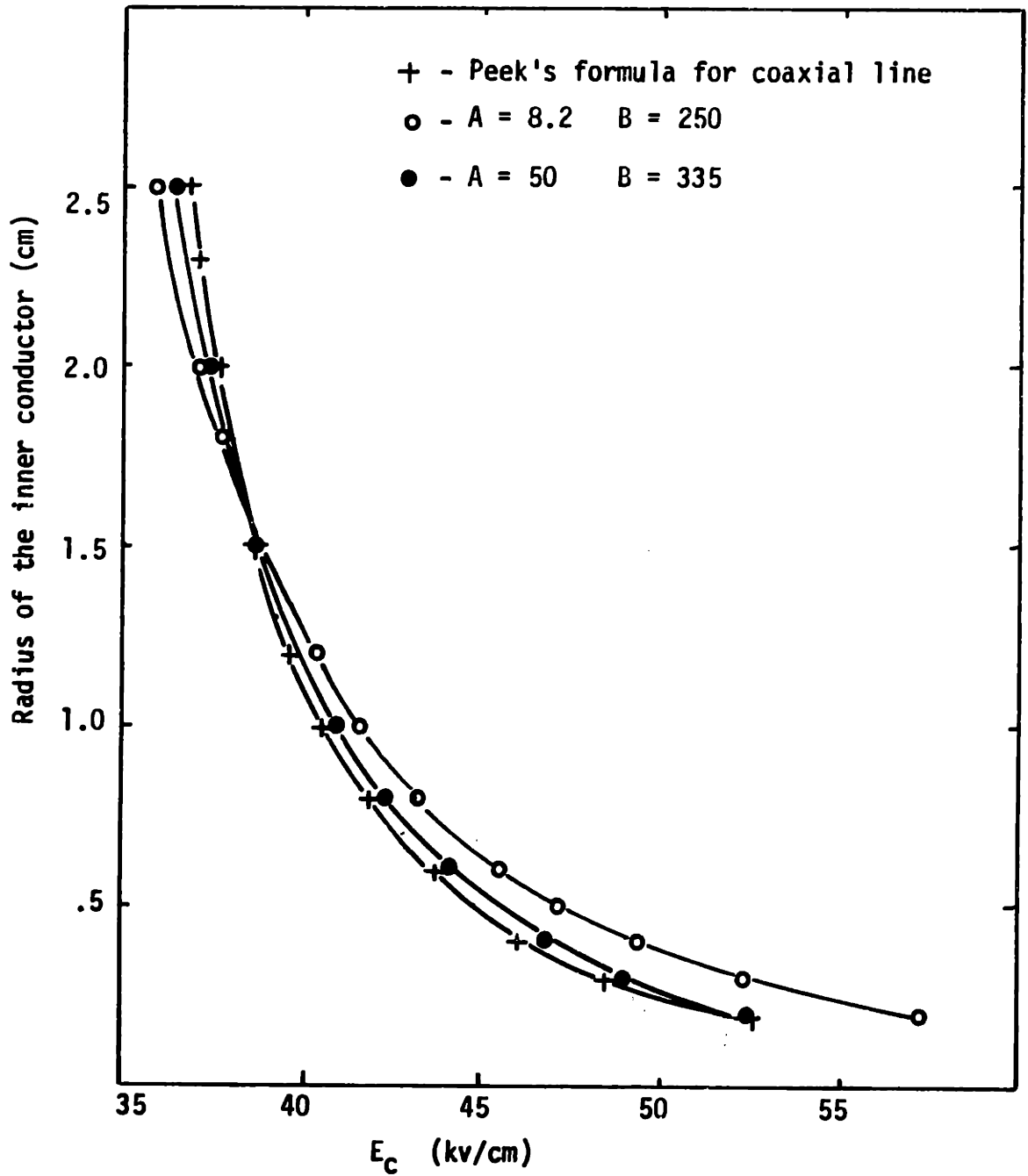


Figure 5.2 Analytic calculation of critical corona onset gradient and comparison against Peek's formula.

be much closer to Peek's formula. The values in equation 21 produces a much steeper α/p as function of E/p . This seems to indicate the importance of attachment, because $\alpha - \eta$ for E/p greater than 32 volts/cm-mm Hg is a curve similar to α but steeper.

5.5 The Full Set of Equations Used

Collecting all the equations involved, they are

$$\vec{J}_e = -v_e(E)\rho_e \quad (22)$$

$$\vec{J}_- = -\mu_- \vec{E} \rho_- \quad (23)$$

$$\vec{J}_+ = \mu_+ \vec{E} \rho_+ \quad (24)$$

$$\vec{E} = -\nabla V \quad (25)$$

$$\nabla \cdot \epsilon_0 \vec{E} = \rho_{++} + \rho_{-+} + \rho_e \quad (26)$$

$$\nabla \cdot \vec{J}_e = -(\alpha - \eta)J_e - 10q - Ph \quad (27)$$

$$\nabla \cdot \vec{J}_- = -\eta J_e \quad (28)$$

$$\nabla \cdot \vec{J}_+ = \alpha J_e + 10q + Ph \quad (29)$$

where

$$Ph = \mu_p Q \int_{R_1}^r G(r') \alpha(r') r' J_e(r') \exp(-\mu_{eff}(r-r')) dr' \quad (30)$$

$$G(r') = \frac{\theta_{max}}{2\pi} + \frac{1}{\pi} \tan^{-1} \left(\left(\frac{r+r'}{r-r'} \right) \tan \left(\frac{\theta_{max}}{2} \right) \right) \quad (31)$$

$$\theta_{max} = \cos^{-1} \left[\frac{1}{rr'} (R_1^2 - ((r'^2 - R_1^2)(r^2 - R_1^2))) \right] \quad (32)$$

α, η and $v_e(E)$ will have to be fitted to experi-

mental data.

Marsh and Sander's data can be fitted quite well by

$$A = 8.2 \quad \text{l/cm-mm Hg} \quad (33)$$

and $B = 250 \quad \text{volt/cm-mm Hg} .$

Harrison and Geballe's data is probably more accurate for regions of $E/p < 40 \text{ volts/cm-mm Hg}$, since they separated out the effect of attachment. One set of A and B, however, will not fit the whole range of E/p for Harrison and Geballe's data. For $E/p \geq 40 \text{ volts/cm-mm Hg}$, A and B are the same as in equation 5.33. For $E/p < 40 \text{ volts/cm-mm Hg}$,

$$A = 1.44 \quad \text{l/cm-mm Hg} \quad (34)$$

and $B = 180 \quad \text{volts/cm-mm Hg}$

fit better.

For the attachment coefficient, no good explanation exists for the discrepancies between experimental results. For $E/p \geq 26 \text{ volts/cm-mm Hg}$, again Harrison and Geballe's η/p curve is used as a reference. It is fitted by

$$\eta/p = 9.15(10^{-6})\left(\frac{E}{p}\right)^2 - .000567\left(\frac{E}{p}\right) + .0135. \quad (35)$$

For $E/p < 26 \text{ volta/cm-mm Hg}$, Kuffel's data is used as a reference.

$$\eta/p = 1.545(10^{-4})(E/p) + 1.14(10^{-3}). \quad (36)$$

Variations of η on corona is also studied later.

$$v_e(E) = 2.5(10^5)(E/p) + 5(10^6) \quad (37)$$

for $E/p \geq 25$ volts/cm-mm Hg. And

$$v_e(E) = 4.5(10^5)(E/p) \quad (38)$$

for $E/p < 25$ volts/cm-mm Hg.

$v_e(E)$ is used for electron drift velocity instead of using the concept of mobility, because mobility associated with measured data is not a constant as E/p is changed for $E/p > 25$ volts/cm-mm Hg. See Figure 3.1 for electron velocity as measured by Ryzko.

5.6 Numerical Method

Because the equations are nonlinear and coupled, an iterative method is used. For the first iteration only, the electric field is assumed to have a K/r form and $\mu_p = 0$. Equation 5.27 is solved first. The results of $J_e(r)$ is used in calculating J_- and J_+ . All the integrations are done by a fourth-order Runge-Kutta method. From J_e , J_- and J_+ , the space charges are calculated using equations 5.22 to 5.23. Equations 5.25 and 5.26 are used to calculate the new electric field. Then the photoionization term is calculated. Equation 5.27 is solved again with the new electric field and the new photoionization term. This process repeats until the solution of total current density changes only by .5% .

5.7 Method Used in the Calculation of the Electric Field

Once the charge distribution is known, and the voltage between the conductors specified, the electric field distribution can be calculated. The equations used in the program are derived below. Trapezoidal rule is used for integration.

Define $r_j = R_1 + j(\Delta r)$, where j is an integer. All the charges within the radius r_j can be written as

$$\int_{r_0}^{r_j} (\rho_e(r) + \rho_-(r) + \rho_+(r)) r 2\pi dr + \rho_0 \quad (39)$$

where ρ_0 is the total charge on the inner conductor.

Also define

$$\text{charge}(j) = \int_{r_0}^{r_j} (\rho_e(r) + \rho_-(r) + \rho_+(r)) r dr . \quad (40)$$

Then the Gauss's Law can be written as

$$2\pi r_j E(r_j) = (\rho_0 + 2\pi \text{charge}(j)) / \epsilon_0 . \quad (41)$$

$$\text{Since} \quad 2\pi r_0 E(r_0) = \rho_0 / \epsilon_0 . \quad (42)$$

$$E(r_j) = E(r_0) \frac{r_0}{r_j} + \frac{\text{charge}(j)}{\epsilon_0 (r_j)} . \quad (43)$$

Equation 5.25 can be rewritten in the integral form.

$$V(r_0) - V(r_N) = \int_{r_0}^{r_N} \mathbf{E} \cdot d\mathbf{r} \quad (44)$$

where $r_N = R_0 = R_1 + N(\Delta r)$. (45)

Since the difference in voltage is important and not the absolute value, $V(r_N)$ can be set to zero. Using the trapezoidal rule for integration,

$$\text{charge}(j) = \Delta r \left[r_0 (\rho_e(r_0) + \rho_-(r_0) + \rho_+(r_0))/2 + \sum_{k=1}^{j-1} r_k (\rho_e(r_k) + \rho_-(r_k) + \rho_+(r_k)) + r_j (\rho_e(r_j) + \rho_-(r_j) + \rho_+(r_j))/2 \right] . \quad (46)$$

$$V(r_0) = \Delta r \left[\frac{E(r_0)}{2} + \sum_{k=1}^{N-1} E(r_k) + \frac{E(r_N)}{2} \right] \quad (47)$$

$$= \Delta r \left[\left(\frac{1}{2} + \sum_{k=1}^{N-1} \frac{r_0}{r_k} + \frac{r_0}{2r_N} \right) E(r_0) + \frac{1}{\epsilon_0} \sum_{j=1}^{N-1} \frac{\text{charge}(j)}{r_j} + \frac{1}{\epsilon_0} \frac{\text{charge}(N)}{2r_N} \right]$$

$$E(r_0) = \frac{V(r_0)}{\Delta r} - \frac{\left[\frac{1}{\epsilon_0} \sum_{j=1}^{N-1} \frac{\text{charge}(j)}{r_j} + \frac{1}{\epsilon_0} \frac{\text{charge}(N)}{2r_N} \right]}{\frac{1}{2} + \sum_{k=1}^{N-1} \frac{r_0}{r_k} + \frac{r_0}{2r_N}} \quad (48)$$

$E(r_0)$ is the electric field on the surface of the inner conductor. Once that is known, the electric field everywhere can be found.

$$E(r_0) = \frac{1}{\epsilon_0} \frac{\text{charge}(j)}{r_j} + \frac{r_0}{r_j} E(r_0) \quad (49)$$

6. Results for Anode Corona

6.1 A Detailed Analysis of One Special Case

A set of numerically computed current as a function of voltage curves are shown in Figure 6.1. There are two common features in these results: an inner conductor of 1.5 cm radius and with photoionization as the only secondary mechanism. For clarity, a detailed analysis of a specific case is described below.

The outer radius is 4.5 cm. The mobility of positive and negative ions are $2.5 \text{ cm}^2/\text{sec-volt}$. Q is .005 based on data from Raether.¹⁹ μ_p is $.001 \text{ cm}^{-1}$ based on data from Figure 3.5.

$$\alpha/p = 1.44 \exp\left(-\frac{180}{E/p}\right) \quad \text{for } E/p \geq 40 \text{ volts/cm-mm Hg;} \quad (1)$$

$$\alpha/p = 8.2 \exp\left(-\frac{250}{E/p}\right) \quad \text{for } E/p < 40 \text{ volts/cm-mm Hg.} \quad (2)$$

The primary sources of electrons are 10 electron-ion pairs created per second per cm^3 by cosmic radiation, and no electrons coming through at the boundary of the outer radius. Recombination is neglected. This will be called the standard case because most of the others are variations from this one.

The horizontal axis of Figure 6.1 is the electric field at the surface of the inner conductor, E_0 , when the voltage is applied and space charge is non existant.

POSITIVE CORONA

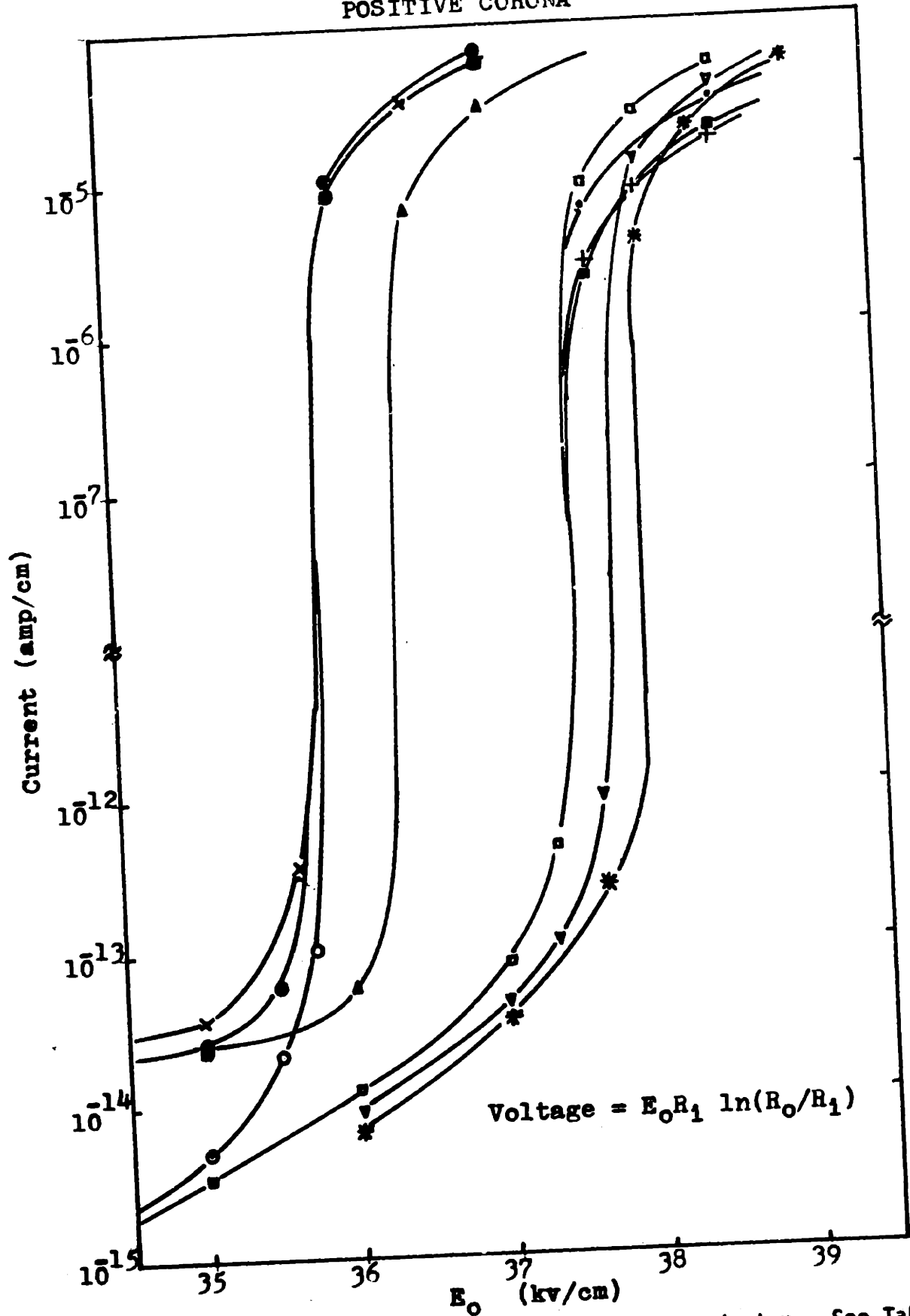


Figure 6.1 Sensitivity tests for 1.5cm inner conductor. See Table 6.1 for reference.

Table 6.1

Explanation for the Figure 6.1

1. - □ - Standard case with or without recombination term

The following are the same as the standard case with the exceptions specified below.

2. - ○ - $\mu_p = .01 \text{ cm}^{-1}$.

3. - × - $\mu_p = .01 \text{ cm}^{-1}$. $J_{e0} = 1 \times 10^{-15} \text{ amp/cm}^2$.

No cosmic radiation.

4. - Δ - $\mu_p = .01 \text{ cm}^{-1}$. $J_{e0} = 1. \times 10^{-15} \text{ amp/cm}^2$.

No cosmic radiation.

$\alpha/p = 8.2 \exp(-250p/E)$ for $E/p < 40$ volts/cm-mm Hg

5. - ● - $\mu_p = .01 \text{ cm}^{-1}$. $J_{e0} = 1 \times 10^{-15} \text{ amp/cm}^2$.

No cosmic radiation. $\Delta r = .005 \text{ cm}$

$\alpha/p = 8.2 \exp(-250p/E)$ for $E/p < 40$ volts/cm-mm Hg

6. - ▽ - η is increased by 10% for all E/p

7. - +- - $\mu_- = .8 \text{ cm}^2/\text{sec/volt}$

$\mu_+ = .8 \text{ cm}^2/\text{sec/volt}$

8. - . - $R_0 = 5.5 \text{ cm}$

9. - ■ - $R_0 = 7.5 \text{ cm}$

10. - * - α is decreased by 5% for all E/p

From field theory one knows that the electric field without space charge in this case has the form

$$E = K/r. \tag{3}$$

Therefore, the voltage applied between cylinders is

$$\begin{aligned} \text{voltage} &= K \ln(R_0/R_1) \\ &= E_0 R_1 \ln(R_0/R_1) \end{aligned} \tag{4}$$

To plot current against voltage is inconvenient because the curves cannot be compared when the outer cylinder's dimensions are changed.

For the standard case, when E_0 is below 37.5 kv/cm, the total current is below 10^{-12} amp/cm. The current decreases steadily as voltage is decreased. When the electric field at R_1 is slightly above 37.5 kv/cm. the current jumps above 10^{-6} amp/cm, and increases slowly again as voltage is increased. The voltage versus current curves are very similar to the ones measured by Miller in Figure 2.2. The electric field at which the current changes by many orders of magnitude is designated as the onset of positive corona for a given sized inner conductor. For all the cases tested, the onset is very sharp.

Consider the case $E_0 = 37$ kv/cm, below onset. Figure 6.2 shows the current densities as a function of position. For most of the region in between conductors, the current is carried by positive ions. The electron and negative ion current densities are roughly the same

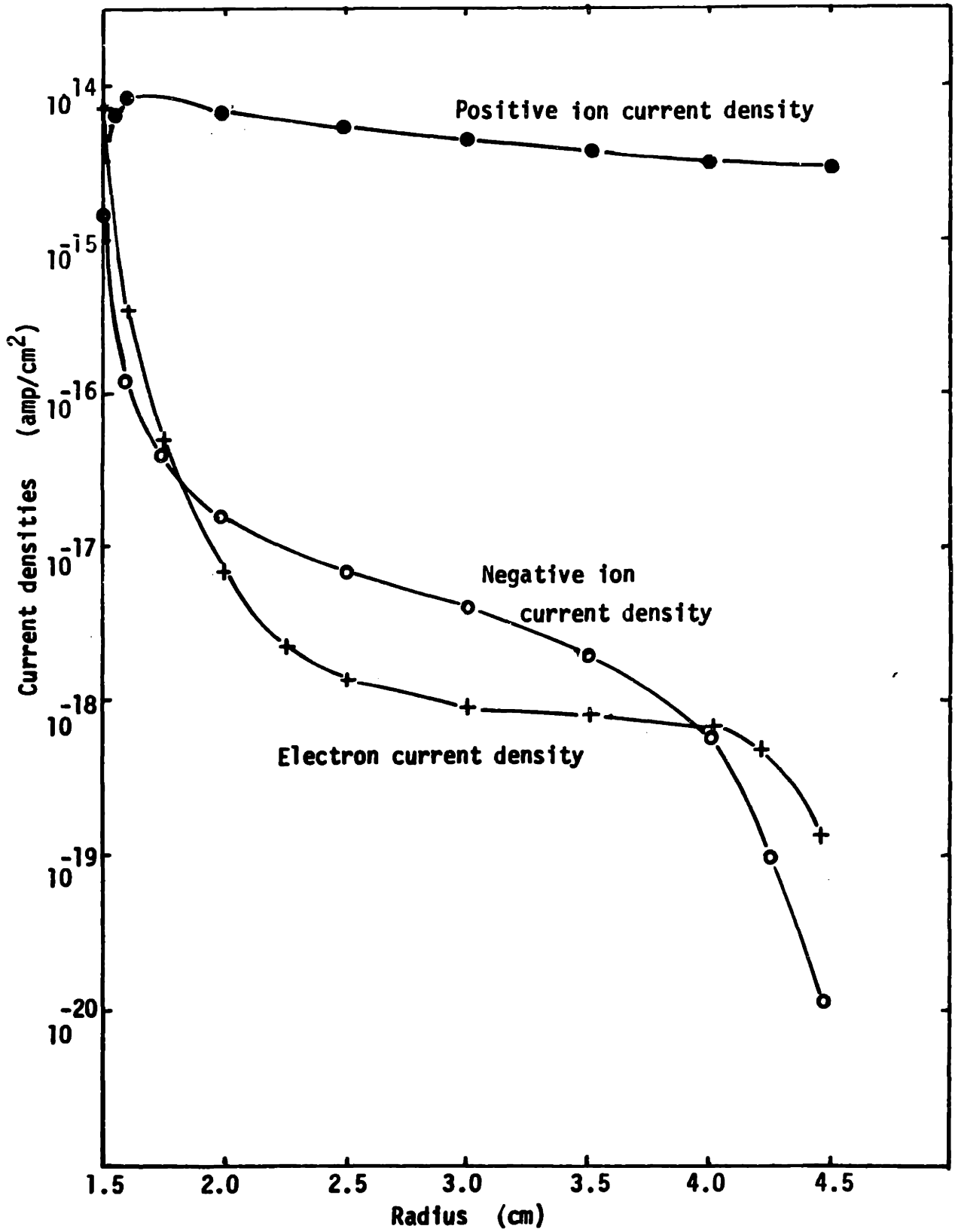


Figure 6.2 Current densities for $E_0 = 37$ kv/cm standard case.

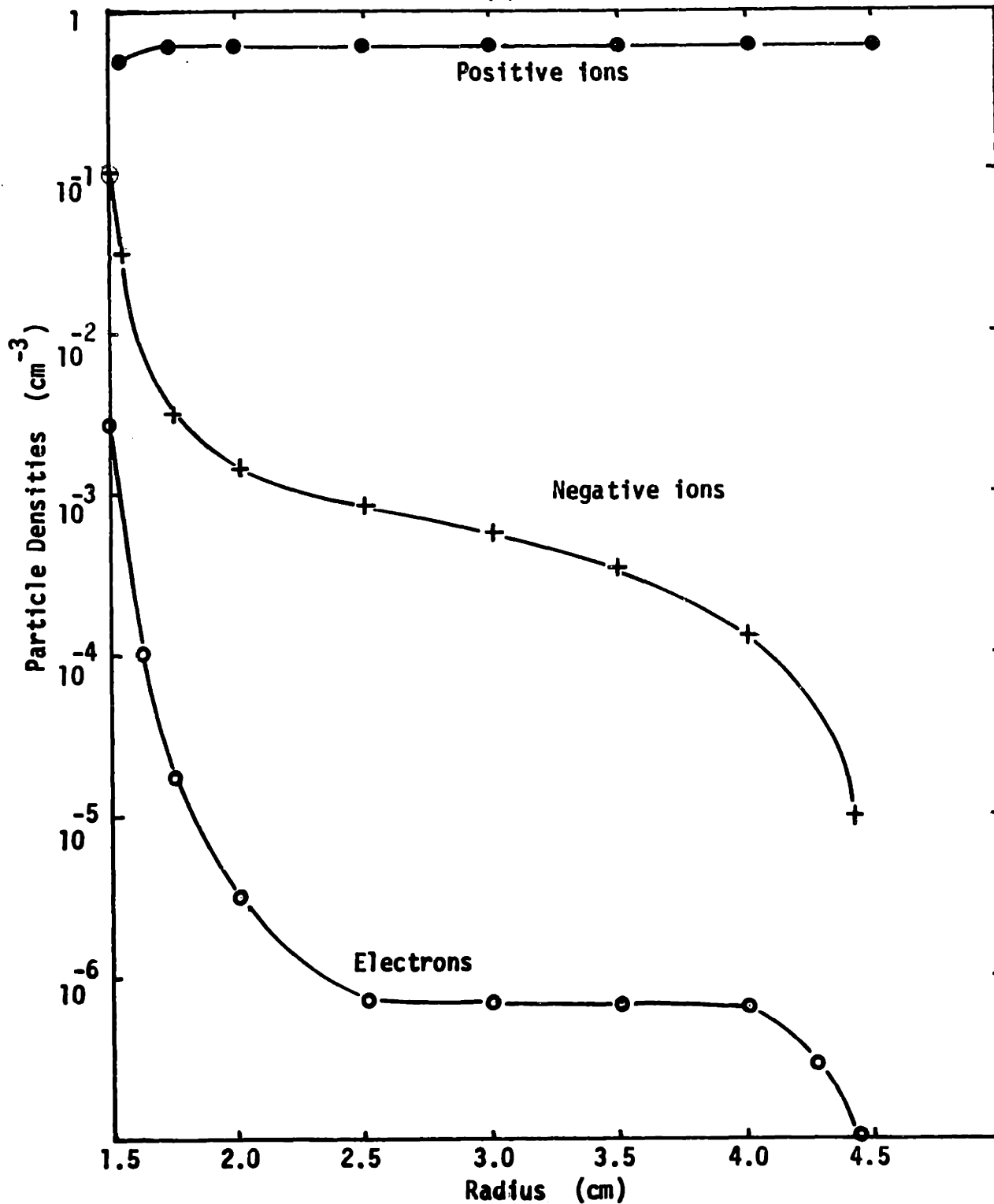


Figure 6.3 Particle densities for $E_0 = 37$ kv/cm standard case.

order of magnitude. There are two regions of interest: ionization versus attachment dominated. Figure 6.4 shows the values of α and η as a function of position. For this case, they cross around 2.35 cm from the center. At distances greater than 2.35 cm the electron current density stayed about the same. The negative ion current density increased as radius decreased. It could not increase by too much since free electrons are created too slowly. Attachment of electrons to neutrals provides a check on the growth of electrons. When electrons eventually drifted into the region of $\alpha > \eta$, their number starts to increase sharply.

Figure 6.3 shows the charge densities. Negative ions are important only in a very small region roughly 1 mm thick on the surface of anode, while the rest of the space between conductors is occupied by positive ions. Electrons are insignificant because of their large velocity. Compare the case above to the results of higher applied electric field, $E_0 = 38$ kv/cm, above the onset. The shape of the current densities and charge densities are roughly the same as the previous case. See Figures 6.5 and 6.6. However, they are many orders of magnitude larger. Figure 6.4 shows that η as a function of radius barely changed. α changed only slightly also. This slight change provides a gain greater than one in the feedback loop, resulting in changing the magnitudes of current

Figure 6.4 Values of α and η as a function of position for two different applied voltages.

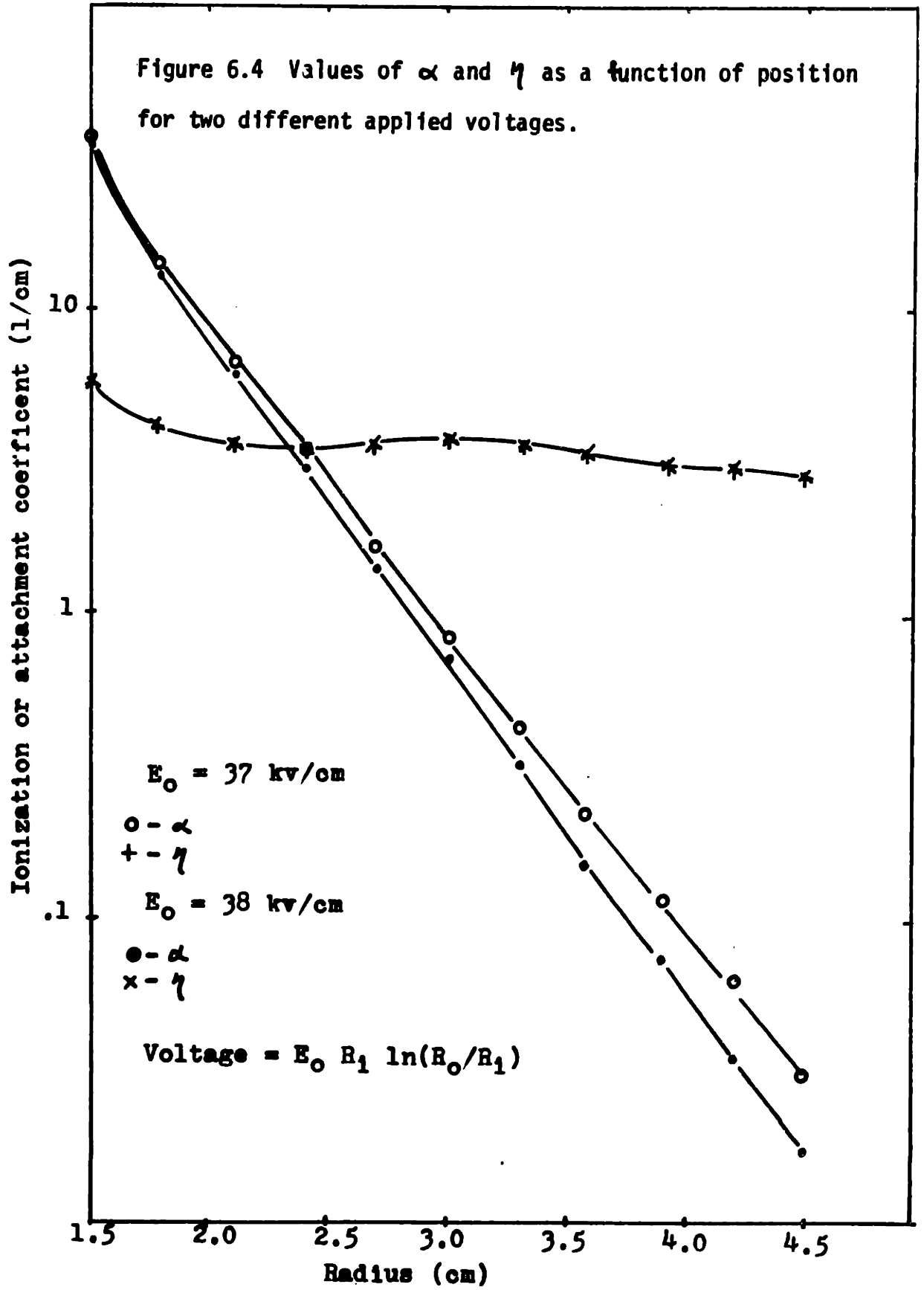
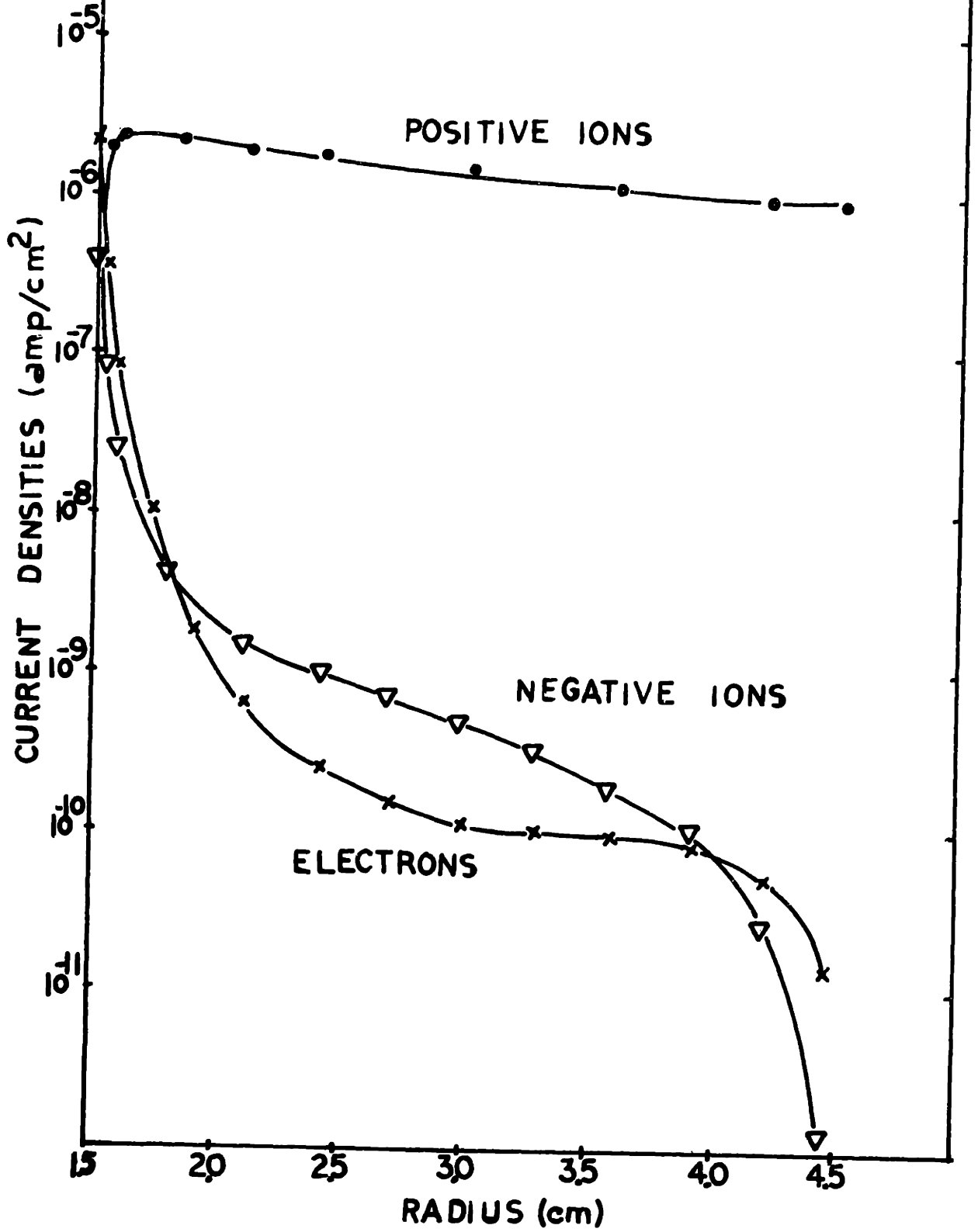
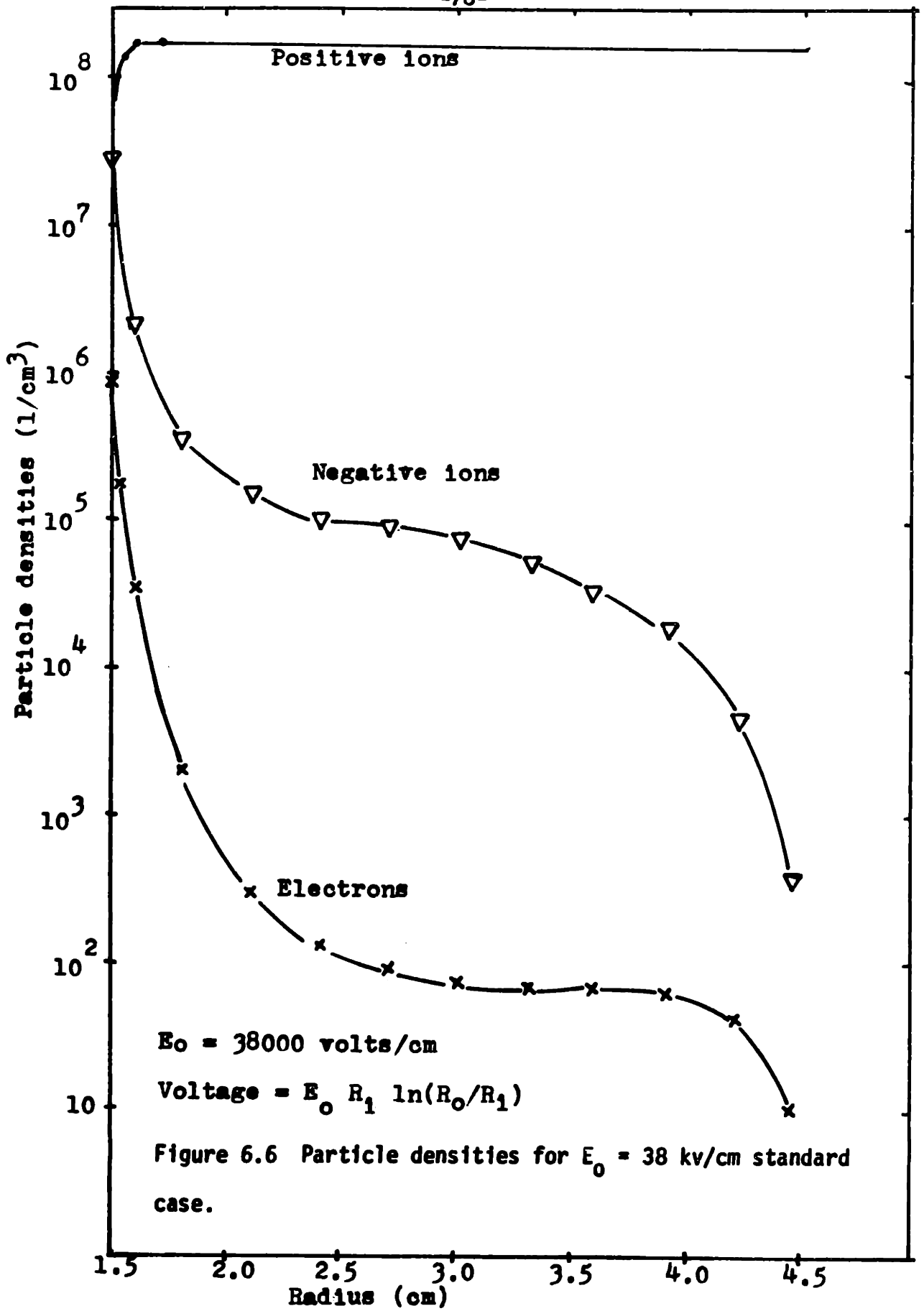


Figure 6.5 Current densities for $E_0 = 38$ kv/cm standard case.





densities by many orders of ten.

The fact that the currents stayed at some finite value after onset means that the space charge has modified the electric field to such an extent the current could not grow unbounded. Below onset the charge densities are too low. The electric field remained as a function of K/r . Figure 6.7 shows the change of the electric field from the K/r field as a function of position for four separate applied voltages. The decrease of electric field near the conductor is known as choking. The deviation is larger for higher applied voltage.

6.2 Electron Current Density Boundary Condition

The standard case had zero electron current density as a boundary condition on the outer radius. If a small electron current density is assumed, the onset and the current densities above onset are unchanged. The current densities below onset level off to a relatively constant value as voltage is decreased. For comparison, see cases 2 and 3 in Figure 6.1.

6.3 Numerical Accuracy

The numerical method used is accurate only when the grid spacing is made very small. The main source of error introduced is in the integration in the high E/p region near the conductor, and possibly in the calculation of the electric field.

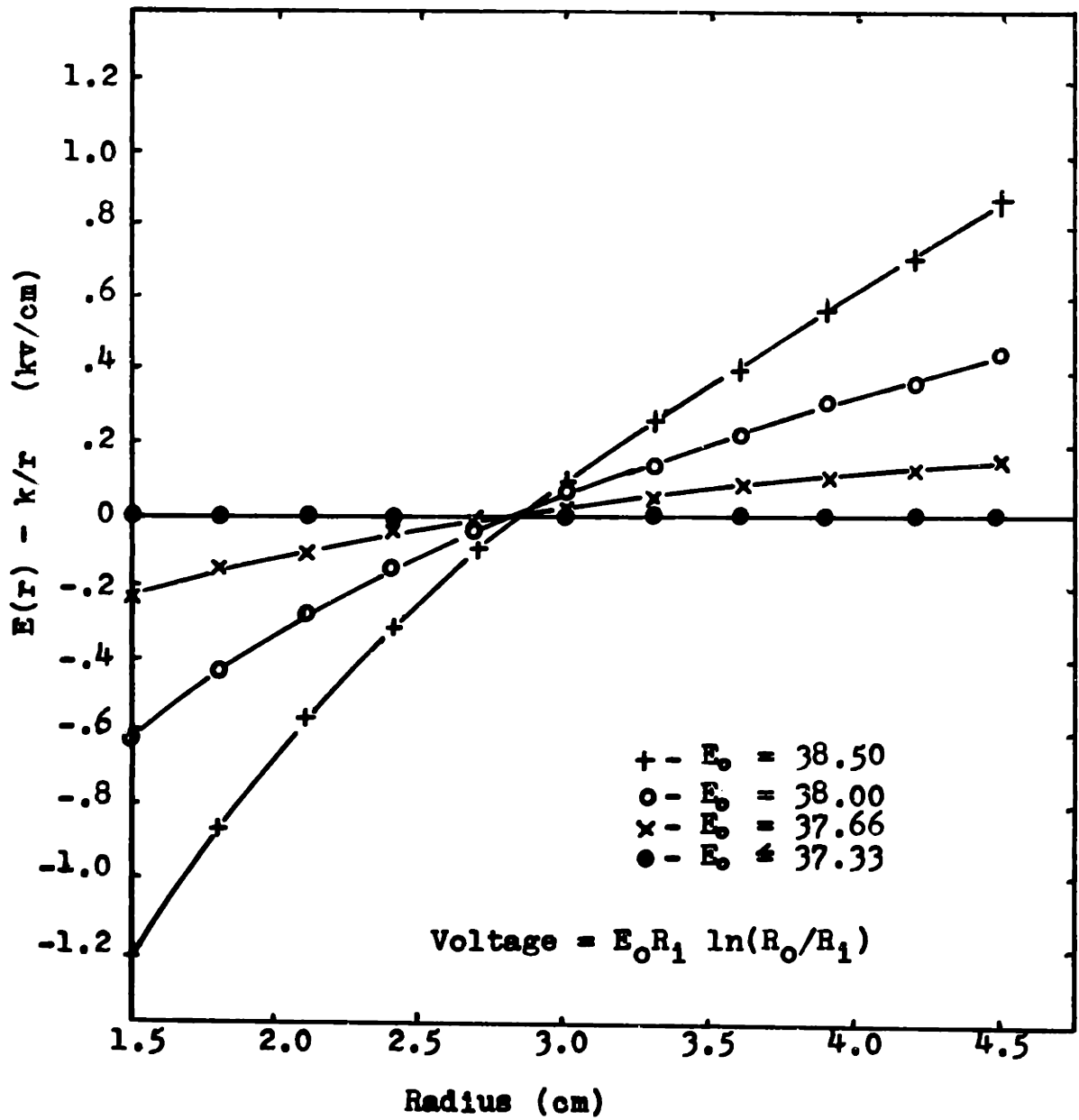


Figure 6.7 Deviation of the electric field from the K/r field as a function of position for different applied voltages.

The current is a very sensitive function of α , and α , in turn, is a very sensitive function of the electric field. Trapezoidal rule is used for numerical integration for the calculation of the electric field and it is only a first order method. This is the only method usable without undue labor.

The test case for accuracy was not performed on the standard case but with the following changes

$$\alpha/p = 8.2 \exp\left(-\frac{250}{E/p}\right) \quad (5)$$

for the whole E/p region, and $\mu_p = .01 \text{ cm}^{-1}$. For an applied voltage of 60973 volts, equivalent to an E_0 of 37 kv/cm at 1.5 cm radius, the calculated voltage is 120 volts higher than the applied for grid size of .01 cm. When the grid size is decreased by half to .005 cm, the error in voltage calculation also decreased by half to 60 volts above the applied. For the .01 cm grid size, the electric field is in error by at most one place in the fifth digit.

The critical onset electric field calculated is approximately at 36.3 kv/cm for the .005 cm grid size case. However, the .01 cm grid size will be used in all other calculations for a 1.5 cm radius anode because decreasing the grid size by half more than doubled the cost of a calculation.

The way to increase accuracy at the same cost is to have variable grid sizes in r , by making a transform-

ation. Let

$$r = f(x). \quad (6)$$

Pick an appropriate function f , such that equal spacing in x will produce more concentrated grids in r in the region of higher E/p . See Figure 6.8. For this study, however, the main objective was devoted to examining the effect of different parameters. The program in its present state will provide the necessary information.

6.4 Rate of Convergence and Stability*

When the applied voltage results in a surface electric field on the inner conductor at a few kv/cm below the critical onset value, the convergence rate is very fast, requiring only three or four iterations. The rate of convergence becomes slower as the critical electric field is reached. See Figure 6.9. The worst situations occur when E_0 is within 1/4 kv/cm above the critical electric field. The climb is slow because the gain is only slightly greater than 1. Sometimes two or three hundred iterations are needed for convergence. It is for these cases, that a relaxation parameter becomes useful. Normally, the relaxation parameter is set to 1. Making it larger than 1, effectively increases the constant Q and

* Material in this section is true for both positive and negative corona cases.

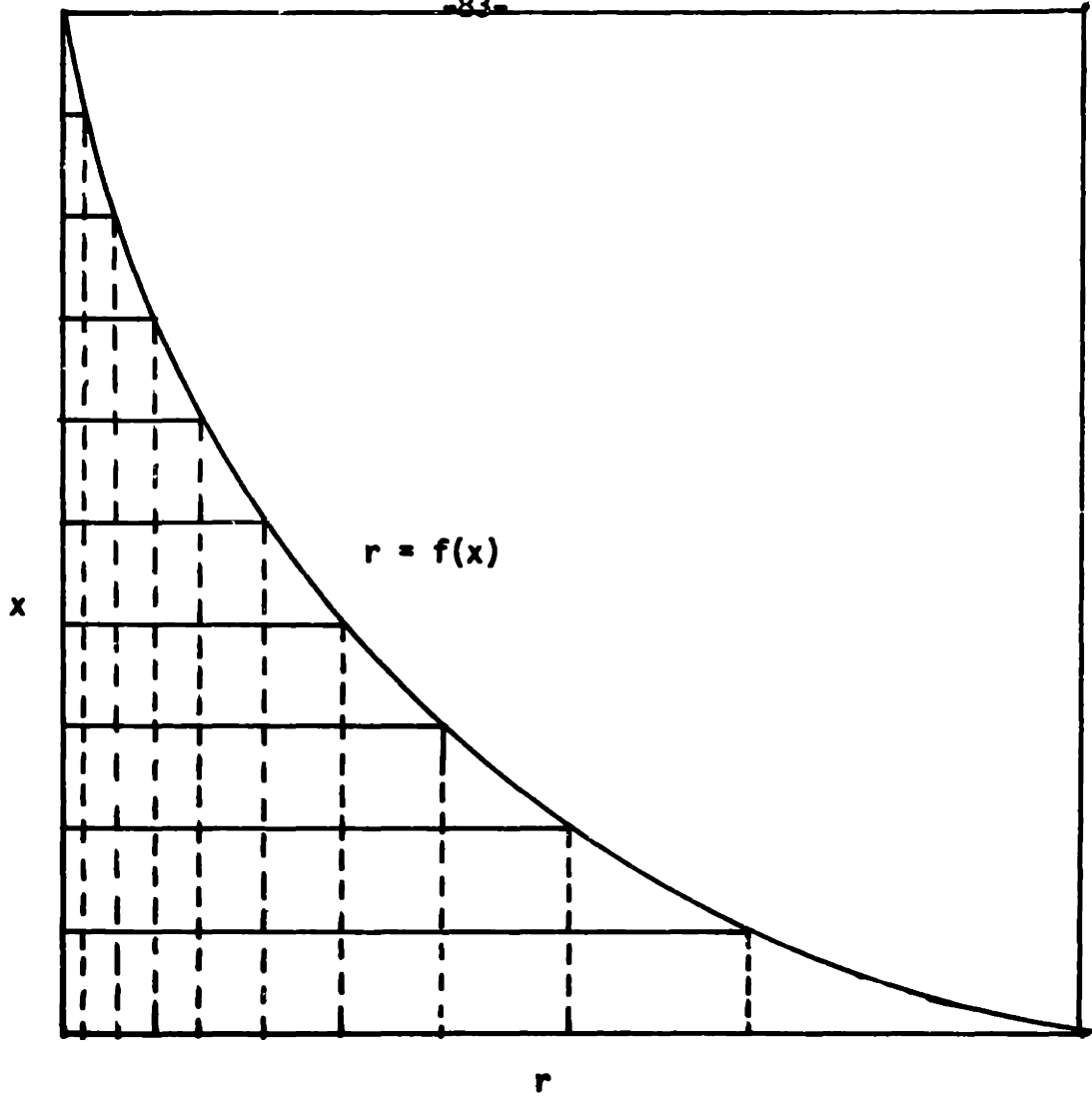


Figure 6.8 With the transformation, $r = f(x)$, equal spacing in x will give variable spacing for r .

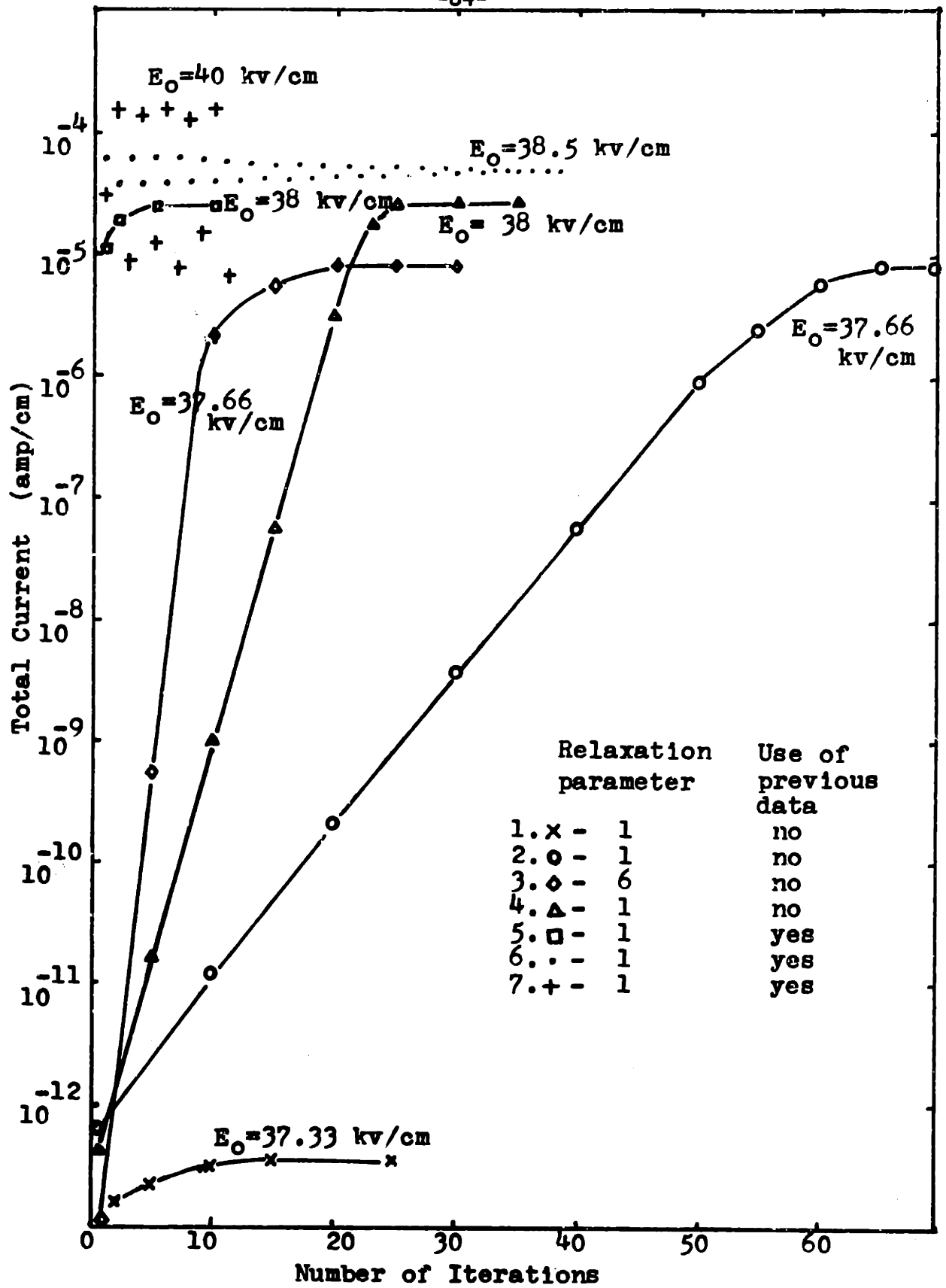


Figure 6.9 Rate of convergence illustrated by the total current at the end of each iteration for the standard case.

and lowers the onset. So in effect, it is the same as moving out of the region of slow convergence. When the current reaches an estimated value, the parameter is set back to 1. Convergence again becomes slow. Case 2 in Figure 6.9 shows that more than 70 iterations are needed for convergence. At the same applied voltage with the relaxation parameter set at 6 and the current estimate set at 10^{-6} amp/cm, the number of iterations required is reduced by more than half.

Another way to speed up convergence is to use data from the previous case. There are two plots of $E_0 = 38$ kv/cm in Figure 6.9. One started when there is no initial space charges. The number of iterations to reach the final value is large. The other case used the space charge distribution from $E_0 = 37.667$ kv/cm. The results converged in a few iterations.

When the applied voltage is increased even higher so that E_0 is in a very narrow neighborhood of 1 kv/cm above the critical electric field, the rate of convergence again becomes very slow. This time the cause is due to problems associated with stability. Look at the case $E_0 = 38.5$ kv/cm in Figure 6.9. The current oscillates about the final value. The reason is that associated with an initially large current there is a large positive space charge distribution, which in turn reduces the electric field. The reduced electric field gives a smaller current

density and space charge density. The electric field near the anode goes back toward the value of unperturbed electric field. The process repeats. Each time the current and the electric field get a little closer to the final value.

If the applied voltage is increased to an even larger value, the solution diverges. The equations try to over stabilize the situation. The current oscillates further and further apart as the iterations are increased. See the case $E_0 = 39$ kv/cm in Figure 6.9.

6.5 Effect of R_0

Peek observed that the size of the outer conductor did not change the critical onset values. This is confirmed by changing the radius of the outer cylinder from 4.5 cm, to 5.5 cm and to 7.5 cm. See Figure 6.1. However, the size of the outer cylinder does effect the electric field and the magnitude of the current after onset. Figure 6.10 is a graph of the current densities when the outer cylinder radius is 7.5 cm. The shape of the curves are very similar to the standard case. Figure 6.11 shows the effect of space charges on the electric field for different outer cylinder radii with voltages set such that E_0 is 38.5 kv/cm. Increasing the radius of the outer cylinder decreases the current above onset. It is consistant with the electric field, because

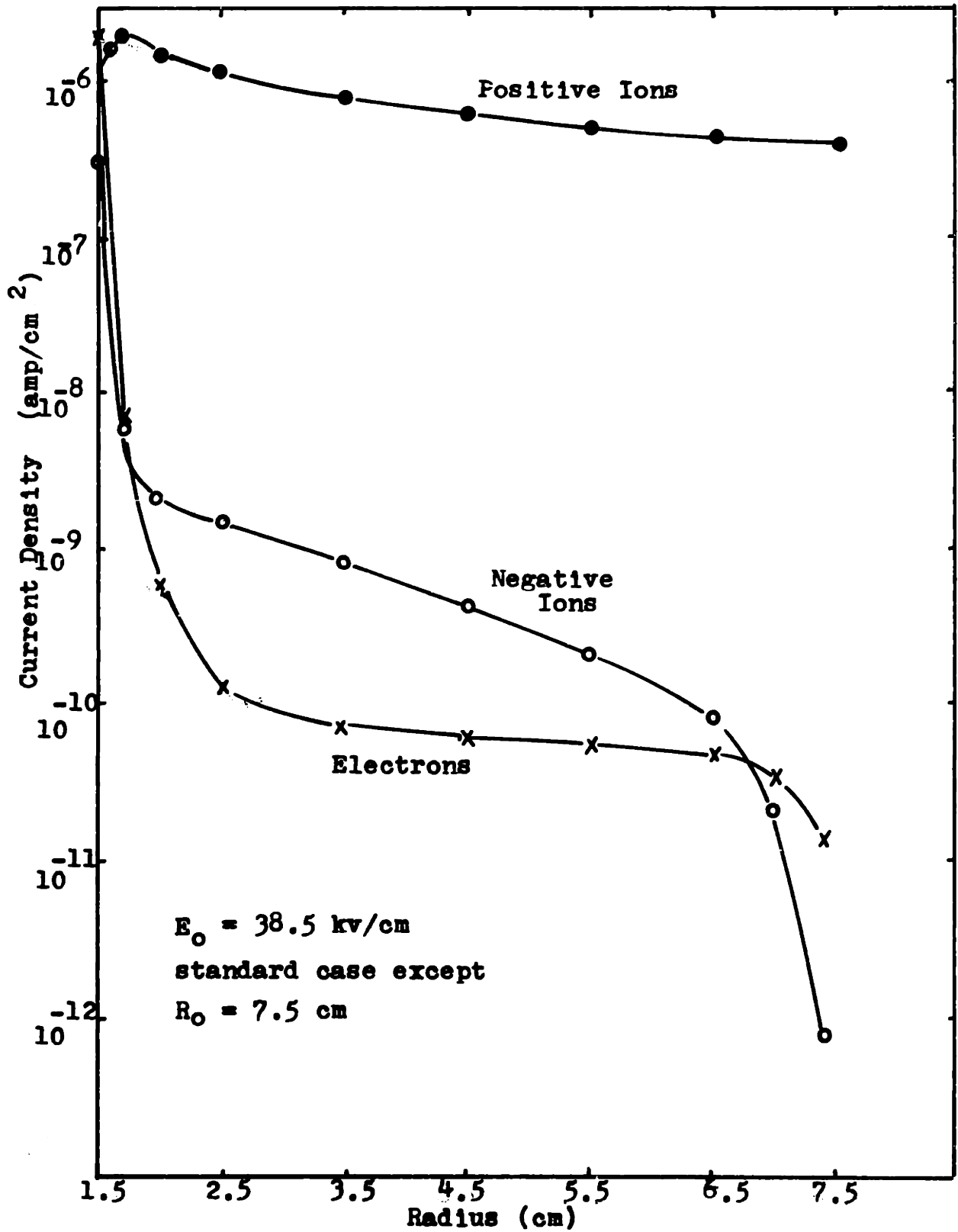


Figure 6.10 Current density when the radius of the outer cylinder is changed to 7.5 cm.

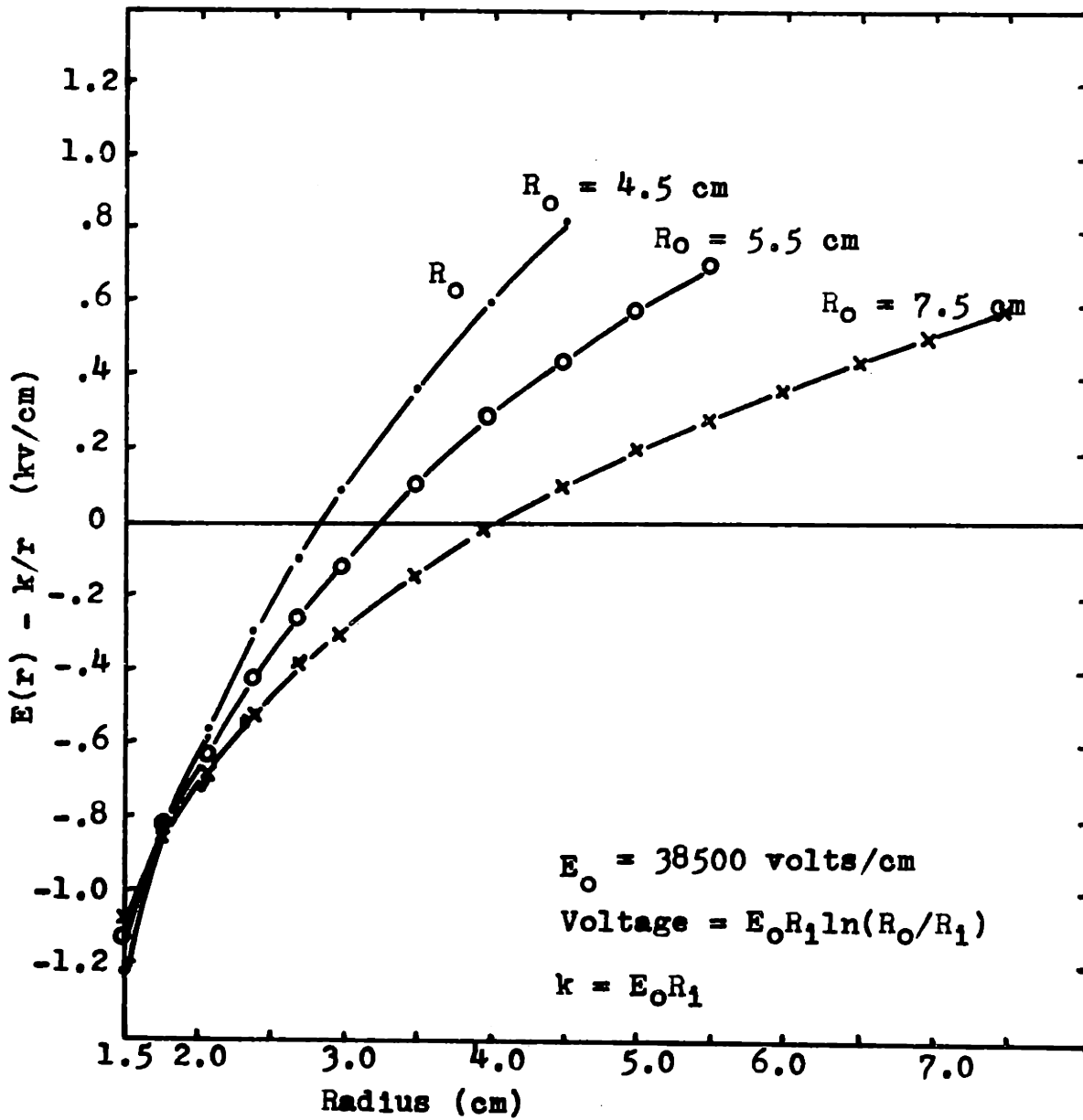


Figure 6.11 The effect of the dimension of the outer cylinder on the electric field.

larger outer cylinder radii results in a larger region where the electric field fell below the K/r field near the anode.

6.6 Modifying Alpha

The value of α is very important and its effects show up in almost every aspect. Let alpha decrease by 5% for all E/p . The onset increases by about $\frac{1}{2}$ kv. This is expected without even going through the calculations, because decreasing the α curve by 5% is the same as moving the curve to the higher E/p region, in this case to the right, by approximately $\frac{1}{2}$ kv.

In the region of $E/p < 40$ volts/cm-mm Hg, the data on α measured by different experimentalists do not have good agreement. One would like to see how important are these variations. The first case was done with the parameters of the standard case except $\mu_p = .01$ cm⁻¹. The onset is about 35.8 kv/cm. Then α is fitted by

$$8.2p \exp(-250p/E) \quad (7)$$

For all E/p . This lowers the value of α for the region $E/p < 40$ volts/cm-mm Hg. With μ_p still set at $.01$ cm⁻¹, the onset increases to 36.3 kv/cm. There is about half a kilovolt difference. In section 6.12, another effect as a result of modifying α will also be pointed out.

6.7 Modified η

Attachment is not only a process of increasing the negative ion current density. It also effectively decreases α . If attachment is increased by 10% for all the E/p values, the onset increases from 37.5 kv/cm of the standard case to 37.75 kv/cm. See case 6 of Figure 6.1.

Compare the current densities of Figure 6.12 to Figure 6.5. They both have the same applied voltage. The increase in attachment did not increase the negative ions by any noticeable amount relative to electron current density. The effect is just moving all current densities lower due to a net decrease in free electrons.

The experimental variations on η are more than $\pm 10\%$ of the fitted curve. That means the onset could be more than $\frac{1}{2}$ kv/cm off just due to uncertainties in η . This error is on the same order of magnitude as the others observed so far.

6.8 Modifying μ_p and Q

The absorption rate of photons by gas molecules is not a very well defined quantity. It depends on the energy of the photons, which in turn depends on the value of E/p and the type of gas molecules. If μ_p is increased by a factor of 10 to $.01 \text{ cm}^{-1}$, the critical onset field changes from 37.5 kv/cm of the standard case to 36.3 kv/cm. See

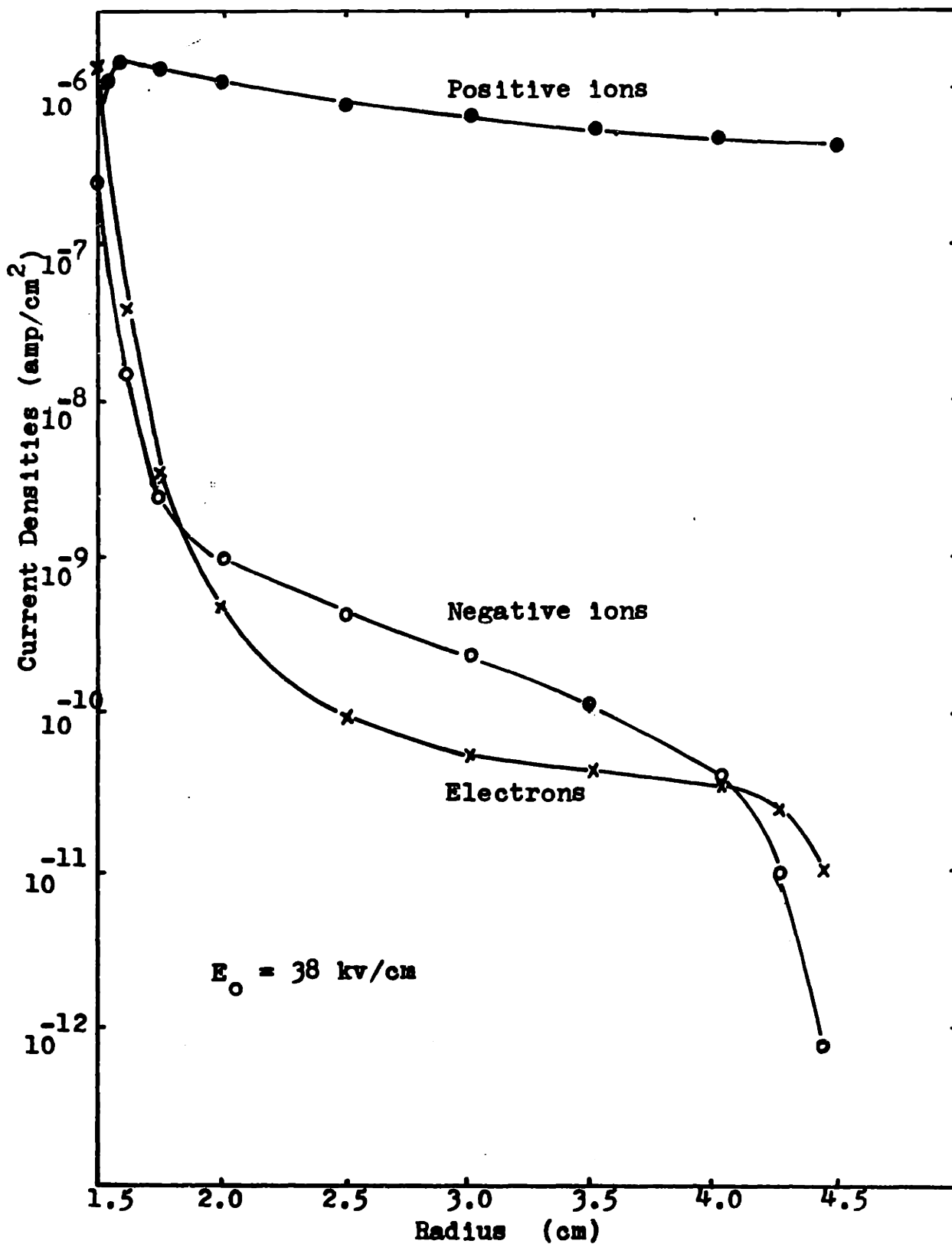


Figure 6.12 The effect of increasing the attachment coefficient for all E/p by 10% on the current densities.

Figure 6.1. For the large variations in μ_p as shown in Figure 3.5, this can be one of the most important factor on the critical onset electric field.

Figure 6.13 shows the calculated photoionization term as a function of position. The shape between $\mu_p = .01 \text{ cm}^{-1}$ and $\mu_p = .001 \text{ cm}^{-1}$ is not very different and stayed relatively constant over most of the region. The reason is that the photon density decays according to

$$\exp(-\mu_p r) \quad (8)$$

and $\mu_p r \ll 1$ in both cases. If μ_p is a larger number, the photoionization will have a noticeable peak close to the anode.

6.9 Mobility

The velocities of charged particles are a function of the humidity in air. The change of velocity of the electron is unimportant because its charge density is many orders smaller than both positive and negative ions.

In dry air the mobility of positive ions is $2.85 \text{ cm}^2/\text{sec-volt}$. The mobility decreases steadily for humid air. For water vapor the ion mobility is as low as $.8 \text{ cm}^2/\text{sec-volt}$. See Figure 6.1 for the result when mobility of both positive and negative ions are set to $.8 \text{ cm}^2/\text{sec-volt}$. The critical onset field did not change, but the current after onset decreased in value. A smaller mobility means a greater charge density, which in turn modifies the

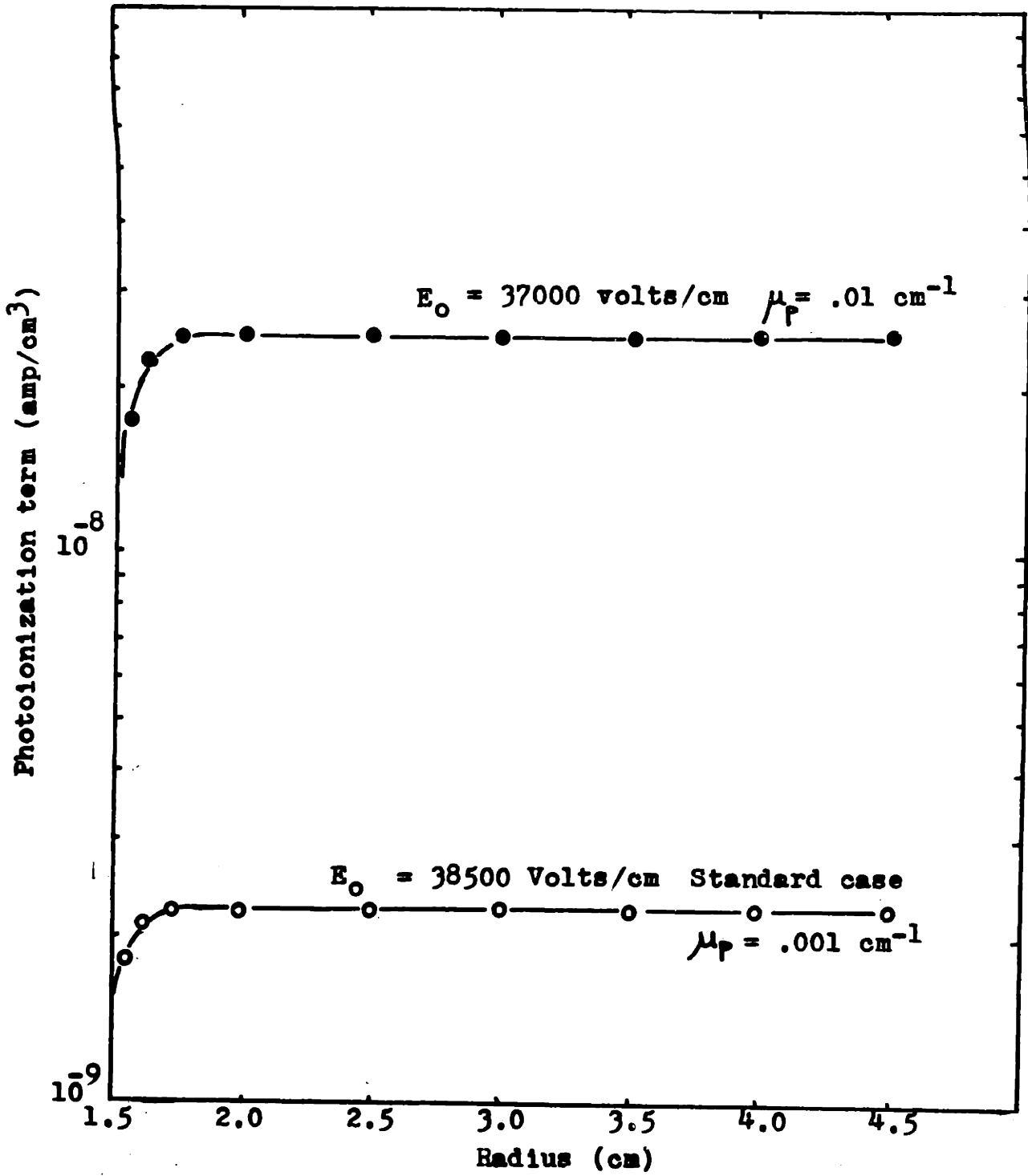


Figure 6.13 The photoionization term as a function of position.

electric field more. The final solution shows that the electric field differed from the case mobility is 2.5 cm²/sec-volt only in the sixth significant figure. However, it is enough to reduce the total current by 60% for some voltages.

6.10 Recombination

When there is recombination, the continuity equations become

$$\nabla \cdot \vec{J}_e = -(\alpha - \eta) J_e - 10q - Ph \quad (9)$$

$$\nabla \cdot \vec{J}_- = -\eta J_e + \beta p_- p_+ / q \quad (10)$$

$$\nabla \cdot \vec{J}_+ = \alpha J_e + 10q + Ph - \beta p_- p_+ / q \quad (11)$$

where β is the recombination constant of positive and negative ions.

$$\beta = 2.3 \times 10^{-6} \text{ cm}^3/\text{sec.} \quad (12)$$

Figure 6.14 has plots of each of the terms on the right hand side of the continuity equations for the standard case with $E_0 = 38$ kv/cm. The recombination term is much smaller than all other terms. Numerical results in Figure 6.1 confirm that recombination is unimportant.

6.11 Diffusion

Diffusion, another primary process mentioned, will also be proven to be unimportant. The current due to diffusion has the form

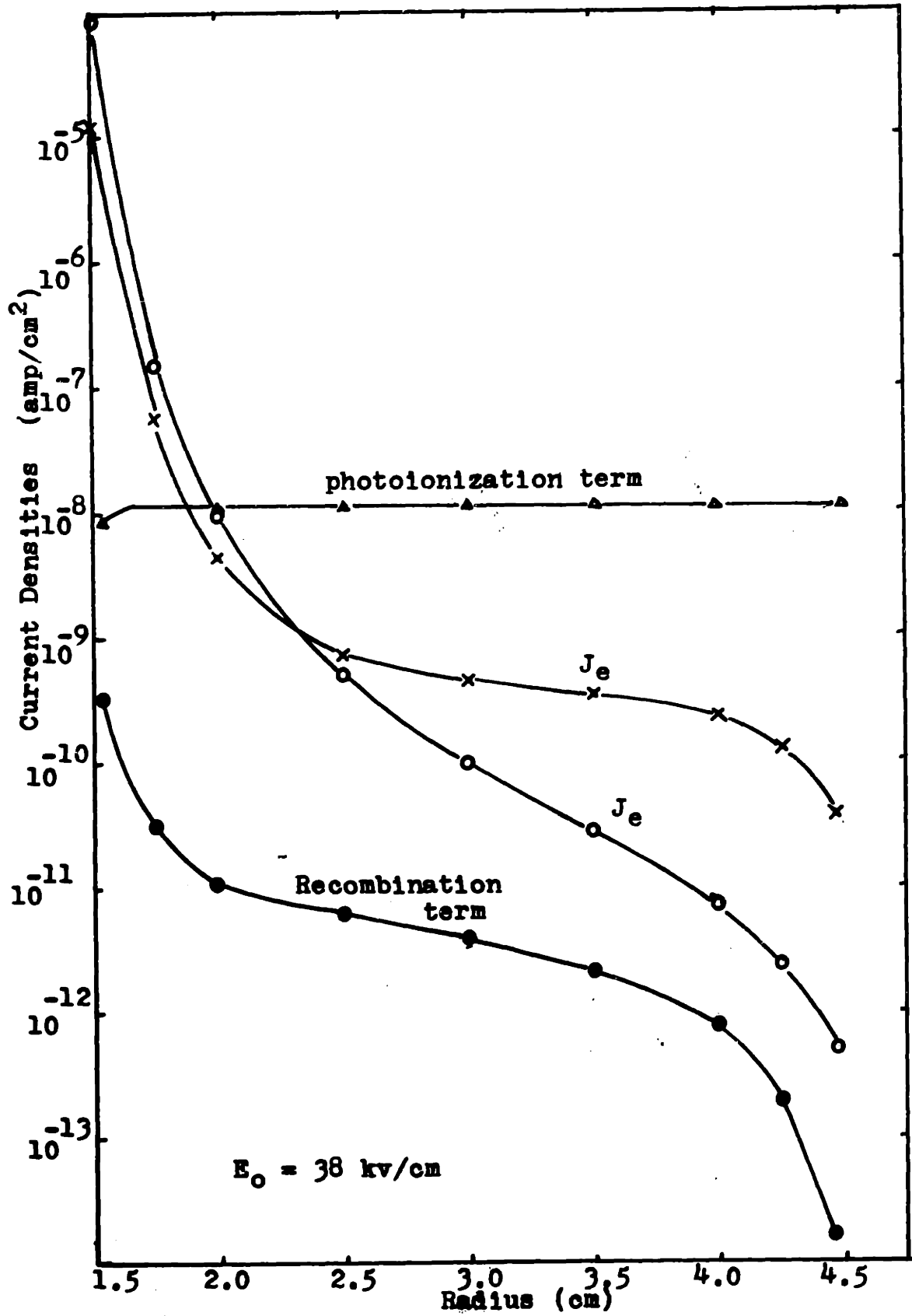


Figure 6.14 Comparing the recombination term to other terms.

$$\vec{j} = - (D_e \nabla \rho_e + D_+ \nabla \rho_+ + D_- \nabla \rho_-). \quad (13)$$

The steepest gradients of all the charge densities occur at the surface of the anode. With

$$\begin{aligned} D_e &= 400 \quad \text{cm}^2/\text{sec} \\ D_- &= .043 \quad \text{cm}^2/\text{sec} \\ D_+ &= .03 \quad \text{cm}^2/\text{sec} \end{aligned} \quad (14)$$

The diffusion current at the largest is only about 5×10^{-11} amp/cm length of wire, for the standard case at $E_0 = 38$ kv/cm. This is much smaller than the calculated total current, 2.5×10^{-5} amp/cm of length.

6.12 Variations on Anode Size and Comparison of Results to Peek's Formula

A set of voltage versus current curves for 2.0 cm, 1.0 cm, .5 cm and .2 cm anode radius with all other input parameters the same as the standard case, are plotted in Figures 6.18, 6.17, 6.16 and 6.15 respectively. Their onset values are plotted with Peek's formula in Figure 6.19. The agreement is poor. In section 5.4, the calculations showed that the curves will agree better if α had a steeper slope as function of E/p . With μ_p fixed at $.01 \text{ cm}^{-1}$ one case was tested for .2 cm radius anode with

$$\alpha/p = 8.2 \exp(-250p/E). \quad (15)$$

Along with the point at 1.5 cm radius, extrapolations show that the general shape agrees with Peek's formula

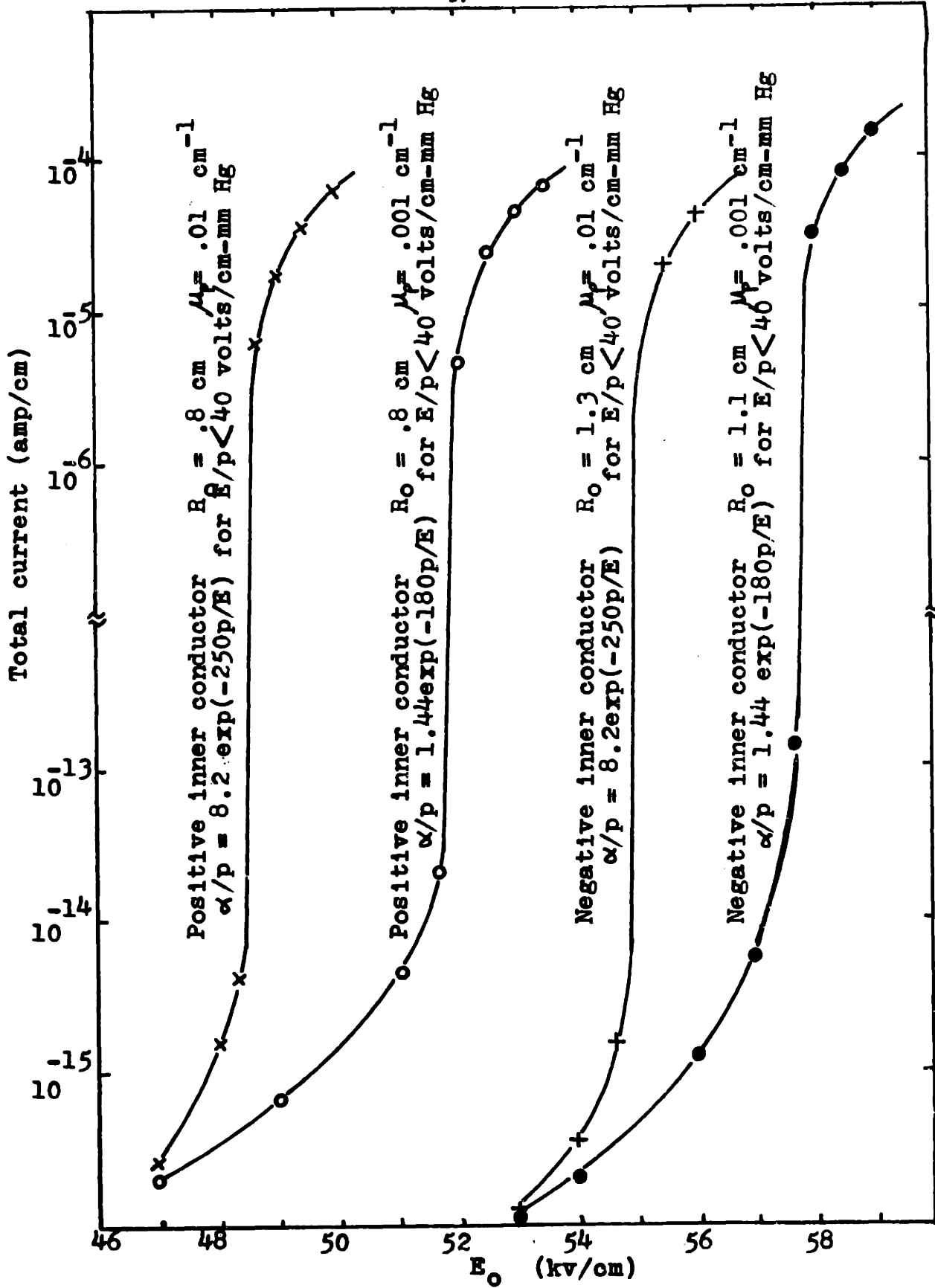


Figure 6.15 Current as a function of the applied voltage when the radius of the inner conductor is .2 cm.

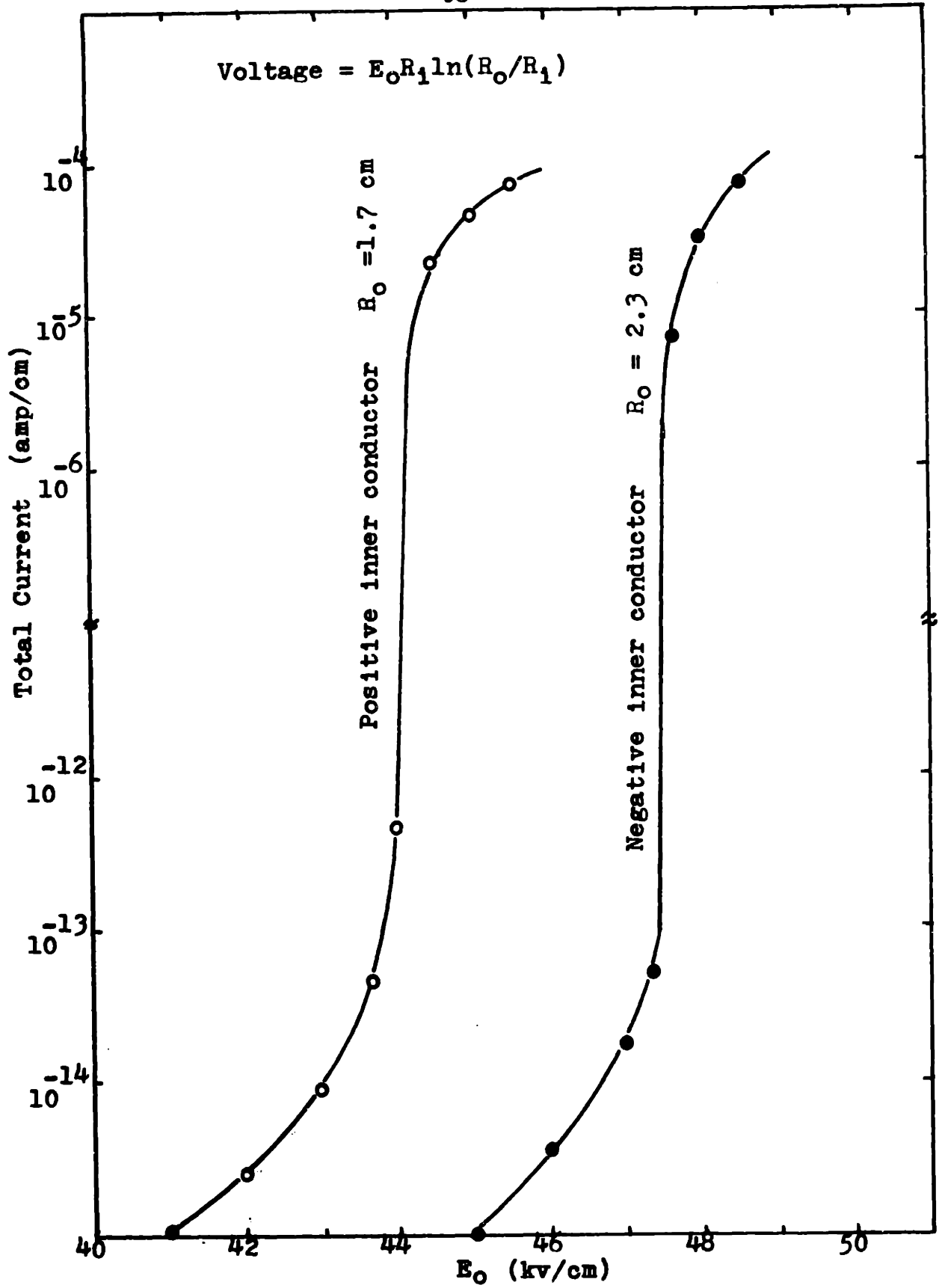


Figure 6.16 Current as a function of the applied voltage when the radius of the inner conductor is .5 cm.

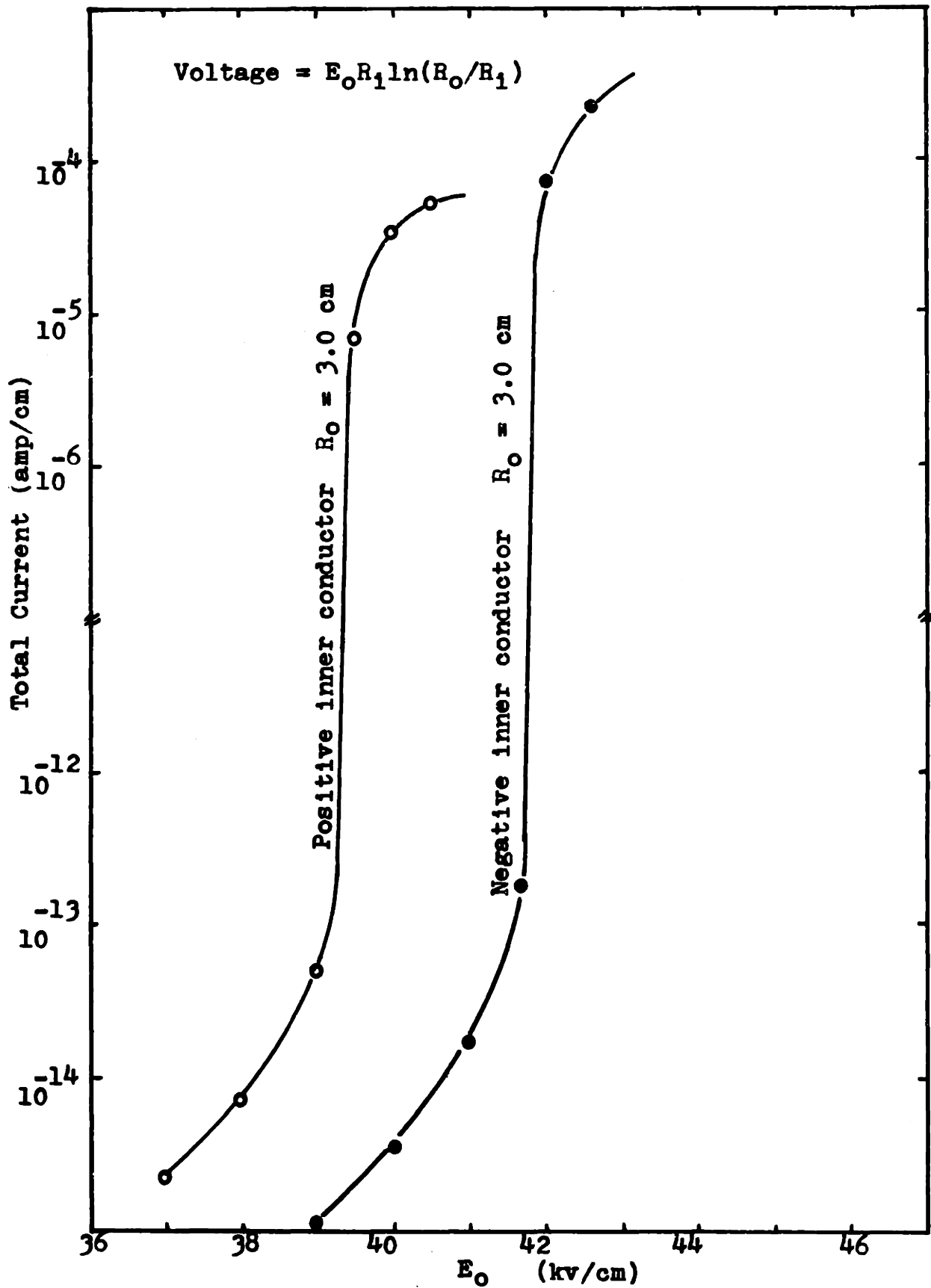


Figure 6.17 Current as a function of the applied voltage when the radius of the inner conductor is 1.0 cm.

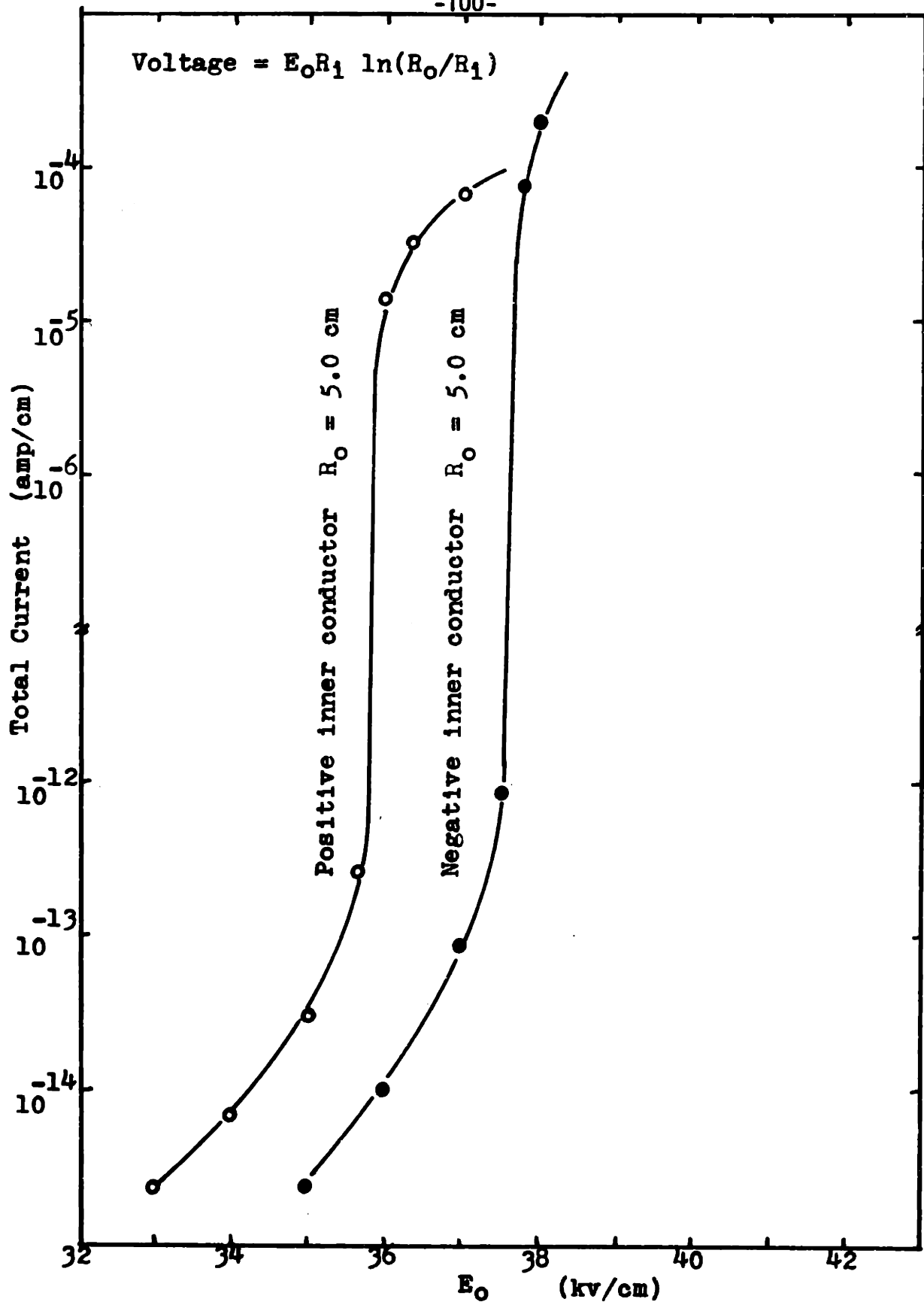


Figure 6.18 Current as a function of the applied voltage when the radius of the inner conductor is 2.0 cm

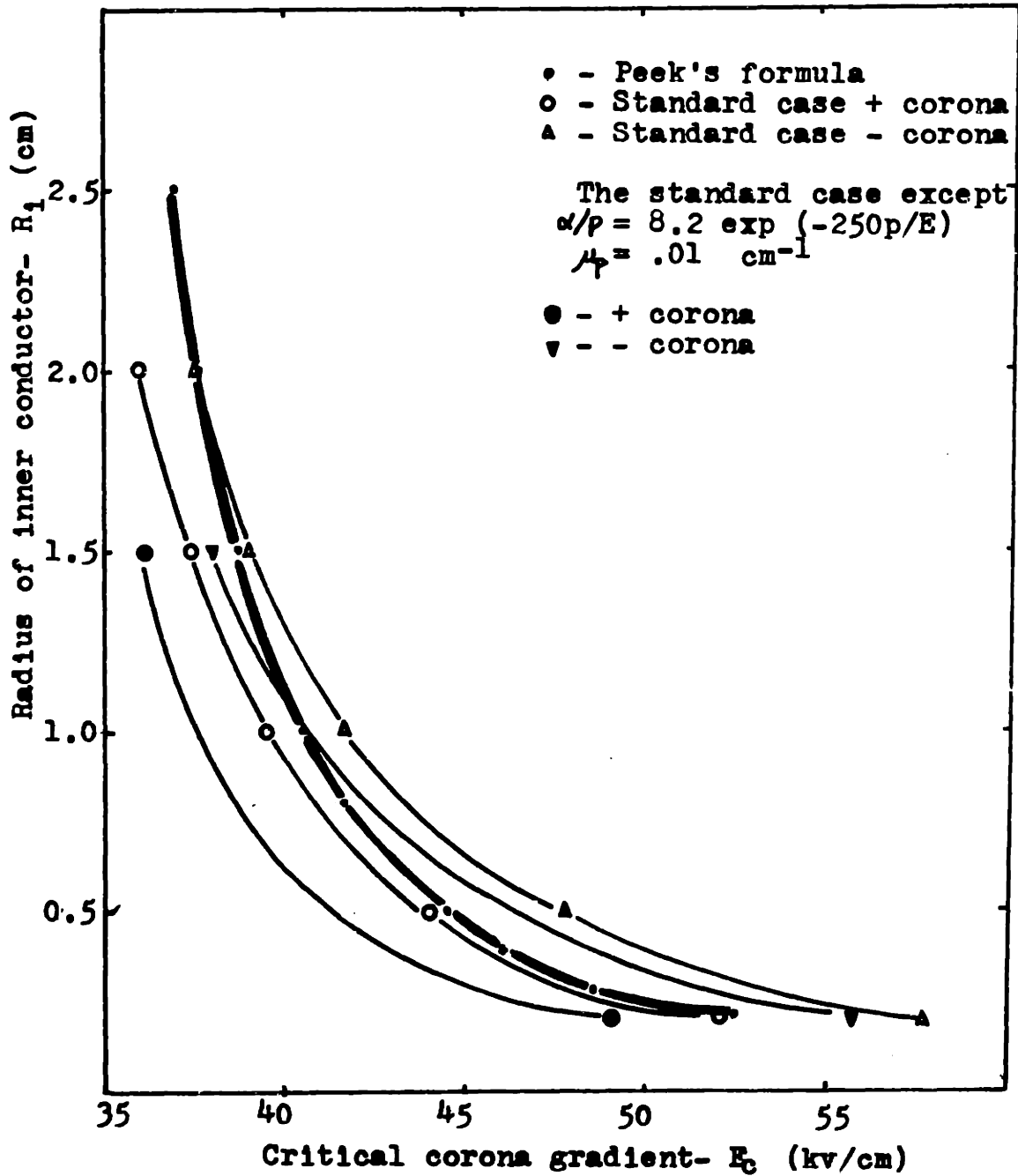


Figure 6.19 Comparison of results to Peek's Formula

but lower values for critical onset field.

If α is assumed to be correct. A curve similar to Peek's could also be obtained if μ_p is allowed to have larger values for smaller anode. Figure 3.5 shows that μ_p is indeed a strongly increasing function of E/p , and supports the above assumption.

7. Model for Negative Corona

7.1 Derivation of Equation without Feedback

All the assumptions stated in the beginning of the anode corona section hold for the cathode corona case as well. The geometry is the same, but the polarity of the voltage is switched. Consequently

$$\vec{E}(r) = E(r)\hat{i}_r = -|E(r)|\hat{i}_r \quad (1)$$

$$\vec{J}(r) = J(r)\hat{i}_r = -|J(r)|\hat{i}_r \quad (2)$$

where $|E(r)|$ and $|J(r)|$ are magnitudes of electric field and of current densities respectively.

Without any kind of feedback mechanisms, the derivation of the continuity equations follow the same approach as in the positive corona case. See Figure 7.1.

$$r\Delta r(\nabla \cdot \vec{J}_e) = (r+\Delta r)|J_e(r+\Delta r)|(-\hat{i}_r) \cdot (\hat{i}_{n1}) \quad (3)$$

$$+ r|J_e(r)|(-\hat{i}_r) \cdot (\hat{i}_{n2})$$

$$= r|J_e(r)| - (r+\Delta r)|J_e(r+\Delta r)|$$

$$|J_e(r)| = |-\rho_e(r)\mu_e E(r)| \quad (4)$$

$$= q n_e(r)\mu_e |E(r)|$$

To first order

$$r\Delta r(\nabla \cdot \vec{J}_e) = q\mu_e |E(r)| (r n_e(r) - (r+\Delta r)n_e(r+\Delta r)) \quad (5)$$

Due to Townsend ionization and attachment processes,

$$(r+\Delta r)n_e(r+\Delta r) - r n_e(r) = (\alpha(r) - \eta(r))n_e(r)r\Delta r.$$

So

$$(6)$$

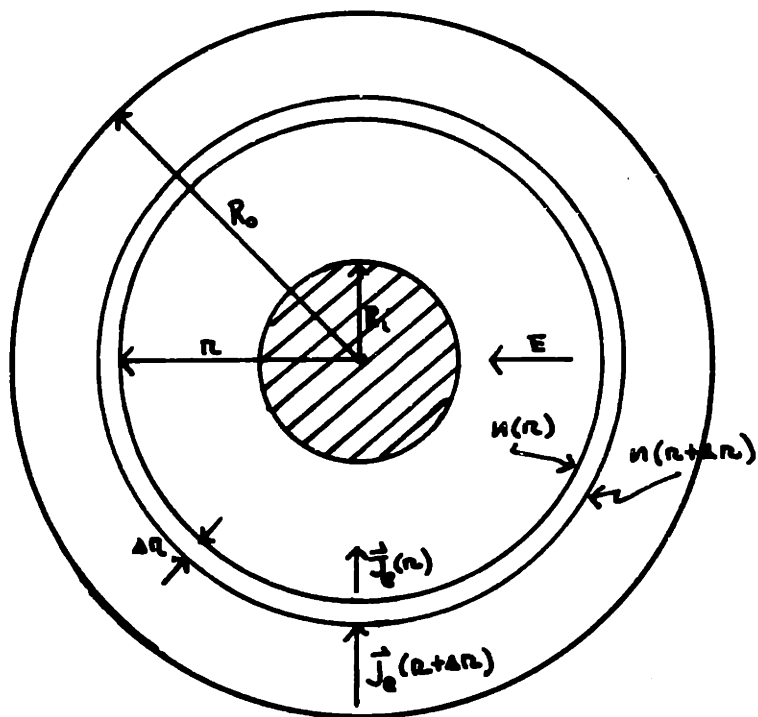


Figure 7.1 The diagram used in the explanation of the derivation for the electron continuity equation for negative corona.

$$\begin{aligned}
 r \Delta r (\nabla \cdot \vec{J}_e) &= -q \mu_e |E(r)| (\alpha(r) - \eta(r)) n_e(r) r \Delta r & (7) \\
 &= - (\alpha(r) - \eta(r)) |J_e(r)| r \Delta r.
 \end{aligned}$$

The continuity equations are, therefore,

$$\nabla \cdot \vec{J}_e = -(\alpha - \eta) |J_e|, \quad (8)$$

$$\nabla \cdot \vec{J}_- = -\eta |J_e|, \quad (9)$$

$$\nabla \cdot \vec{J}_+ = \alpha |J_e|, \quad (10)$$

and these equations are also applicable to the positive corona case.

The boundary conditions for electron and negative current densities has to be set at the surface of the inner conductor and positive ion current density set at the outer cylinder.

Rewriting the current densities in the form

$$\vec{J} = J(r) \hat{i}_r, \quad (11)$$

the continuity equations reduce to

$$\frac{d}{dr}(rJ_e) = (\alpha - \eta)(rJ_e), \quad (12)$$

$$\frac{d}{dr}(rJ_-) = \eta(rJ_e), \quad (13)$$

$$\frac{d}{dr}(rJ_+) = -\alpha(rJ_e). \quad (14)$$

Boundary conditions can be written as

$$J_e(R_1) = J_{e0}, \quad (15)$$

$$J_-(R_1) = 0, \quad (16)$$

$$J_+(R_0) = J_{+0}. \quad (17)$$

7.2 The Exact Solution

The current densities can be solved easily.

$$J_e(r) = \frac{R_1 J_{e0}}{r} \exp \int_{R_1}^r (\alpha(r') - \eta(r')) dr' \quad (18)$$

where $0 < R_1 < r' < r < R_0$.

$$J_-(r) = \frac{R_1 J_{e0}}{r} \int_{R_1}^r \eta(r'') \exp \left(\int_{R_1}^{r''} (\alpha(r') - \eta(r')) dr' \right) dr'' \quad (19)$$

where $0 < R_1 < r' < r'' < r < R_0$

$$J_+(r) = \frac{R_1 J_{e0}}{r} \int_r^{R_0} \alpha(r'') \exp \left(\int_{R_1}^{r''} (\alpha(r') - \eta(r')) dr' \right) dr'' \quad (20)$$

$$+ \frac{R_0 J_{+0}}{r}$$

where $0 < R_1 < r < r' < r'' < R_0$.

Note that the current densities are not the same as the positive corona case. Even though at first glance, they look very similar. The electron current density is not necessarily a monotonically increasing function of radius. If r is taken far enough so that attachment dominates, $J_e(r)$ will start to grow slower and finally decrease. However, $J_-(r)$ is a monotonically increasing function of radius and $J_+(r)$ increases as radius decreases.

The total current

$$I = 2\pi \left[R_0 J_{+0} + R_1 J_{e0} \int_{R_1}^{R_0} (r'') \exp \int_{R_1}^{r''} (\alpha(r') - \eta(r')) dr' dr'' \right] \quad (21)$$

The same type of approximation as for the positive corona case are employed. Take R_0 to where α is the same as η . Let

$$\alpha/p = A \exp\left(-\frac{B}{E/p}\right) \quad (22)$$

and set J_{+0} and attachment coefficient to zero.

$$I = 2\pi R_1 J_{e0} \left[\exp\left(\frac{AK}{B}\left(\exp\left(-\frac{BpR_1}{K}\right) - \exp\left(-\frac{B}{32}\right)\right) - 1 \right] \quad (23)$$

This is the same as the positive corona case except for the constant in front.

7.3 With Cosmic Radiation

$$\frac{d}{dr}(rJ_e) = (\alpha - \eta)(rJ_e) - 10qr. \quad (24)$$

$$\frac{d}{dr}(rJ_-) = \eta(rJ_e). \quad (25)$$

$$\frac{d}{dr}(rJ_+) = -\alpha(rJ_e) + 10qr. \quad (26)$$

The solutions are

$$J_e(r) = \frac{-10q}{rS(r)} \int_{R_1}^r r'S(r')dr' + \frac{R_1 J_{e0} S(R_1)}{rS(r)}. \quad (27)$$

$$J_-(r) = \frac{-10q}{r} \int_{R_1}^r \frac{\eta(r'')}{S(r'')} \int_{R_1}^{r''} r'S(r')dr' dr'' \quad (28)$$

$$+ \frac{R_1 J_{e0} S(R_1)}{r} \int_{R_1}^r \frac{\eta(r'')}{S(r'')} dr''.$$

$$J_+(r) = \frac{10q}{r} \int_{R_0}^r \frac{\alpha(r'')}{S(r'')} \int_{R_0}^{r''} r' S(r') dr' dr'' + \frac{J_{+0} R_0}{r} \quad (29)$$

$$- \frac{R_1 J_{e0} S(R_1)}{r} \int_{R_0}^r \frac{\alpha(r'')}{S(r'')} dr'' + \frac{10q}{r} \int_{R_0}^r r'' dr''$$

where $S(r) = \exp \int (\alpha(r') - \eta(r')) dr'$. (30)

The total current

$$I = -2\pi(10q) \int_{R_1}^{R_0} r'' dr'' \quad (31)$$

$$+ 10q \int_{R_1}^{R_0} \frac{\alpha(r'')}{S(r'')} \int_{R_1}^{r''} r' S(r') dr' dr''$$

$$+ 2\pi R_1 J_{e0} S(R_1) \int_{R_1}^{R_0} \frac{\alpha(r'')}{S(r'')} dr'' + 2\pi R_0 J_{+0}$$

Now make the same assumptions as in section 4.4 when calculating total current. Then

$$I = - (10q)(R_0^2 - R_1^2) \quad (32)$$

$$+ 10q \int_{R_1}^{R_0} A \exp\left(-\frac{Bpr''}{K}\right) \exp\left(-\frac{AK}{B} \exp\left(-\frac{Bpr''}{K}\right)\right) \cdot$$

$$\int_{R_1}^{r''} r' \exp\left(\frac{Ak}{B}\right) \exp\left(-\frac{Bpr'}{K}\right) dr' dr''$$

$$+ 2\pi R_1 J_{e0} \left[\exp\left(\frac{AK}{B}\right) \left(\exp\left(-\frac{BpR_1}{K}\right) - \exp\left(-\frac{B}{JZ}\right) - 1 \right) \right] + 2\pi R_0 J_{+0} .$$

7.4 Photoionization Term

The photoionization term to be added into the continuity equation cannot be just the term added for positive corona. For negative corona, the distribution of electron creation as a function of radius is

$$\alpha(r)J_e(r) = \frac{R_1 J_{e0}}{r} \alpha(r) \exp \int_{R_1}^r (\alpha(r') - \eta(r')) dr' \quad (33)$$

It is no longer true that most ionization by alpha process occur at the inner cylinder surface; and that implies the maximum photon creation too has moved away from the inner cylinder surface. At the same time the important secondary electrons are the ones photoionized near the cathode surface. Therefore the creation of electrons by photons coming from outside the cylinder of radius r will have to be taken into account also. See Appendix 2.

Now the continuity equations with cosmic radiation and the photionization term looks like

$$\frac{d}{dr}(rJ_e) = (\alpha - \eta)(rJ_e) - 10q - Ph, \quad (34)$$

$$\frac{d}{dr}(rJ_-) = \eta(rJ_e), \quad (35)$$

$$\frac{d}{dr}(rJ_+) = -\alpha(rJ_e) + 10q + Ph, \quad (36)$$

where

$$Ph = \mu_p Q \int_{R_1}^r G(r') \alpha(r') |J_e(r')| r' \exp(-\mu_{eff}(r-r')) dr' \quad (37)$$

$$+ \mu_p Q \int_r^{R_0} G'(r, r') \alpha(r') |J_e(r')| r' \exp(-\mu_{eff}(r'-r)) dr'$$

where

$$G'(r, r') = 1 - \frac{1}{\pi} \cos^{-1} \left(\frac{2r^2 - r'^2}{r'^2} \right) + GG(r'), \quad (38)$$

$$GG(r') = \frac{\theta_{max}}{2\pi} - \frac{1}{\pi} \tan^{-1} \left[\left(\frac{r'+r}{r'-r} \right) \tan \left(\frac{\theta_{max}}{2} \right) \right], \quad (39)$$

$$G(r') = \frac{\theta_{max}}{2\pi} + \frac{1}{\pi} \tan^{-1} \left[\left(\frac{r+r'}{r-r'} \right) \tan \left(\frac{\theta_{max}}{2} \right) \right]. \quad (40)$$

$G'(r, r')$ is a function of both r and r' . Therefore, for each new grid point r_j , the second integral has to be evaluated completely from scratch. One way to get around this difficulty is to try to take the r dependence outside the integral. This can be accomplished by approximating

$$1 - \frac{1}{\pi} \cos^{-1} \left(\frac{2r^2 - r'^2}{r'^2} \right) \quad (41)$$

by a polynomial of r/r' . A straight line is good enough for purposes here. One possible choice is

$$.93 \left(\frac{r}{r'} \right) - .112 \quad (42)$$

See Figure 7.2 for comparison. The photionization term now looks like

$$Ph = \mu_p Q \int_{R_1}^r G(r') \alpha(r') |J_e(r')| r' \exp(-\mu_{eff}(r-r')) dr' \quad (43)$$

$$+ \mu_p Q \int_r^{R_0} GG(r') \alpha(r') |J_e(r')| r' \exp(-\mu_{eff}(r'-r)) dr'$$

$$- .112 \mu_p Q \int_r^{R_0} \alpha(r') |J_e(r')| r' \exp(-\mu_{eff}(r'-r)) dr'$$

$$+ .93 \mu_p Q r \int_r^{R_0} \alpha(r') |J_e(r')| \exp(-\mu_{eff}(r'-r)) dr'$$

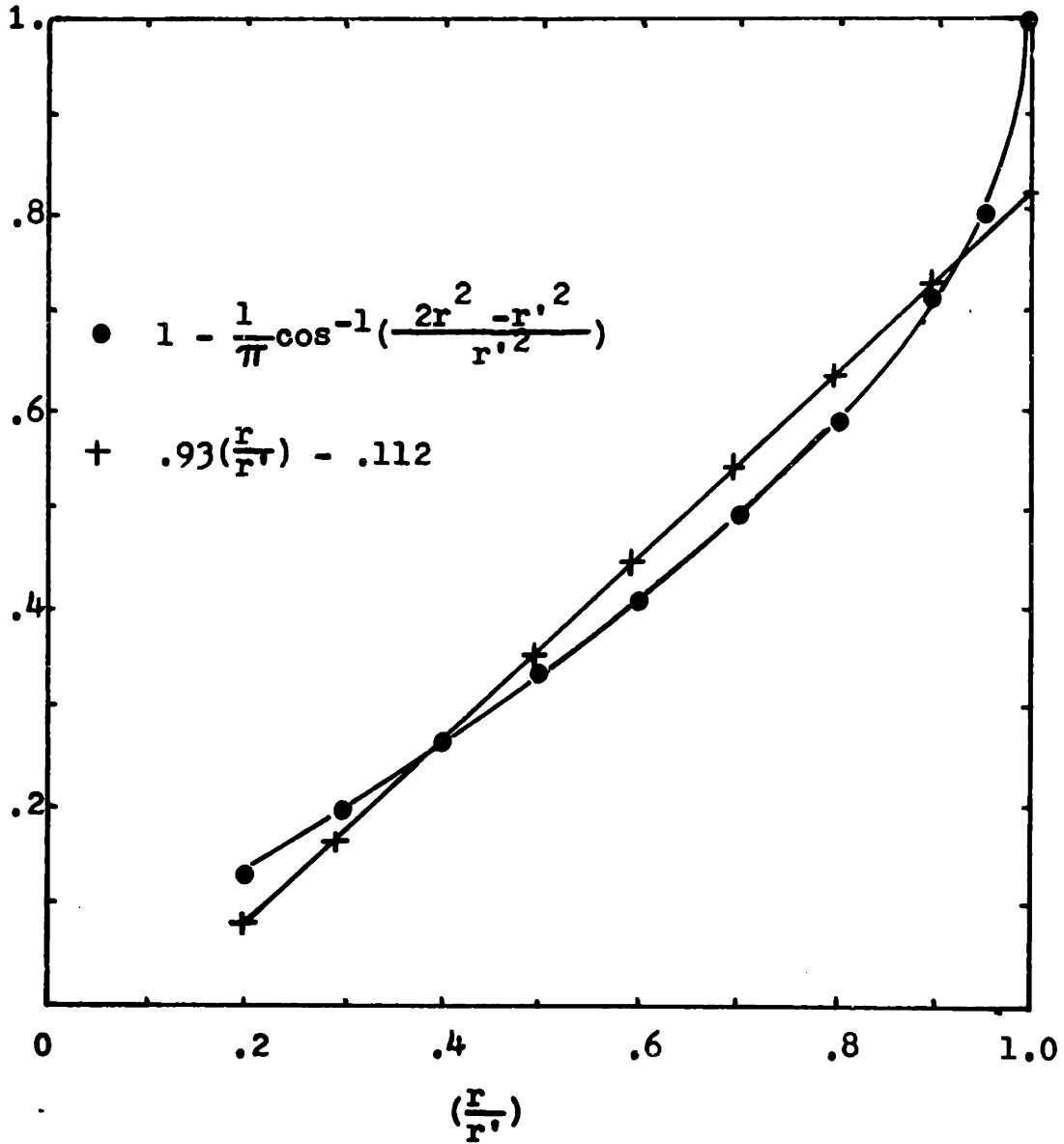


Figure 7.2 Approximating a term of the geometric factor by a linear function of $\left(\frac{r}{r'} \right)$

8. Results for Negative Corona

8.1 A Detailed Analysis of the Standard Case

The shape of the voltage versus current curve has the basic characteristics as the curves for positive corona. The critical onset electric field for the standard case is at E_0 approximately equal to 39.4 kv/cm, higher than that of the positive corona. This phenomenon is expected if photoionization is the only secondary mechanism. All secondary electrons for positive corona could be effective ionizers. While for negative corona only the secondary electrons produced in the region $\alpha > \eta$ could be effective ionizers because electrons are moving from a high electric field into a low electric field.

Figure 8.2 shows the current density for the case $E_0 = 39$ kv/cm, below the onset. Starting with no electrons at the surface of the cathode, the electron current density increases very sharply. The peak occurs where $\alpha = \eta$. In the region where α is important, the positive ion current density dominates, while in the region where attachment is greater than α , the negative ions dominate.

When the voltage is increased above onset until E_0 is 40 kv/cm, the current density still has the same shape except the magnitude has increased by factor of 10^9 . In general for the identical configuration, the current for negative corona is larger than that of positive corona

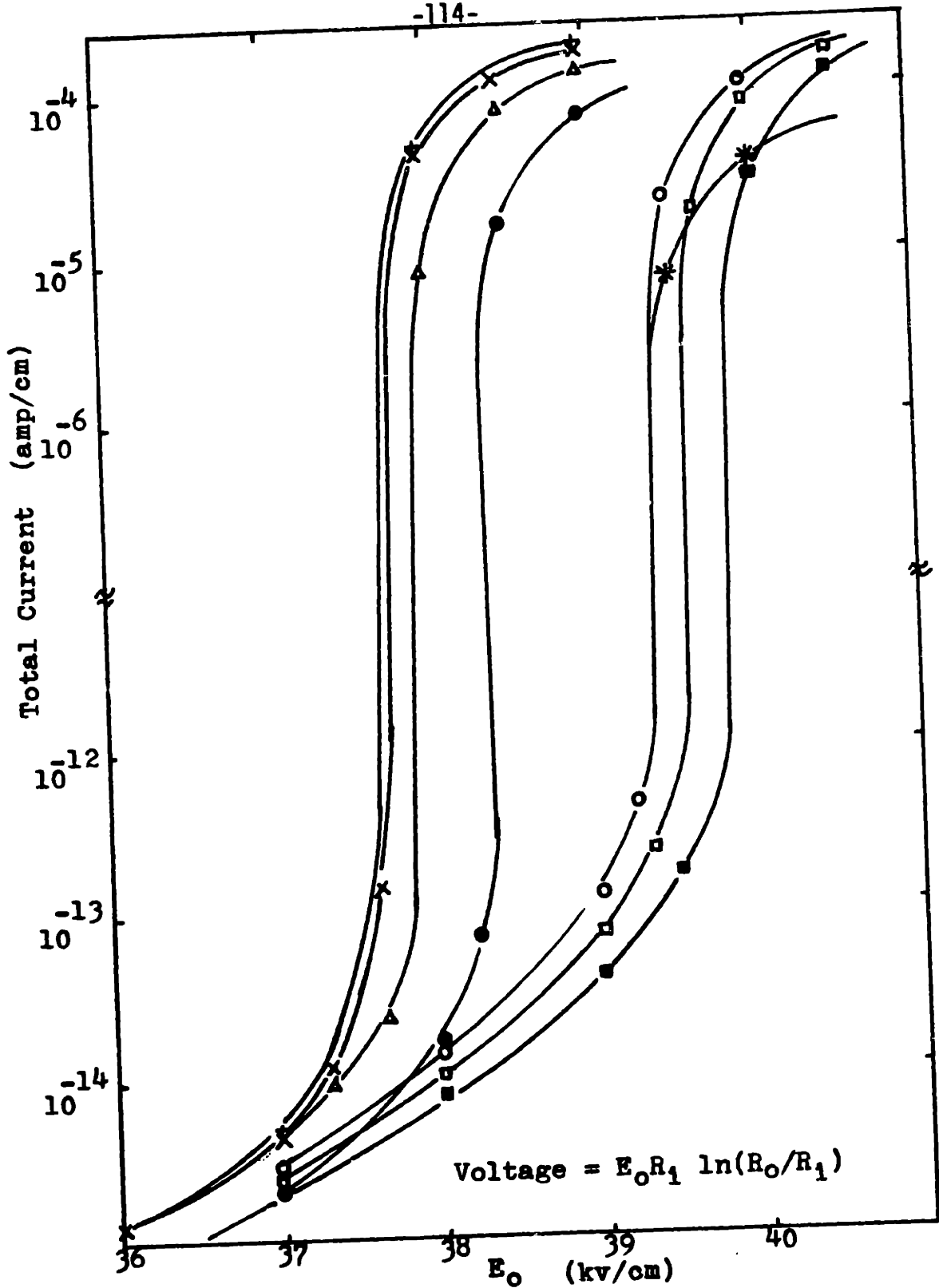


Figure 8.1 Sensitivity tests when the applied voltage on the 1.5 cm inner conductor is negative with respect to the outer conductor. See Table 8.1 for reference.

Explanation for the Figure 8.1

1. - o - Standard case with or without recombination term

The following are the same as the standard case with the exception specified below.

2. - ■ - α is decreased by 5% for all E/p

3. - □ - η is increased by 10% for all E/p

4. - Δ - $\mu_p = .01 \text{ cm}^{-1}$

5. - ● - $\mu_p = .01 \text{ cm}^{-1}$. $\mu_p = 8.2 \exp(-250p/E)$ for E/p 40
volts/cm-mm Hg

6. - * - $\mu_- = .8 \text{ cm}^2/\text{sec/volt}$
 $\mu_+ = .8 \text{ cm}^2/\text{sec/volt}$

7. - X - $\gamma_1 = .0001$

8. - t - $\gamma_p = .001$

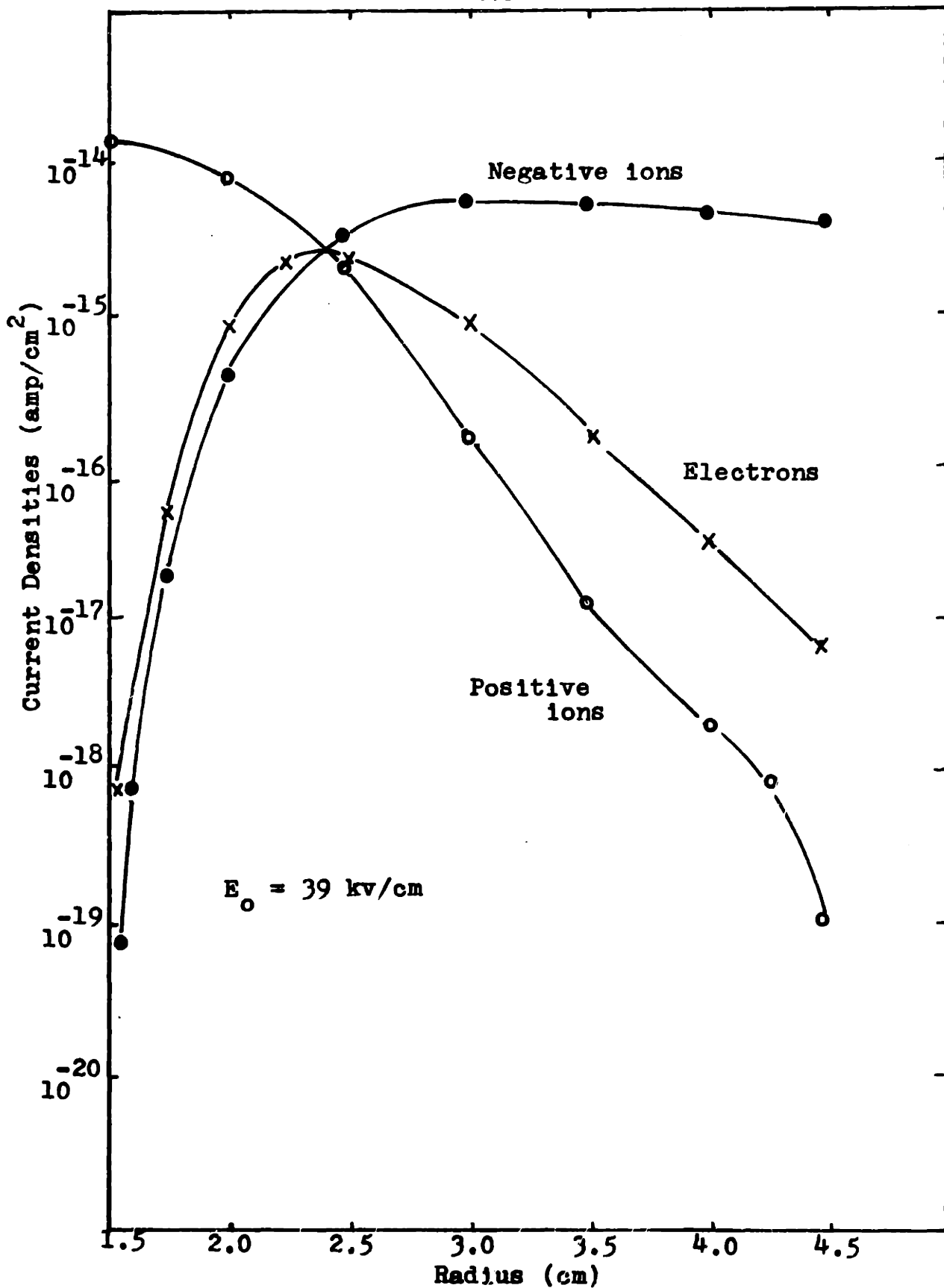


Figure 8.2 Current densities for $E_0 = 39 \text{ kv/cm}$ standard case.

above the onset. See Figure 8.3.

The corresponding charge densities for $E_0 = 39$ kv/cm are shown in Figure 8.4. Both positive ions and negative ions are important in modifying the electric field. Again electron charge density is insignificant.

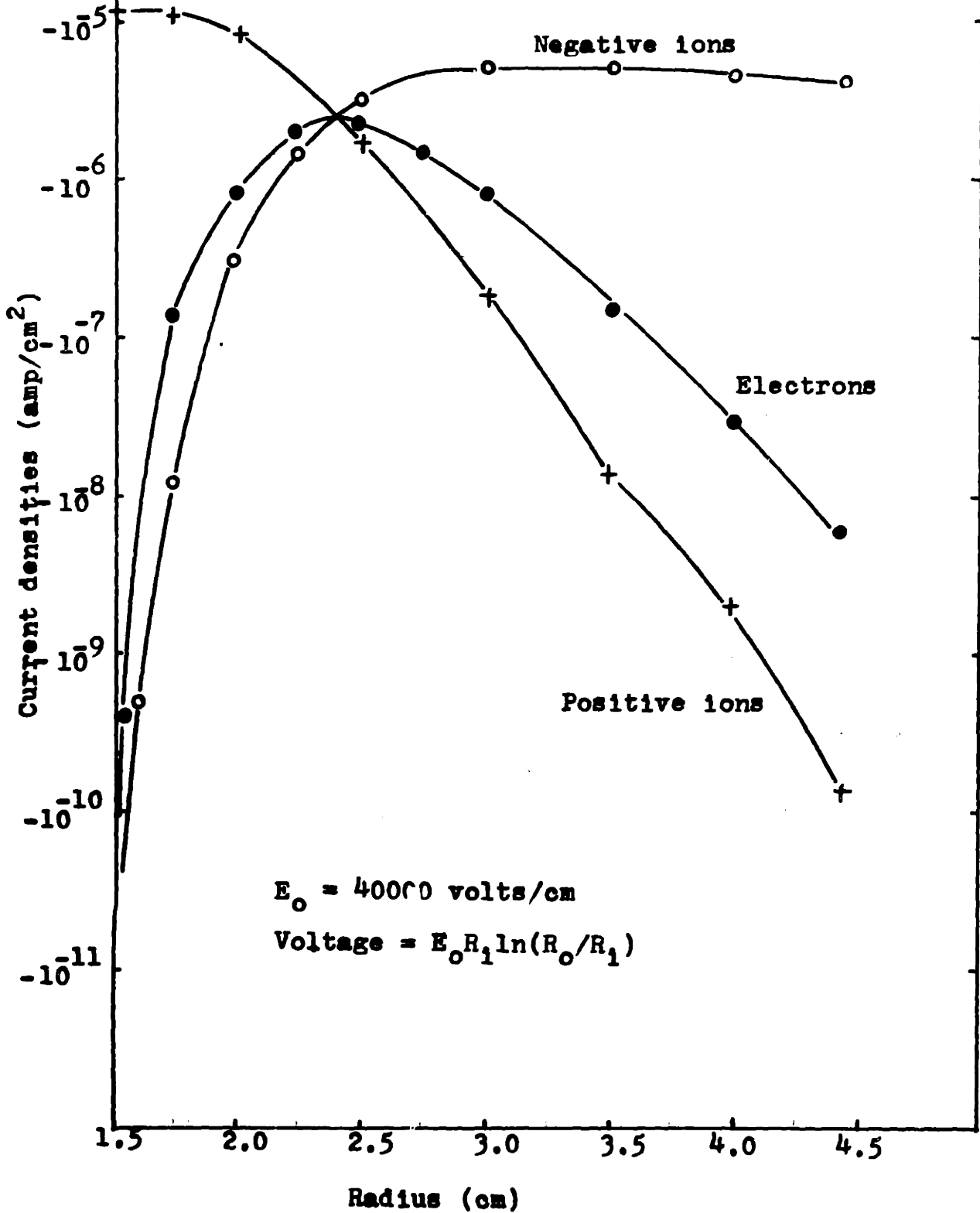
Figure 8.6 shows the effect of space charges on the electric field. Below onset the charge densities are so small that the electric field is unaltered from its K/r form. Above onset, the electric field near the center falls below the unperturbed K/r field and it deviates further until a minimum is reached approximately at where $\alpha = \eta$. This phenomenon is caused by the layer of positive space charge on the surface of the cathode. At distances far from the cathode, the electric field starts to increase and eventually becomes larger than the K/r field. Increases in voltage results in an increase in deviation from the K/r field. This is known as choking similar to the positive corona case.

The deviation of the electric field is reflected on the plots of α and η as a function of radius in Figure 8.7.

8.2 Sensitivity Tests

A set of sensitivity tests similar to the positive corona case are performed for the negative corona also.

Figure 8.3 Current densities for $E_0 = 40 \text{ kv/cm}$ standard case.



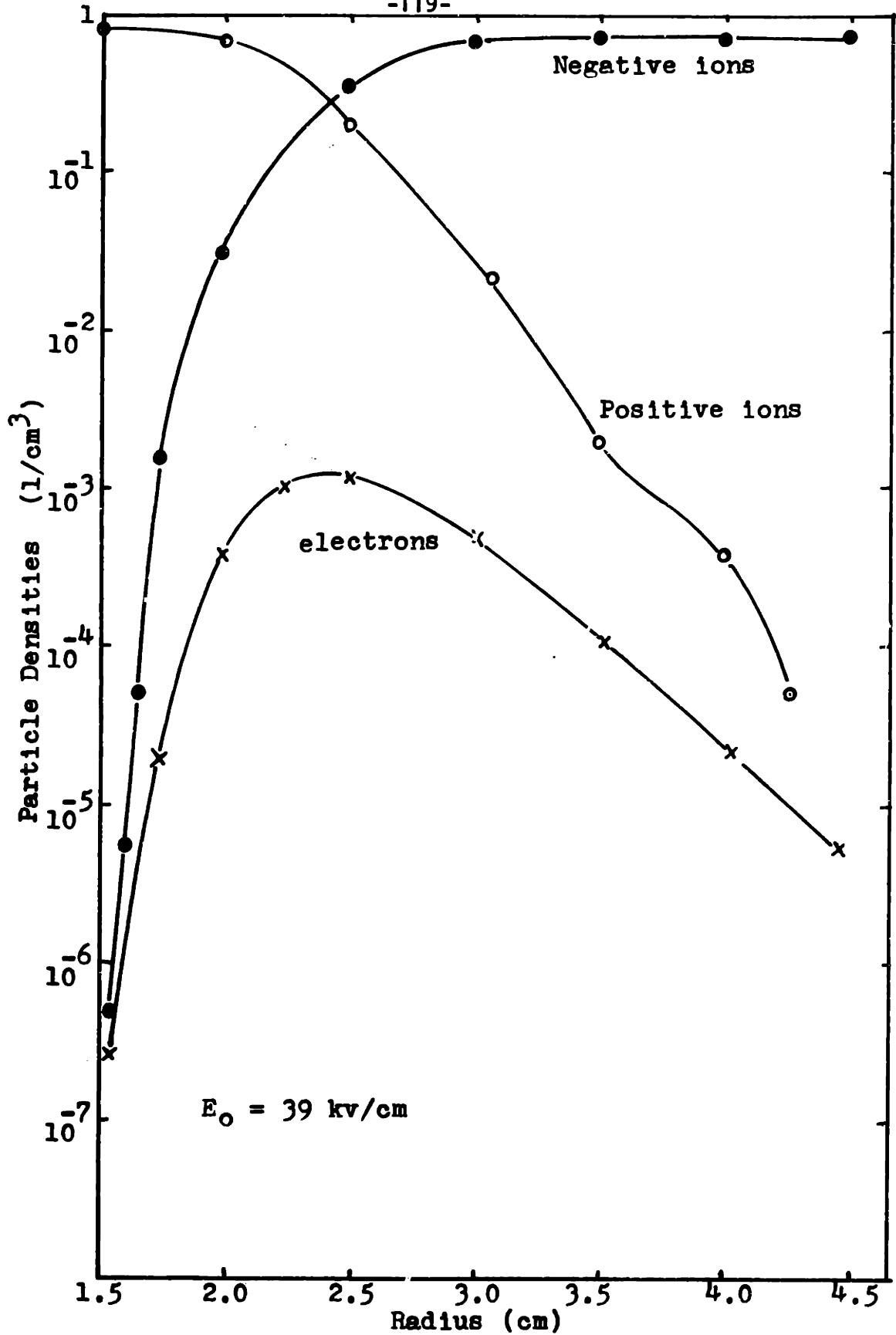


Figure 8.4 Particle densities for E₀ = 39 kv/cm standard case.

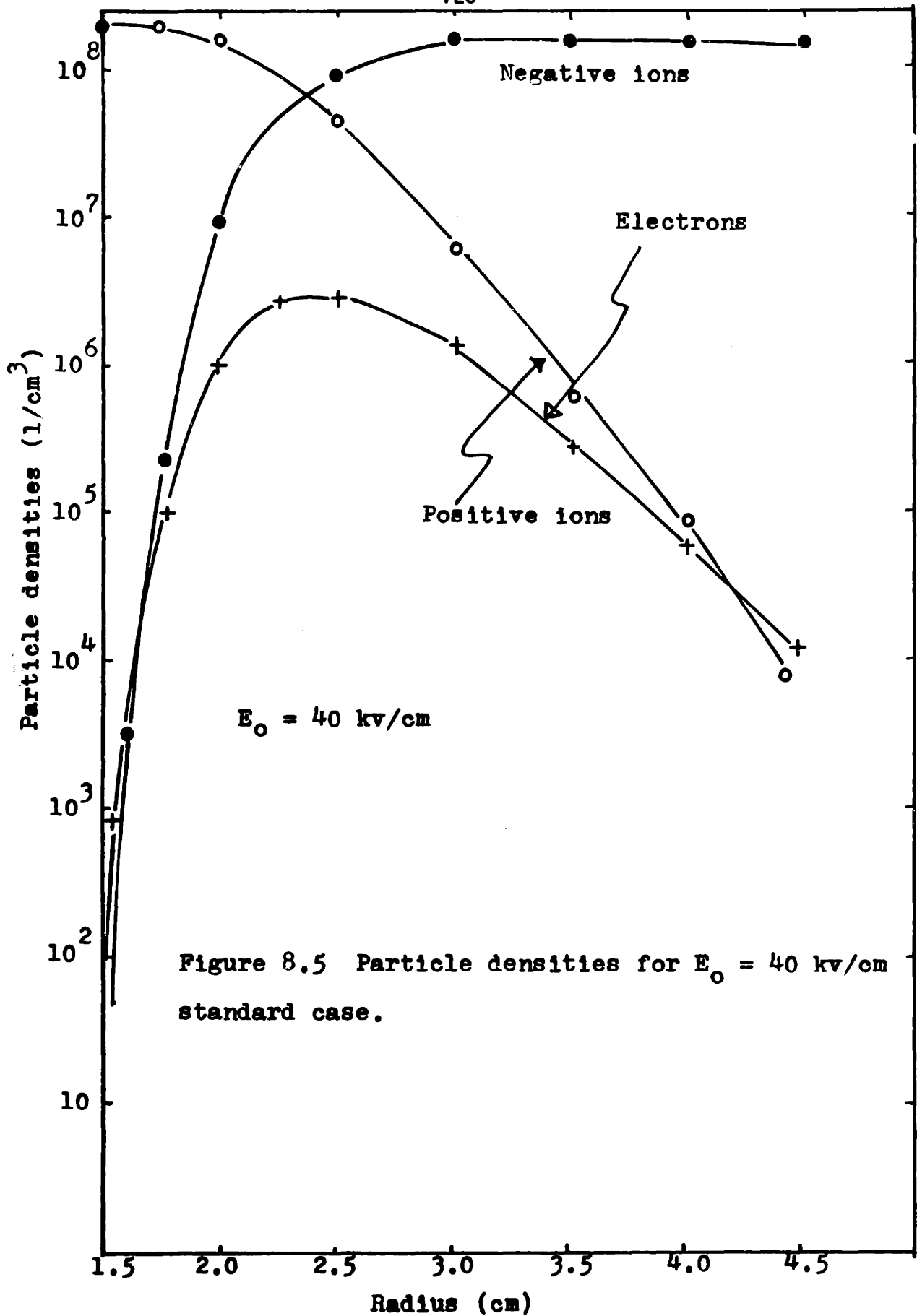


Figure 8.5 Particle densities for $E_0 = 40 \text{ kv/cm}$ standard case.

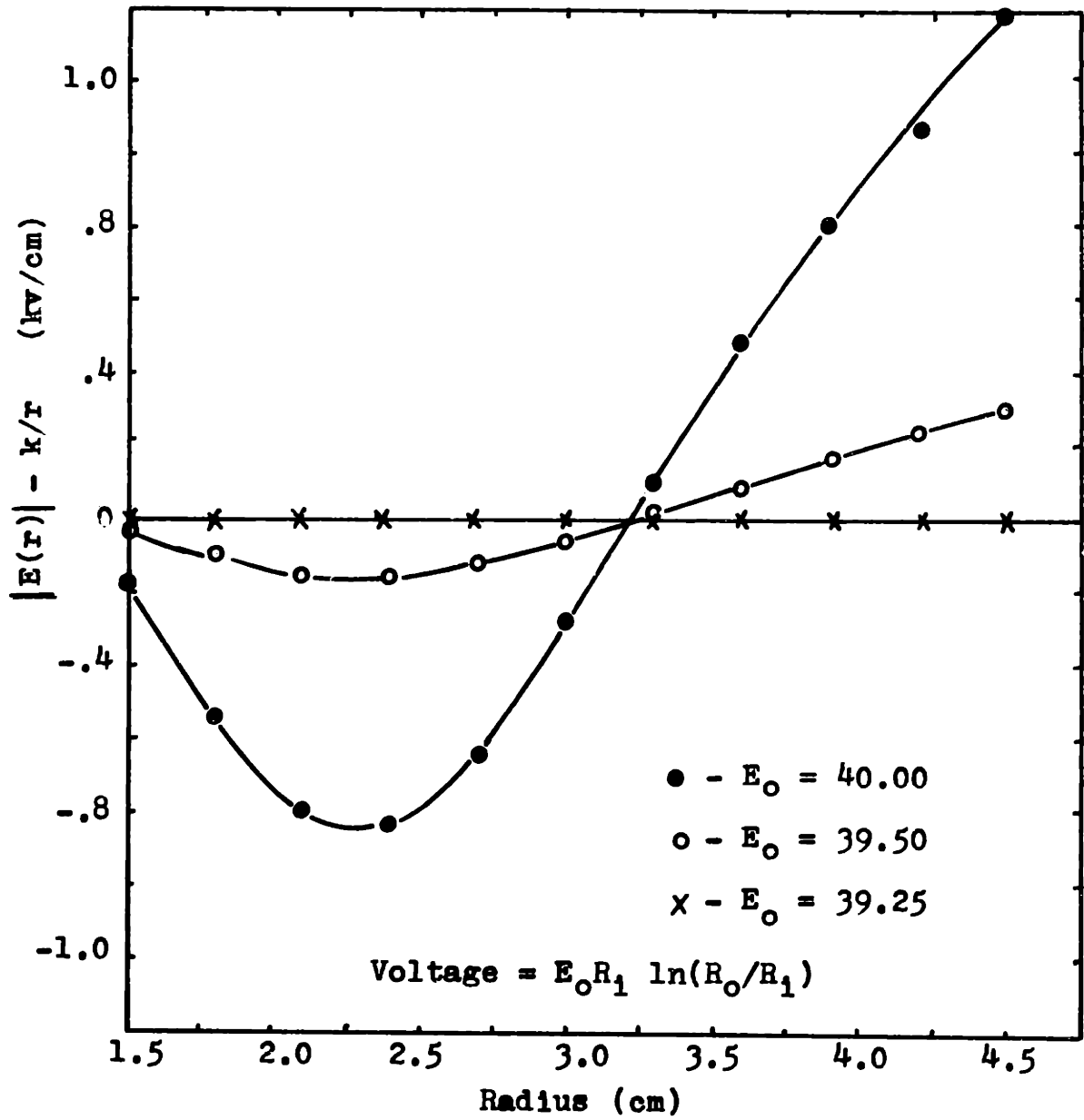


Figure 8.6 Deviation of the electric field from the k/r field as a function of position for different applied voltages.

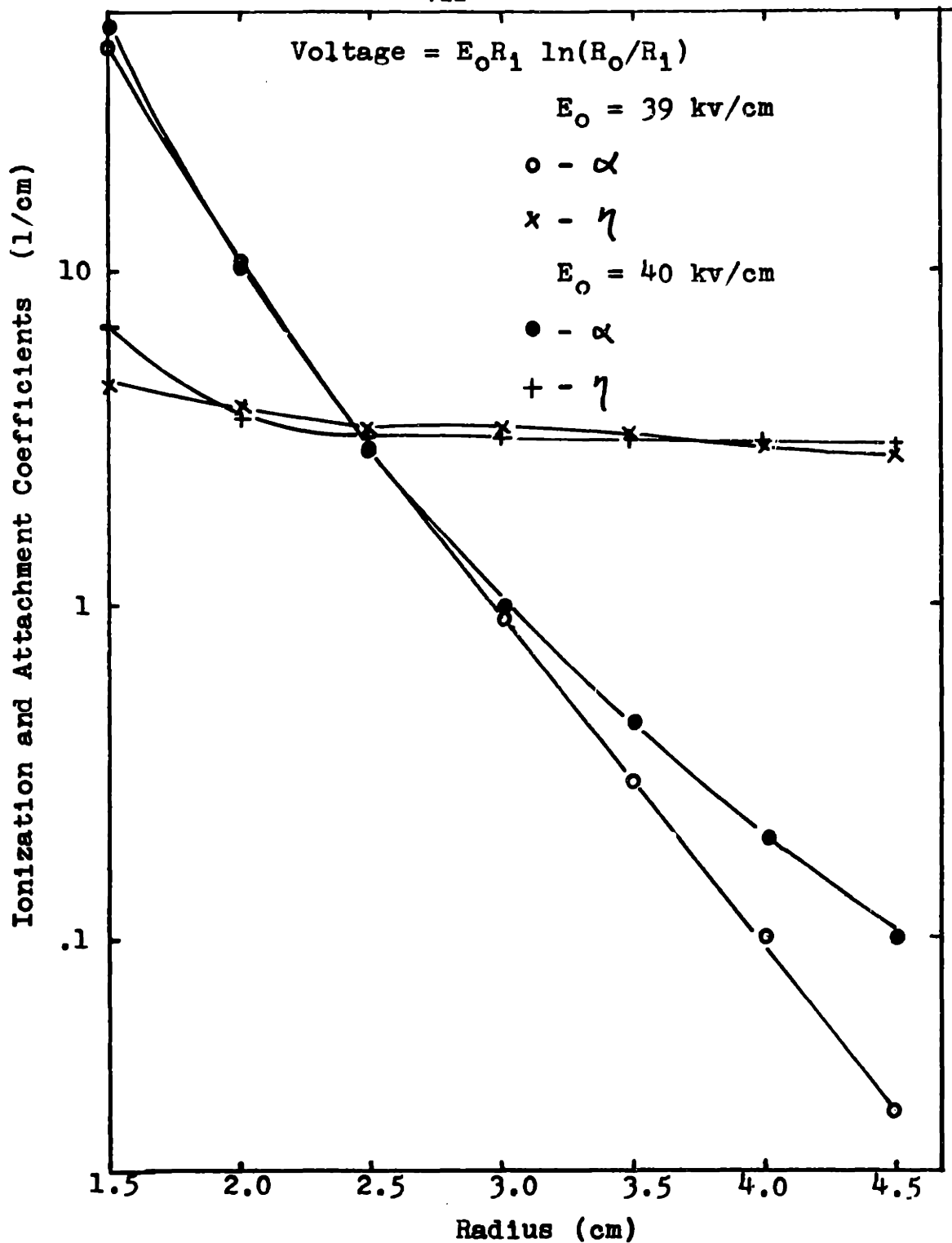


Figure 8.7 Values of α and η as a function of position for two different applied voltages.

Their curves are shown in Figure 8.1. First, consider the decrease in α by 5%. The onset increases by about $\frac{1}{2}$ kv/cm, Then the value of α in the region $E/p = 40$ volts/cm-mm Hg is allowed to vary from

$$\alpha/p = 1.44 \exp\left(-\frac{180}{E/p}\right) \quad (1)$$

to

$$\alpha/p = 8.2 \exp\left(-\frac{250}{E/p}\right) \quad (2)$$

with $\mu_p = .01 \text{ cm}^{-1}$ for both cases. The critical onset electric field is at 37.9 kv/cm-mm Hg for the first α used. The critical onset field is increased to 38.5 kv/cm for the second α .

Similar to the positive corona case, when μ_p is changed from $.001 \text{ cm}^{-1}$ to $.01 \text{ cm}^{-1}$, the onset dropped from 39.4 kv/cm to 37.9 kv/cm. The photoionization term for the standard case with $E_0 = 40$ kv/cm at the center electrode, when there is no space charges, is shown in Figure 8.8. If μ_p is a much larger number, the photoionization term will have a distinct peak between the two conductors. For changes in ion mobilities, recombination coefficient, and attachment coefficient, the effects are exactly the same as the positive case.

8.3 Variations on the Size of the Outer Conductor

If the size of the outer conductor is many times the

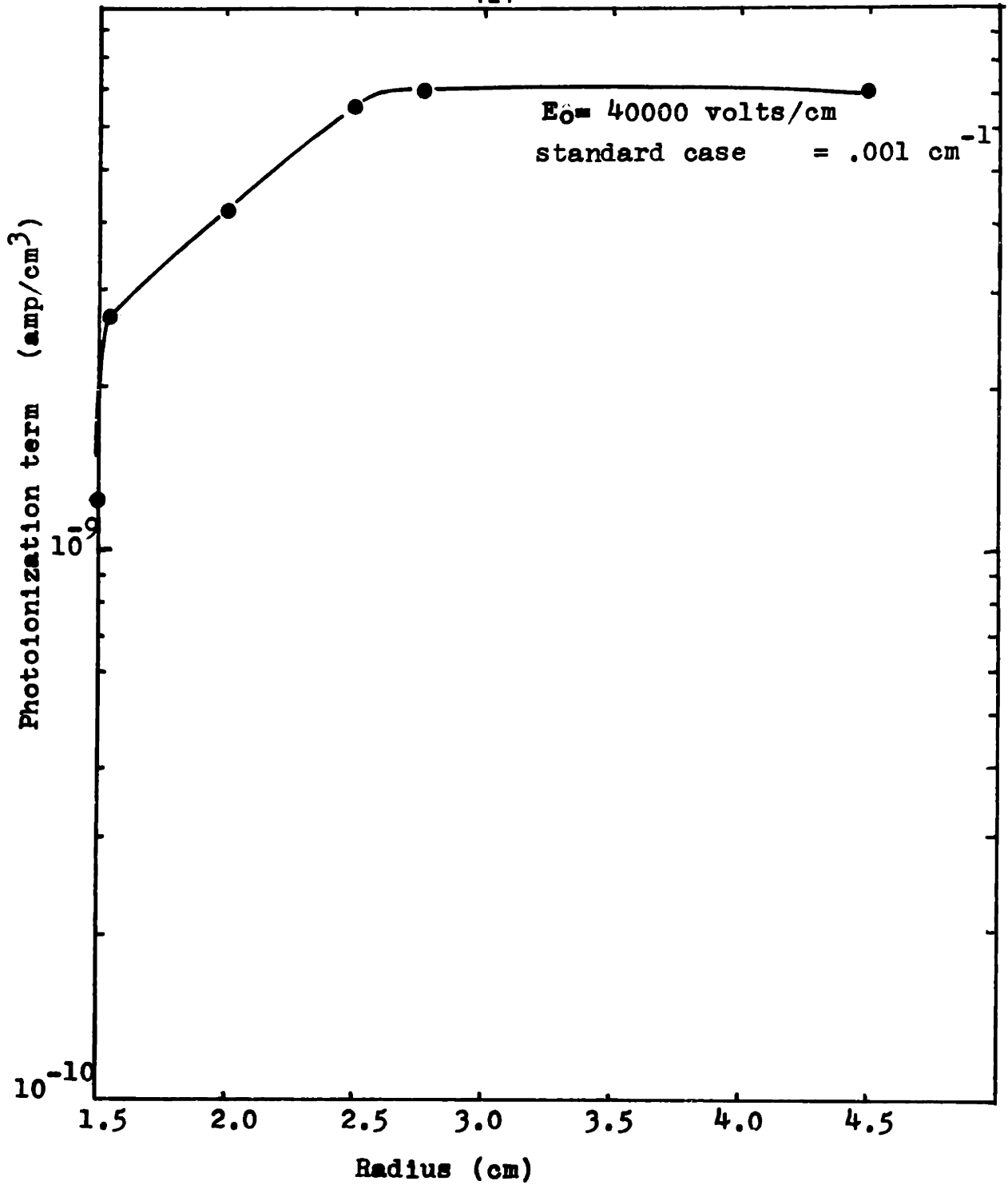


Figure 8.8 The photoionization term as a function of position.

distance from the inner conductor to the peak of electron current density, then the change in the outer cylinder radius only changes the current above onset. The electric field will be decreased near the conductor and increased further away from the K/r field as described in section 6.5.

If the outer conductor is made too small, the electric field at the surface of the cathode could actually be increased above the K/r field. If the deviation is not too large as in the case shown in Figure 8.9, the situation is still stable. If the outer conductor is further decreased in size, the large increase of the electric field on the surface of the cathode produces a larger current, and the larger current increases the electric field more near the cathode. This is similar to a complete breakdown. The effect is opposite to choking. It could not happen in the positive corona case, unless the outer cylinder is only a few mm away from the inner cylinder.

8.4 Ion Bombardment and Photoelectric Emission.

Negative Corona is noted to occur on or above the positive corona onset for a polished and oxidized wire. γ_1 can at most be .00001 if the onset is to occur at Peek's prediction for a 1.5 cm radius cathode. Case 7 in Figure 8.1 is a current as a function of voltage curve

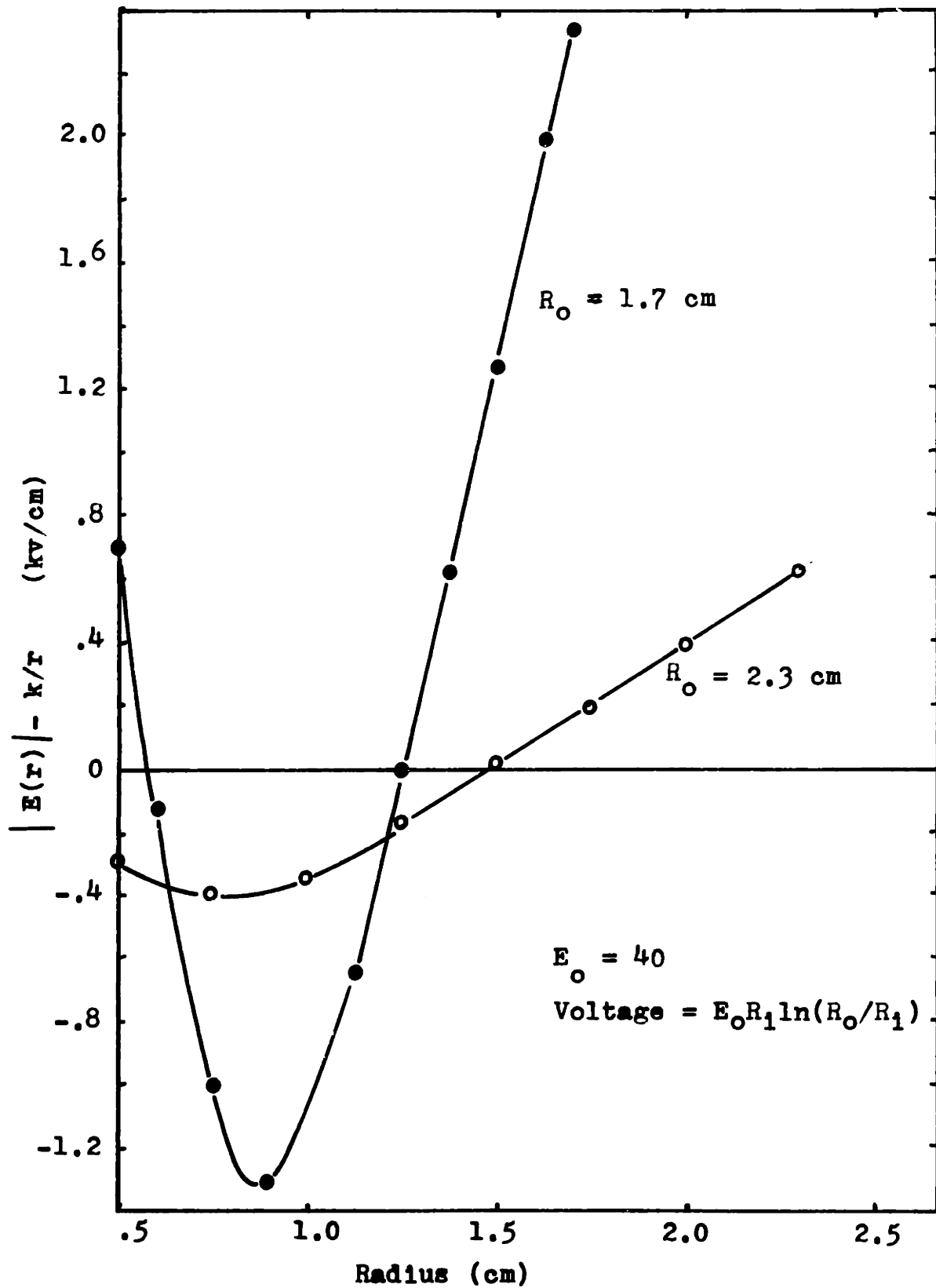


Figure 8.9 The effect of the dimension of the outer cylinder on the electric field.

when $\gamma_1 = .0001$. The critical onset field is at 37.9 kv/cm. The current densities are shown in Figure 8.10. There is no marked difference in current distribution between the photoionization case and the case with ion impact.

Similarly if photoelectric emission is the only secondary feedback mechanism, γ_p has to be less than .0001.

There is no way to distinguish the three different secondary mechanisms using steady state measurements. Possibly, measurements of the time lag for an applied current impulse is one method to distinguish the three secondary processes.

8.5 Variations on Cathode Size and Comparison of Results to Peek's Formula

For all size inner conductors tested, the onset for negative corona is higher than positive as shown in Figures 6.15, 6.16, 6.17 and 6.18 in the positive corona section. The shape of the critical onset electric field as function of radius in Figure 6.1 again is different from Peek's formula, but the same as analytical predictions in Figure 5.2. By changing α in the low E/p region, however, did not have as big a change on the shape of the onset curve. The reason is the electrons move from high field into low E/p region. Changes in μ_p as a function of E/p could twist the curve the correct way. However, the correctness

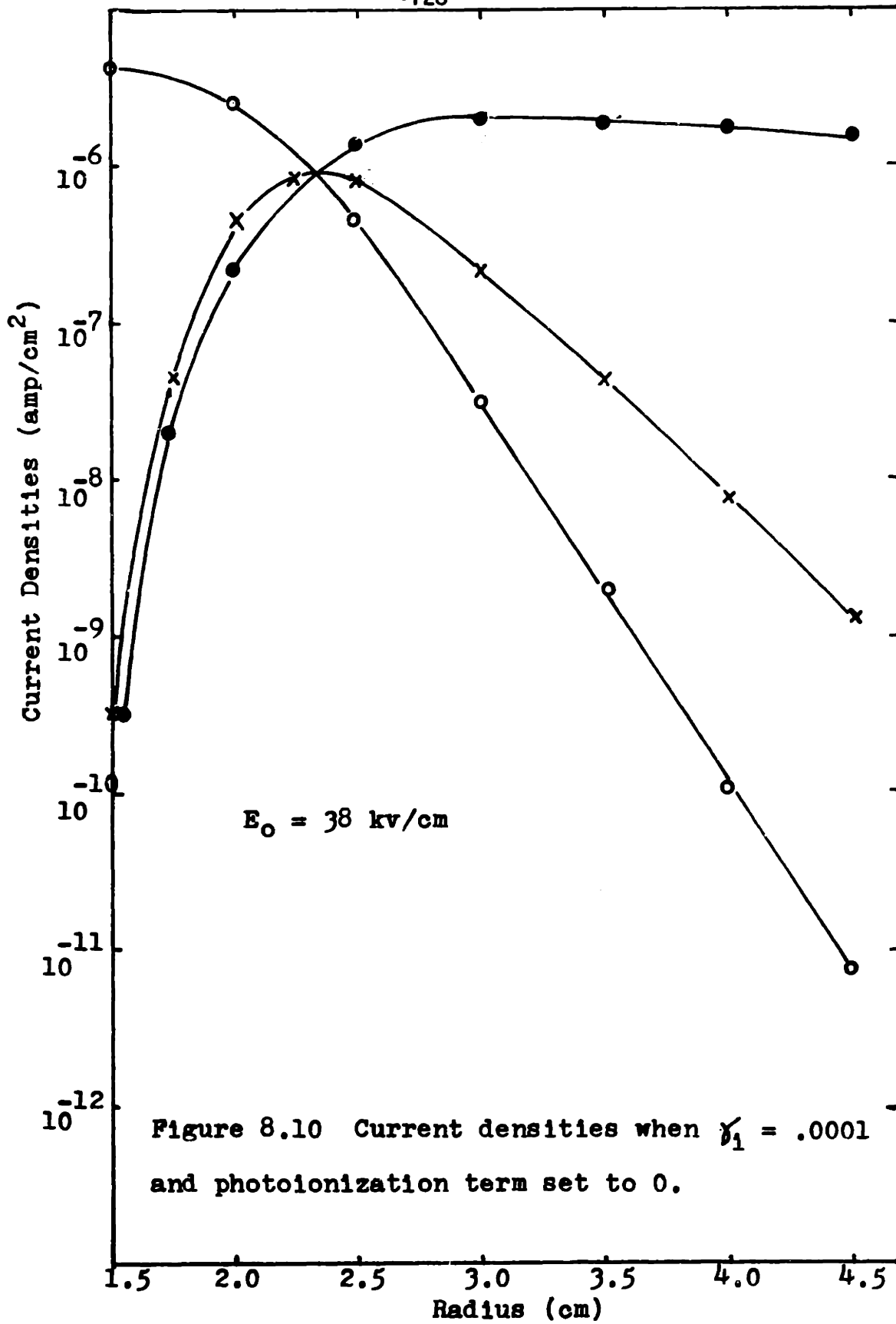


Figure 8.10 Current densities when $\gamma_1 = .0001$ and photoionization term set to 0.

of Peek's formula for direct current measurements in negative corona is very questionable.

9. Conclusions

The model used can generate a total current as a function of voltage similar to observations. The important primary processes are ionization by electron neutral collisions and attachment of electrons to neutrals. Recombination and diffusion are insignificant. Changes of ion mobilities only effect the current above onset. Changes in electron velocity only changes the electron charge densities, while the current densities are not effected at all. Both the positive and the negative corona can be produced when the only secondary process included is photoionization in the bulk of the gas. The negative corona onset then is always above the positive corona onset. There is no way to differentiate the type of secondary process using this model.

The model can be improved if the photon absorption rate, μ_p , is made to be a function of E/p . A better approximation for the geometric factor for negative corona will also improve the accuracy of onset.

The program too can be improved, such as a second order method for evaluation of the electric field. To increase the accuracy at minimum cost, variable grid sizes should be allowed.

The next logical step would be to include time depen-

dence. The equations used in this assume that the average time from electron neutral collision to emission of a photon and eventual absorption is short compared to the characteristic distance over the electron velocity. The continuity equations for the case with time dependence become

$$\frac{\partial f_e}{\partial t} = - \nabla \cdot \vec{J}_e - (\alpha - \eta) |J_e| - 10q - Ph \quad (1)$$

$$\frac{\partial f_-}{\partial t} = - \nabla \cdot \vec{J}_- - \eta |J_e| \quad (2)$$

$$\frac{\partial f_+}{\partial t} = - \nabla \cdot \vec{J}_+ + \alpha |J_e| + 10q + Ph \quad (3)$$

The greatest difficulty associated with the model when time is incorporated is the difference in the velocity of electrons versus the ions in an electric field.

Appendix 1

Derivation of Geometric Factor for Positive Corona

This section is devoted to deriving an expression for the percentage of photons created at a point P located r' away from the axis that reach an imaginary cylinder of radius r , for $r > r'$.

Consider a small area dA on the imaginary cylinder with radius r . See Figure A1.2. The solid angle $d\Omega$ subtended by dA as seen at point P is

$$d\Omega = \frac{\cos \gamma}{D^2} dA \quad (1)$$

where D = distance between point P and dA ,

and γ = angle between the vector D and the normal vector of dA .

$d\Omega/4\pi$ is the percentage of rays from point P that get to area dA when there is no absorption of photons in the intermittant space. With absorption, the actual percentage of rays leaving P and arriving at dA is decreased to

$$\frac{d\Omega}{4\pi} \exp(-\mu_p D) \quad (2)$$

Summing over all the area S on a cylinder with radius r , where rays from point P could reach, the percentage of photon, K arriving is

$$K = \iint_S \exp(-\mu_p D) \frac{\cos \gamma}{4\pi D^2} dA \quad (3)$$

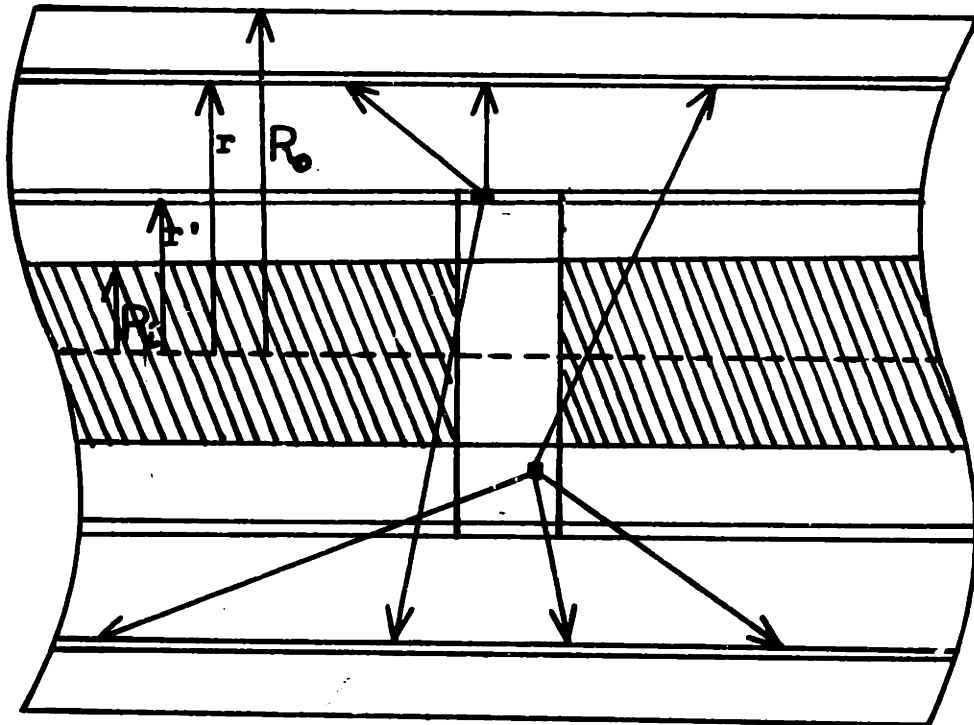
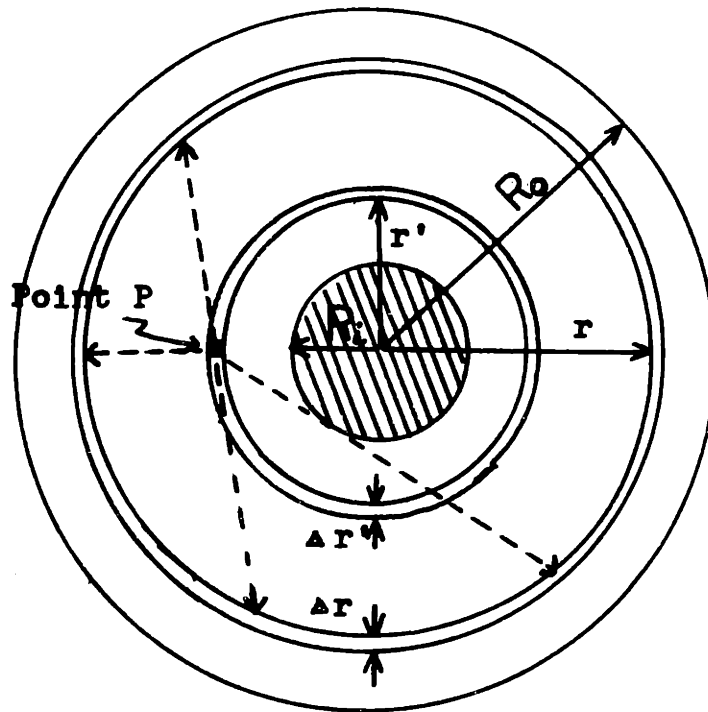


Figure A1.1 Two different view points for the derivation of geometric factor of positive corona.

$$K = 4 \int_0^{\infty} \int_0^{\theta_{\max}} \frac{\cos \gamma}{4\pi D^2} \exp(-\mu D) r d\theta dz. \quad (4)$$

The expressions for θ_{\max} , γ and D will be derived below.

Consider the configuration shown in Figure A1.2 .

dA is located at (x,y,z) and the point P is at $(r',0,0)$.

The results derived below are very general. The distance D between point P and dA is

$$\begin{aligned} |D| &= ((x - r')^2 + y^2 + z^2)^{\frac{1}{2}} \\ &= (r'^2 + r^2 - 2rr'\cos\theta + z^2)^{\frac{1}{2}} \end{aligned} \quad (5)$$

The definition of γ is

$$\cos \gamma = \hat{i}_n \cdot \hat{i}_D \quad (6)$$

$$\text{where } \hat{i}_n = (x\hat{i}_x + y\hat{i}_y)/r \quad (7)$$

$$\text{and } \hat{i}_D = ((x-r')\hat{i}_x + y\hat{i}_y + z\hat{i}_z) / D \quad (8)$$

$$\begin{aligned} \cos \gamma &= (x(x-r') + y^2) / (rD) \\ &= (r - r' \cos\theta) / D \end{aligned} \quad (9)$$

The last unknown is θ_{\max} . θ_{\max} is the angle between the x -axis and a line that includes the origin and a point B on the circle with radius r . Point B is picked in such a way that the line connecting points B and P is tangent to the inner cylinder with radius R_1 ; and the point of contact is called C .

$$x_c^2 + y_c^2 = R_1^2 \quad (10)$$

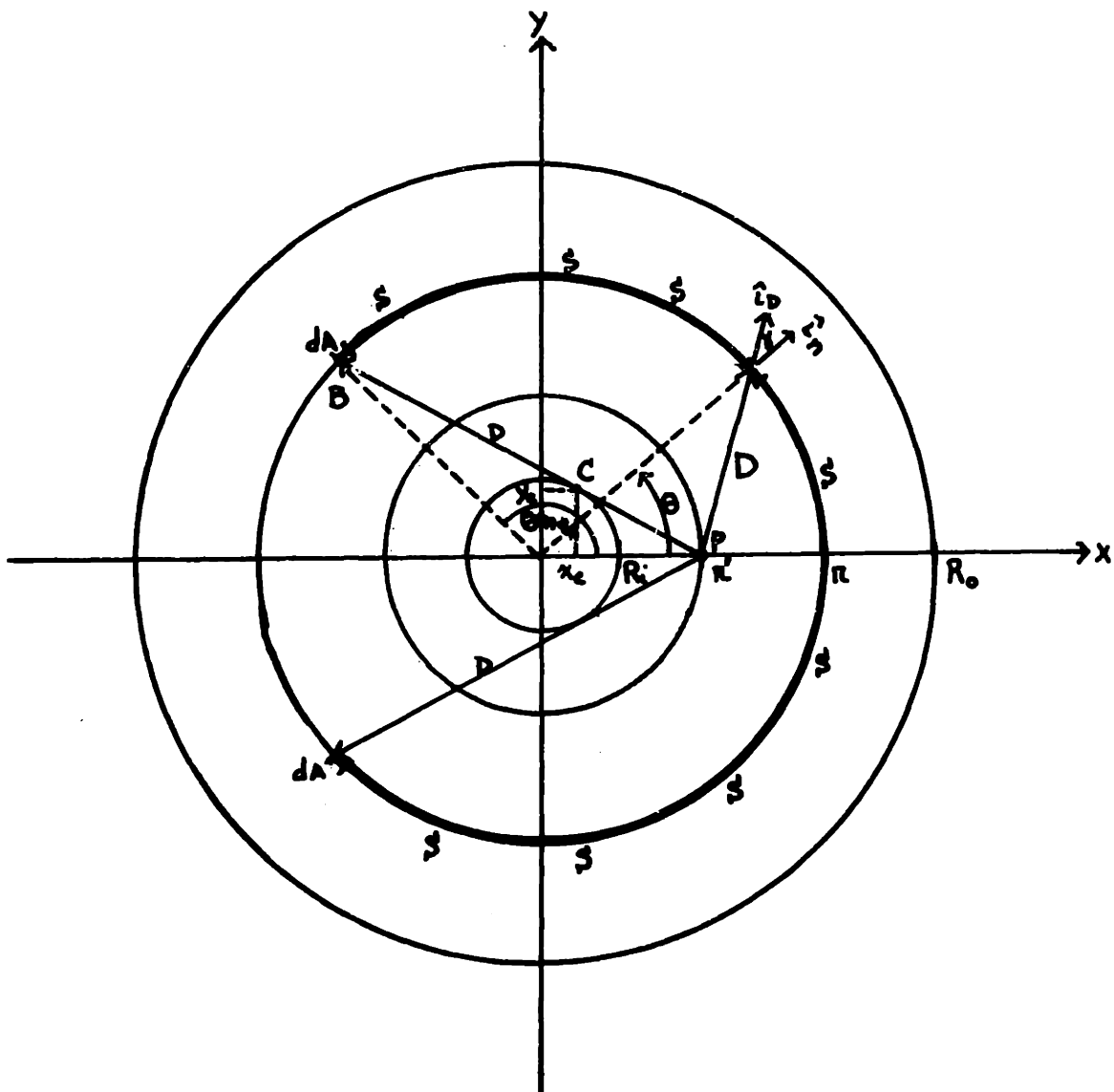


Figure A1.2 Definition of variables used in the derivation.

Definition of the slope of the tangent at point C is

$$\frac{dy}{dx} = \frac{-x_c}{(R_1^2 - x_c^2)^{\frac{1}{2}}} \quad (11)$$

The triangle made of points C, P and $(x_c, 0)$ also can give an expression for tangent.

$$\frac{dy}{dx} = \frac{-y_c}{r' - x_c} = \frac{-(R_1^2 - x_c^2)^{\frac{1}{2}}}{r' - x_c} \quad (12)$$

Solve for x_c .

$$x_c = \frac{R_1^2}{r'} \quad (13)$$

Now the equation of the tangent is known.

$$y = \frac{R_1}{(1 - (R_1/r')^2)^{\frac{1}{2}}} \left(1 - \frac{x}{r'}\right) \quad (14)$$

Solving for the intersection of this equation with the circle

$$x^2 + y^2 = r^2 \quad (15)$$

gives the coordinates of the point B.

$$x_B = \frac{1}{r'} \left(R_1^2 - ((r^2 - R_1^2)(r'^2 - R_1^2))^{\frac{1}{2}} \right) \quad (16)$$

So θ_{\max} can now be found.

$$\cos \theta_{\max} = \frac{x_B}{r} \quad (17)$$

$$= \frac{1}{r r'} \left(R_1^2 - ((r^2 - R_1^2)(r'^2 - R_1^2))^{\frac{1}{2}} \right)$$

$$\theta_{\max} = \cos^{-1} \left[\frac{1}{r r'} \left(R_1^2 - ((r^2 - R_1^2)(r'^2 - R_1^2))^{\frac{1}{2}} \right) \right] \quad (18)$$

Finally the expression for K is completely determined.

$$K = \frac{r}{\pi} \int_0^{\infty} \int_0^{\theta_{\max}} \frac{(r - r' \cos \theta) \exp(-\mu D)}{D^3} d\theta dz \quad (19)$$

$$\text{where } D = (r^2 + r'^2 - 2r r' \cos \theta + z^2)^{\frac{1}{2}}. \quad (20)$$

Unfortunately the above expression cannot be integrated. An expression that is simpler to use in photoionization calculations is

$$K \cong G \exp(-\mu_{\text{eff}}(r-r')) \quad (21)$$

$$\text{where } G = \frac{r}{\pi} \int_0^{\theta_{\max}} \int_0^{\infty} \frac{r - r' \cos \theta}{D^3} dz d\theta \quad (22)$$

and μ_{eff} is calculated from equation 21 for each point after K is integrated numerically.

G can be integrated, first over the variable z giving

$$G = \frac{r}{\pi} \int_0^{\theta_{\max}} \frac{r - r' \cos \theta}{(r^2 + r'^2 - 2rr' \cos \theta)} d\theta \quad (23)$$

$$= \frac{r}{2\pi r'} \int_0^{\theta_{\max}} \frac{d\theta}{\left(\frac{r^2 + r'^2}{2rr'} - \cos \theta\right)}$$

$$- \frac{1}{2\pi} \int_0^{\theta_{\max}} \frac{\cos \theta d\theta}{\left(\frac{r^2 + r'^2}{2rr'} - \cos \theta\right)} .$$

The second term can be written in another form, (24)

$$- \frac{1}{2\pi} \left[-\theta \Big|_0^{\theta_{\max}} + \frac{r^2 + r'^2}{2rr'} \int_0^{\theta_{\max}} \frac{d\theta}{\left(\frac{r^2 + r'^2}{2rr'} - \cos \theta\right)} \right]$$

which when combined with the first term of G, gives

$$\begin{aligned}
 G &= \frac{\theta_{\max}}{2\pi} + \frac{1}{2\pi} \left(\frac{r}{r'} - \frac{r^2 + r'^2}{2rr'} \right) \int_0^{\theta_{\max}} \frac{d\theta}{\frac{r^2 + r'^2}{2rr'} - \cos\theta} \\
 &= \frac{\theta_{\max}}{2\pi} + \frac{1}{2\pi r'} \frac{r^2 - r'^2}{2r} \frac{2}{\left(\frac{r^2 + r'^2}{2rr'} - 1 \right)^{\frac{1}{2}}} \cdot \\
 &\quad \frac{\tan^{-1} \left(\frac{r^2 + r'^2}{2rr'} - 1 \right)^{\frac{1}{2}} \tan\left(\frac{\theta}{2}\right)}{\frac{r^2 + r'^2}{2rr'} - 1} \Bigg|_0^{\theta_{\max}} \\
 &= \frac{\theta_{\max}}{2\pi} + \frac{1}{2\pi} \tan^{-1} \left(\frac{r + r'}{r - r'} \right) \tan\left(\frac{\theta_{\max}}{2}\right) \quad (25)
 \end{aligned}$$

Numerical calculations show that G is not a function of r, which is very reasonable since G is really the percentage of rays emitted from r' that are not blocked by the inner cylinder of radius R₁. The limiting case

$$r' = R_1 \quad (26)$$

gives

$$G = .5. \quad (27)$$

This checks with expectations.

Derivation of Geometric Factor for Negative Corona

For negative corona the percentage of photons created at a point P located r away from the axis that reach an imaginary cylinder of radius r' , for $r > r'$, is also of importance.

This time consider a small area dA on the imaginary cylinder with radius r' . See Figure A2.1. The arguments in deriving K is identical with that in appendix 1.

$$K = 4 \int_0^{\infty} \int_0^{\theta_{\max}} \frac{\cos \gamma \exp(-\mu D)}{4 D^2} r' d\theta dz \quad (1)$$

where $\theta_{\max} = \cos^{-1} \left[\frac{1}{rr'} (R_1^2 - ((r^2 - R_1^2)(r'^2 - R_1^2))^{\frac{1}{2}}) \right]$

and $D = (r^2 + r'^2 - 2rr' \cos \theta + z^2)^{\frac{1}{2}}$

The same as before. However, the expression for $\cos \gamma$ is changed. See Figure A2.2.

$$\hat{i}_D = (x - r')\hat{i}_x + y\hat{i}_y + z\hat{i}_z \quad (2)$$

so $\cos \gamma = \frac{x - r'}{D} = \frac{r \cos \theta - r'}{D} \quad (3)$

Note that $\cos \gamma$ changes sign when

$$\cos \theta = \frac{r'}{r} \quad (4)$$

This can be explained by the fact that rays from point

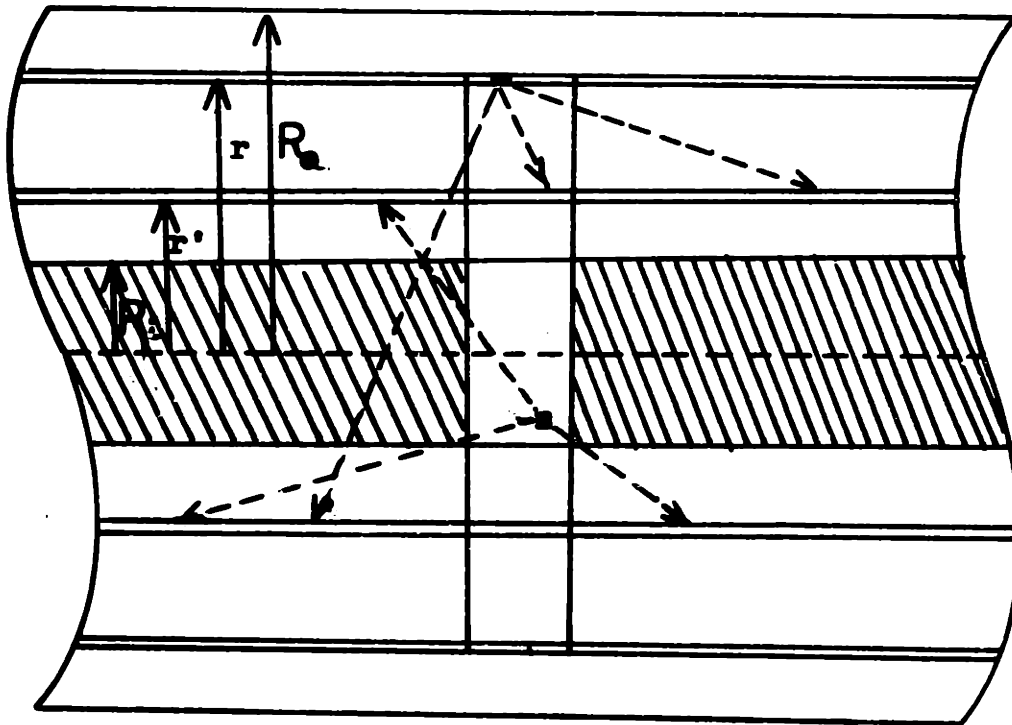
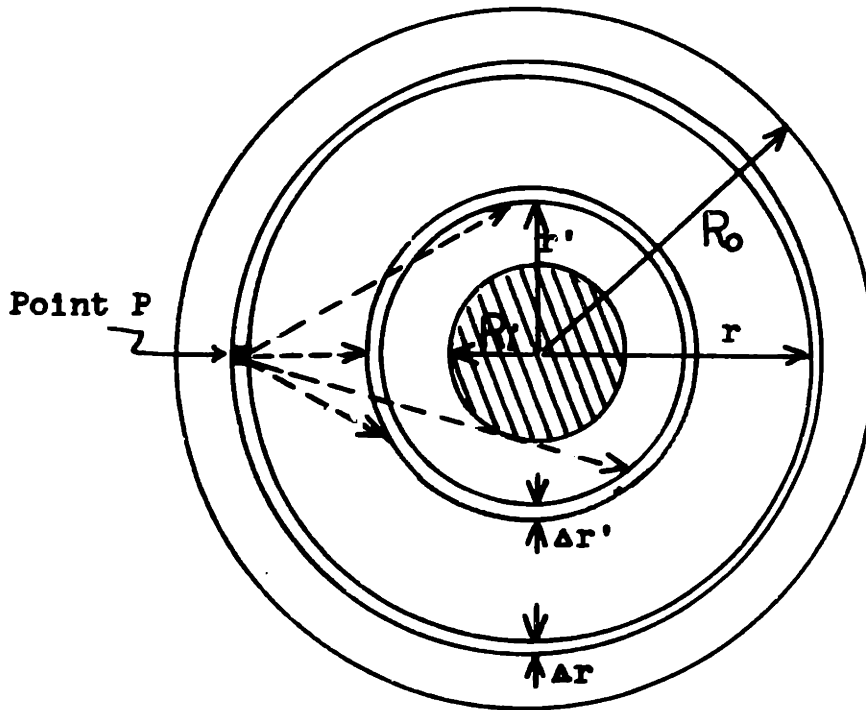


Figure A2.1 Two different view points for the derivation of geometric factor of negative corona.

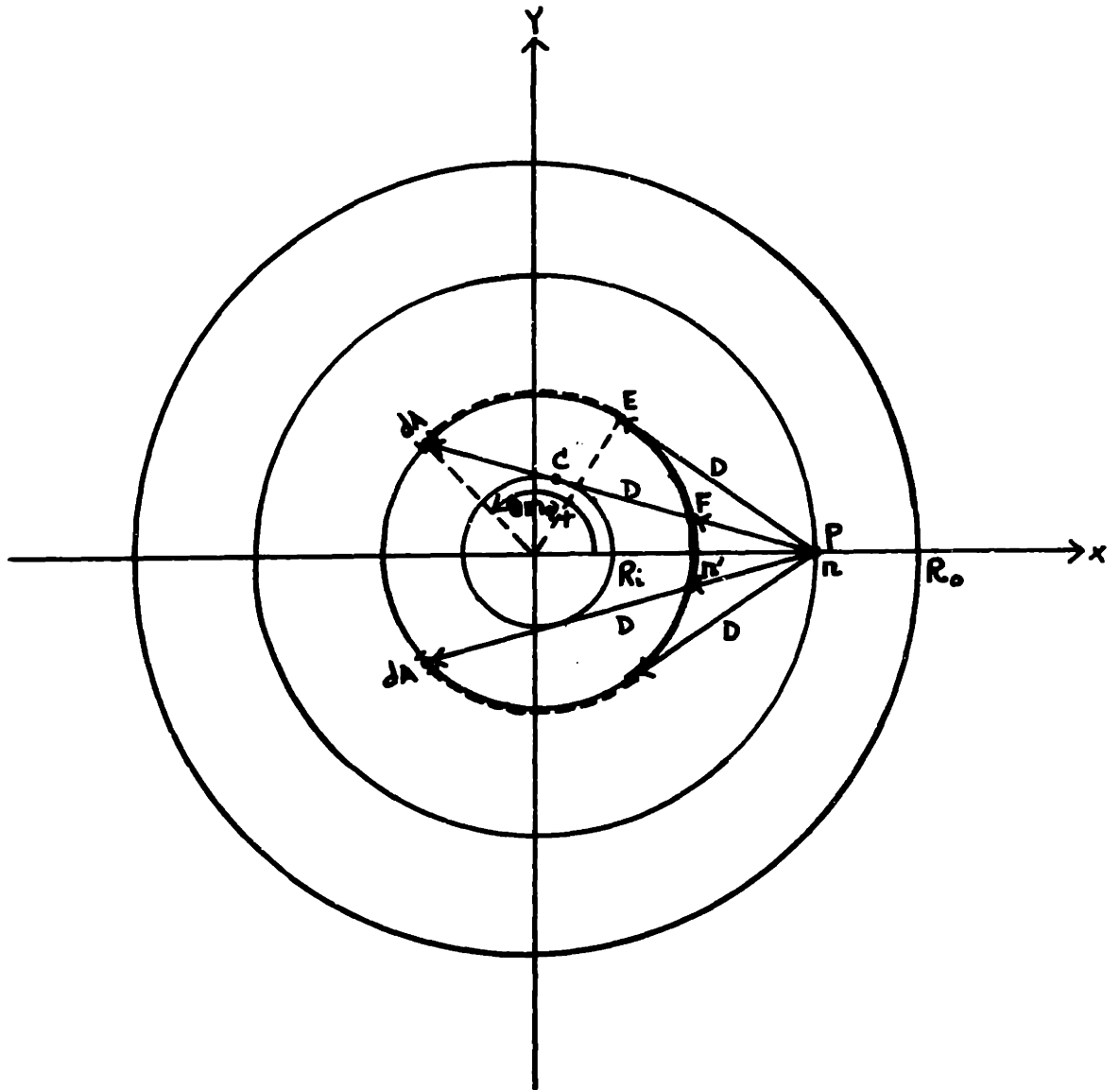


Figure A2.2 Definition of variables used in the derivation.

P. intersect the cylinder of radius r' twice except at the point of tangency, E.

Again assume

$$K \cong G' \exp(-\mu_{\text{eff}}(r - r')) \quad (5)$$

where G' is a new geometric factor

$$\begin{aligned} G' &= \frac{r'}{\pi} \int_0^{\theta_{\text{max}}} \frac{(r \cos \theta - r') d\theta dz}{(r^2 + r'^2 - 2rr' \cos \theta + z^2)^{3/2}} \\ &= \frac{r'}{\pi} \int_0^{\theta_{\text{max}}} \frac{(r \cos \theta - r') d\theta}{r^2 + r'^2 - 2rr' \cos \theta} \end{aligned} \quad (6)$$

$$= \frac{1}{\pi} 2 \tan^{-1} \left(\frac{r + r'}{r - r'} \right) - \cos^{-1} \left(\frac{r'}{r} \right)$$

$$- \frac{1}{2\pi} \left[2 \tan^{-1} \left(\left(\frac{r + r'}{r - r'} \right) \tan \left(\frac{\theta_{\text{max}}}{2} \right) \right) - \theta_{\text{max}} \right]$$

The second term is independent of variable r' because it is the percentage blocked by the inner cylinder.

Further rearrangement of terms gives

$$G' = 1 - \frac{1}{\pi} \cos^{-1} \left(\frac{2r'^2 - r^2}{r^2} \right) \quad (7)$$

$$- \frac{1}{2\pi} \left[2 \tan^{-1} \left(\left(\frac{r + r'}{r - r'} \right) \tan \left(\frac{\theta_{\text{max}}}{2} \right) \right) - \theta_{\text{max}} \right]$$

Appendix 3

Calculating an Approximate Value for μ_{eff}

$$K \cong G \exp(-\mu_{\text{eff}}(r-r')) \quad (1)$$

μ_{eff} is approximated by the average of many exact values of effective photon absorption rate, when reducing a three dimensional problem into two dimensions.

$$\mu_{\text{eff}} \cong \frac{1}{N} \sum_{i=1}^N \frac{1}{(r_1 - r')} \ln\left(\frac{G(r', r_1)}{K(r', r_1)}\right) \quad (2)$$

where $r_1 = R_1 + i\Delta r,$ (3)

$r' = R_1,$ (4)

and $r_N = R_0.$ (5)

r' is assigned to be R_1 because most of the photons are emitted near the surface of inner conductor. G and K are described by equations A1.25 and A1.19 respectively. K has to be integrated numerically. To make the integration bounded, let

$$z = \tan \varphi. \quad (6)$$

$$dz = (1 + \tan^2 \varphi) d\varphi. \quad (7)$$

Then (8)

$$K = \frac{r}{\pi} \int_0^{\pi/2} \int_0^{\theta_{\text{max}}} \frac{(r - r' \cos \theta) \exp(-\mu D)}{D^3} (1 + \tan^2 \varphi) d\varphi d\theta$$

where $D = (r^2 + r'^2 - 2rr' \cos \theta + \tan^2 \varphi)^{\frac{1}{2}}$ (9)

For $\mu = .01 \text{ cm}^{-1}$

$$\mu_{\text{eff}} \cong 1.8 \mu_p. \quad (10)$$

Because μ_p is a very small number, variations of μ_{eff} from μ_p is not large. The error produced in the photoionization term is small.

Appendix 4

Program Listing for Positive Corona

To use the following program, the data should be inputted in the order specified below.

1. N - This is the number of divisions. When end points are included. There are N+1 grid points.
2. SAVE - Input 'YES' if the data from previous case is saved for use in the present case. Otherwise input 'NO'.
3. CARD_IN - Input 'YES' if there are any input data. Note that SAVE and CARD_IN cannot both be 'YES' at the same time.
4. CARD_OUT- Input 'YES' if data from this case is desired to be outputted on cards when iterations did not converge in the specified limit. Otherwise input 'NO'.
5. R_INNER - Input the radius of the inner conductor in units of centimeters.
6. DELTA_R - Input the grid size in centimeters.
7. INCR - For every print out of data associated with a grid point, INCR - 1 grid points are skipped. For example, if the input is 6, every 6th grid point will be printed starting at the inner cylinder.

8. M - The Maximum number of iterations allowed.
9. OUT_NUM - When the number of iterations performed become greater than M - OUT_NUM the data of that iteration will be printed. The input should be within the following limits:

$$1 \leq \text{OUT_NUM} \leq M.$$

10. E0 - Absolute value of the electric field at the surface of the inner conductor when no space charges present. This is same as specifying the voltage applied between conductors.

$$\text{Voltage} = E0 R_1 \ln(R_0/R_1)$$

11. ENTERJE - Input the boundary condition for the electron current density at the outer radius in units of amp/cm². For positive corona this quantity should be greater than or equal to zero.
12. MOB_P_I - Input the mobility of positive ions in units of cm²/sec-volt.
13. MOB_N_I - Input the mobility of the negative ions in units of cm²/sec-volt.
14. A(1) - The constant A used in α for E/p = 40 volts/cm-mm Hg.
15. B(1) - The constant B used in η for E/p = 40 volts/cm-mm Hg.
16. A(2) - The constant A used in α for E/p = 40 volts/cm-mm Hg.

17. B(2) - The constant B used in η for $E/p = 40$ volts/cm-mm Hg.
18. PHOTOMU - This is one over the distance a photon travels before it decays to $1/e$ of its original value. The units of PHOTOMU is in cm^{-1} .
19. EFF - The number of photons created in the frequency of interest for every electron created by electron-neutral collision.
20. MOD_ETA - This is a constant by which the whole attachment curve is multiplied by, so as to increase or decrease η . If η is not to be changed from the fitted values, Then set MOD_ETA to 1.
21. OVER - This is the relaxation parameter. If OVER is set greater than 1, it effectively increase the value of EFF to $\text{OVER} \cdot \text{EFF}$, and it is used when iterations converges too slowly. Normally set over to 1.
22. EST - This is the estimated current for the specified voltage. If OVER is 1, EST can be set to any value. The units of EST is in amp/cm^2 .
23. RECOMB - This is the recombination coefficient for

positive and negative ions with units in
cm³/sec.

24. PAIRS - Input the number of electron-ion pairs
created by cosmic radiation percm³ per
second.

If CARD_IN is 'YES' then the charge density data
cards should be placed after the input data PAIRS. To
terminate the run, place the following card at the
very end of the input data.

-1 'NO' 'NO' 'NO'

```

SS: PROCEDURE OPTIONS (MAIN);
/*****
/* ** POSITIVE CORONA ** ANODE CORONA **
/* ** THIS PROGRAM CALCULATES THE STEADY STATE CHARGE DENSITY
/* ** WHEN THE SOURCE IS ELECTRON CURRENT DENSITY AT THE OUTER
/* ** BOUNDARY AND PHOTOIONIZATION IN THE INTERIOR. PREVIOUS
/* ** RESULTS WILL BE USED IF ANY. OVERSHUT PARAMETER IS USED
/* ** FOR FASTER CONVERGENCE. RUNGE-KUTTA METHOD IS USED IN THE
/* ** INTEGRATION.
*****/
DECLARE (R_INNER, /* RADIUS OF INNER CYLINDER
OVER, /* ADJUSTED OVERSHUT PARAMETER.
R_OLD, /* INNER RADIUS
MOD_ETA, /* FACTOR BY WHICH ETA IS CHANGED
DELTA_R) FIXED (7,4),
(N, /* ACTUAL NUMBER OF DIVISIONS.
INCR, /* OUTPUT INCREMENT.
OUT_NUM, /* # OF TIMES OUTPUT WILL BE PRINTED
X, /* GRID PT. E/P=40
Y, /* GRID PT. E/P=25
I, J, K, CASE, M, T) FIXED(15,0) BINARY,
(SAVE, /* SAVING PREVIOUS DATA?
CARD_IN, /* ANY INPUT DATA
CARD_OUT) /* OUTPUT DATA ON CARDS
CHARACTER(3),
(SUM1, SUM2,
PAIRS, /* ELECTRON/ION PAIRS/CC BY COSMIC RAY
COSMIC, /* PAIRS*1.602E-19
RECOMB, /* RECOMBINATION COEFFICIENT
A(2),B(2),AA(2),BB(2), /* USED IN ALPHA
EO, /* VALUE OF E
TEMP, TEMP1, TEMP2, /* APPLIED VOLTAGE
VOLT, /* DIFFERENT BOUNDARY CONDITIONS
ENTERJE, /* R(K) * J_E(K)
R_JE,

```

```

POS-0001
POS-0002
POS-0003
POS-0004
POS-0005
POS-0006
POS-0007
POS-0008
POS-0009
POS-0010
POS-0011
POS-0012
POS-0013
POS-0014
POS-0015
POS-0016
POS-0017 1-149
POS-0018 49
POS-0019 1
POS-0020
POS-0021
POS-0022
POS-0023
POS-0024
POS-0025
POS-0026
POS-0027
POS-0028
POS-0029
POS-0030
POS-0031
POS-0032
POS-0033
POS-0034
POS-0035
POS-0036

```

```

EST,                               /* ESTIMATE OF FINAL TOTAL CURRENT.          POS-0037
R_J_N,                             /* R * J_N_I                                 POS-0038
R_J_P,                             /* R * J_P_I                                 POS-0039
K0, K1, K2, K3,                   /* KK/R(0) IS E(0) FOR NO SPACE CHG        POS-0040
K0P, K1P, K2P, K3P,              /* MOBILITY OF NEGATIVE IONS                POS-0041
K0N, K1N, K2N, K3N,              /* MOBILITY OF POSITIVE IONS                POS-0042
KK,                                /* PHOTON IONIZATION COEFFICIENT           POS-0043
MOB_N_I,                           /* PHOTON ABSORPTION COEFFICIENT *1.86     POS-0044
MOB_P_I,                           /* NUMBER OF PHOTONS CREATED PER ELECTRON   POS-0045
PHOTOMU,                           CREATED                                     POS-0046
ABS_MU,                             /* CONSTANT                                  POS-0047
EFF,                                /* CHANGE OF TOTAL I BETWEEN ITERATIONS    POS-0048
INT,                                /* FOR CALCULATING GEOMETRIC FACTOR       POS-0049
PI,                                 /* EPSILON) BINARY FLOAT,                  POS-0050
OLD_CHG, NEW_CHG,                 /* THE SIZE OF THE FOLLOWING ARRAYS IS NOT FIXED. THEY WILL BE * /
I_DIFF,                             /* ALLOCATED WHEN N IS KNOWN.              POS-0051
R_OUT, ANGLE,                      /* *****                                  POS-0052
EPSILON) BINARY FLOAT,             /* *****                                  POS-0053
*****                              /* *****                                  POS-0054
/* THE SIZE OF THE FOLLOWING ARRAYS IS NOT FIXED. THEY WILL BE * /
/* ALLOCATED WHEN N IS KNOWN.      /* *****                                  POS-0055
*****                              /* *****                                  POS-0056
(R(*) FIXED (8,5) CONTROLLED,     /* *****                                  POS-0057
(CHARGE(*),                        /* TOTAL CHARGE WITHIN A CERTAIN RADIUS.   POS-0058
J_P_I(*),                          /* POSITIVE ION CURRENT DENSITY            POS-0059
J_N_I(*),                          /* NEGATIVE ION CURRENT DENSITY           POS-0060
J_E(*),                            /* ELECTRON CURRENT DENSITY                POS-0061
E(*),                              /* ELECTRIC FIELD                          POS-0062
CURRENT(*),                        /* TOTAL CURRENT.                          POS-0063
VOLTAGE(*),                        /* VOLTAGE AS DEFINED FROM R(0)           POS-0064
ALPHA(*),                          /* NUMBER OF ELECTRONS CREATED /CM        POS-0065
ETA(*),                            /* NUMBER OF ELECTRONS ATTACHED/CM       POS-0066
ALPHA2(*), ETA2(*),               /* SOURCE DUE TO PHOTOIONIZATION         POS-0067
PHOTO_ELE(*),                      /* *****                                  POS-0068
PHOTO_ELE2(*),                    /* *****                                  POS-0069
*****                              /* *****                                  POS-0070
*****                              /* *****                                  POS-0071
*****                              /* *****                                  POS-0072

```

```

G(*),          /* GEOMETRIC FACTOR
TOTAL_CUR(*), /* VALUE OF SUM OF ALL THE CURRENT.
KP(*),         /* KOP+2*K1P+2*K2P+K3P
KN(*),         /* KON+2*K1N+2*K2N+K3N
P_I_CHG_D(*), /* POSITIVE ION CHARGE DENSITY
N_I_CHG_D(*), /* NEGATIVE ION CHARGE DENSITY
ELE_CHG_D(*), /* ELECTRON CHARGE DENSITY
BINARY FLOAT CONTROLLED;

/*****
/* THE PROCEDURE E_FIELD CALCULATES THE ELECTRIC FIELD WHEN THE
/* VOLTAGE AND CHARGE DENSITIES ARE KNOWN BETWEEN THE TWO
/* ELECTRODES. SUM2 IS CALCULATED IN THE NO_SAVE DO LOOP OF THE
/* MAIN PROCEDURE.
/*****
E_FIELD: PROCEDURE;
ALLOCATE CHARGE (0:N);
VOLT = KK * LOG(R(N)/R(0));
SUM1 = 0;
CHARGE(0) = 0;
OLD_CHG = R(0) * DELTA_R * (ELE_CHG_D(0) +
N_I_CHG_D(0) + P_I_CHG_D(0) )/2;
DO J = 1 TO N;
NEW_CHG = R(J) * DELTA_R * ( ELE_CHG_D(J) +
N_I_CHG_D(J) + P_I_CHG_D(J) ) /2;
CHARGE(J) = (OLD_CHG+ NEW_CHG) + CHARGE(J-1);
OLD_CHG = NEW_CHG;
SUM1 = SUM1 + CHARGE(J) / R(J);
END;
SUM1 = SUM1 - CHARGE (N) /2/R(N);
E(0) = (VOLT /DELTA_R-SUM1/EPSILON) /
(R(0) * (SUM2 + .5 /R(N) ) + .5);
X = 0;
Y = N;
DO J = 1 TO N;
E(J) = ( CHARGE(J) /EPSILON+ R(0)*E(0) )/R(J);

```

```

POS-0073
POS-0074
POS-0075
POS-0076
POS-0077
POS-0078
POS-0079
POS-0080
POS-0081
POS-0082
POS-0083
POS-0084
POS-0085
POS-0086
POS-0087
POS-0088
POS-0089
POS-0090
POS-0091
POS-0092
POS-0093
POS-0094
POS-0095
POS-0096
POS-0097
POS-0098
POS-0099
POS-0100
POS-0101
POS-0102
POS-0103
POS-0104
POS-0105
POS-0106
POS-0107
POS-0108

```

POS-0109
 POS-0110
 POS-0111
 POS-0112
 POS-0113
 POS-0114
 POS-0115
 POS-0116
 POS-0117
 POS-0118
 POS-0119
 POS-0120
 POS-0121
 POS-0122
 POS-0123
 POS-0124
 POS-0125¹
 POS-0126²⁵
 POS-0127¹
 POS-0128
 POS-0129
 POS-0130
 POS-0131
 POS-0132
 POS-0133
 POS-0134
 POS-0135
 POS-0136
 POS-0137
 POS-0138
 POS-0139
 POS-0140
 POS-0141
 POS-0142
 POS-0143
 POS-0144

```

IF E(J) >= 30400 THEN X=J;
  ELSE IF E(J) >= 19000 THEN Y =J;
END;
FREE CHARGE;
END E_FIELD;

/*****
/* THE PROCEDURE OUT IS CALLED WHEN OUTPUT IS DESIRED.
/* THE FIRST DO LOOP CALCULATE THE VOLTAGE AS A FUNCTION OF
/* POSITION ONCE THE ELECTRIC FIELD DISTRIBUTION IS KNOWN. IT
/* PROVIDES A CHECK ON THE ACCURACY OF THE ELECTRIC FIELD.
*****/
OUT: PROCEDURE;
  ALLOCATE VOLTAGE(0:N);
  VOLTAGE (N) =0;
  DO J = N-1 TO 0 BY -1;
    VOLTAGE(J) = VOLTAGE(J+1) + E(J) * DELTA_R;
  END;

/*****
/* NOW OUTPUT THE VALUES ASSOCIATED WITH INPUT DATA.
*****/
PUT LIST ('CASE:|CASE|', '|||'|TH. ITERATION.
  '|DELTA_R = '|DELTA_R||', OVERSHUT = '|
OVER||', RECOMBINATION = '|RECOMB) PAGE;
PUT LIST (' PHOTO_MU = '|PHOTOMU||', EFF = '|EFF|
  ' MOD_ETA = '|MOD_ETA) SKIP;
PUT LIST (' MOB_P_I = '|MOB_P_I||', MOB_N_I = '|MOB_N_I
  '| VELOCITY OF ELECTRON IS 4.5E5*E/P '|
  'FOR E/P<25. IT IS 2.5E5*E/P+5.E6 FOR '|
  'E/P>=25.') SKIP;
PUT LIST ('AT R = '|R(0)||'CM J_P_I = 0.
  'VOLTAGE = '|VOLT||', E = '|KK/R(0)||
  ' (WHEN FREE OF SPACE CHARGES) ') SKIP;
PUT LIST ('AT R = '|R(N)||'CM J_N_I = 0.
  
```



```

***** VOLTAGE = 0. J_E = '||J_E(N)) SKIP:
/* THE NEXT 3 PUT EDIT STATEMENTS PRINT OUT THE HEADINGS FOR THE */
/* LIST OF DATA.
*****
PUT EDIT ('RADIUS', 'E FIELD', 'VOLTAGE', 'POSITIVE',
'NEGATIVE', 'ELECTRON', 'POSITIVE', 'NEGATIVE',
'ELECTRON', 'TOTAL', 'ALPHA', 'ETA', 'PHOTO_ELE')
( A(6), X(1), A(7), X(2), A(9), X(3), A(8), X(3),
A(8), X(3), A(8), X(2), A(8), X(4), A(8), X(4),
A(8), X(3), A(5), X(4), A(5), X(4), A(3), X(4), A(9))
SKIP(2);

PUT EDIT ('ION CHARGE', 'ION CHARGE', 'CHARGE',
'ION CURRENT', 'ION CURRENT', 'CURRENT', 'CURRENT')
( X(28), A(10), X(1), A(10), X(1), A(6), X(4),
A(11), X(1), A(11), X(1), A(7), X(4), A(7)) SKIP:

PUT EDIT ('DENSITY', 'DENSITY', 'DENSITY', 'DENSITY',
'DENSITY', 'DENSITY')
( X(28), A(7), X(4), A(7), X(4), A(7), X(3),
A(7), X(5), A(7), X(5), A(7), X(6) ) SKIP:
*****
/* THIS SECTION ACTUALLY OUTPUT THE DATA . ONLY ONE OUT OF A */
/* SPECIFIED NUMBER OF GRID POINTS IS ACTUALLY PRINTED TO SAVE */
/* PRINTING COST. THE VARIABLE INCR TAKES CARE OF THE SPECIFIED */
/* NUMBER.
*****
DO J=0 TO N BY INCR:
PUT EDIT (R(J), E(J), VOLTAGE(J), P_I_CHG_D(J),
N_I_CHG_D(J), ELE_CHG_D(J), J_P_I(J), J_N_I(J),
J_E(J), CURRENT(J), ALPHA(J), ETA(J), PHOTO_ELE(J))
( F(6,4), E(11,4), E(10,3), X(1), E(10,3), X(1),
E(10,3), X(1), E(10,3), E(11,4), E(11,4),
E(11,4), E(11,4), E(9,2), E(9,2), E(9,2))SKIP:

END:
FREE VOLTAGE:

END OUT:

```

```

POS-0145
POS-0146
POS-0147
POS-0148
POS-0149
POS-0150
POS-0151
POS-0152
POS-0153
POS-0154
POS-0155
POS-0156
POS-0157
POS-0158
POS-0159
POS-0160
POS-0161
POS-0162
POS-0163
POS-0164
POS-0165
POS-0166
POS-0167
POS-0168
POS-0169
POS-0170
POS-0171
POS-0172
POS-0173
POS-0174
POS-0175
POS-0176
POS-0177
POS-0178
POS-0179
POS-0180

```

POS-0181
 POS-0182
 POS-0183
 POS-0184
 POS-0185
 POS-0186
 POS-0187
 POS-0188
 POS-0189
 POS-0190
 POS-0191
 POS-0192
 POS-0193
 POS-0194
 POS-0195
 POS-0196
 POS-0197
 POS-0198
 POS-0199
 POS-0200
 POS-0201
 POS-0202
 POS-0203
 POS-0204
 POS-0205
 POS-0206
 POS-0207
 POS-0208
 POS-0209
 POS-0210
 POS-0211
 POS-0212
 POS-0213
 POS-0214
 POS-0215
 POS-0216

```

/*****
/* DATA ARE INPUTED AND VALUES INITIALIZED IN THE NEXT SECTION */
/* BEFORE THE II DO LOOP. */
/*****
/*****
EPSILON= 8.854E-14; /* COULOMB /VOLTS /CM */
PI = 3.14159;
CASE = 0;
GET LIST (N, SAVE, CARD_IN, CARD_OUT);
R_OLD = -1;
/*****
/* THE CONDITION THAT THE PROGRAM WILL CONTINUE IS THAT THE VALUE */
/* OF N INPUTED IS GREATER THAN ZERO. THE MAIN PORTION OF */
/* THE PROGRAM IS LOCATED IN THE CC DO LOOP. */
/*****
CC: DO WHILE (N>0);
CASE = CASE +1;
GET LIST (R_INNER, DELTA_R, INCR, M, OUT_NUM, EO, ENTERJE,
MOB_P_I, MOB_N_I, A(1), B(1), A(2), B(2), PHOTOMU,
EFF, MOD_ETA, OVER, EST, RECOMB, PAIRS);
ALLOCATE TOTAL_CUR(0:M);
KK = EO*R_INNER;
TOTAL_CUR(*) = 0;
TOTAL_CUR(0) = -1;
I-DIFF = 10;
COSMIC = PAIRS * 1.602E-19;
AA(1) = A(1)*760;
AA(2) = A(2)*760;
BB(1) = B(1)*760;
BB(2) = B(2)*760;
/*****
/* IF NO DATA IS SAVED, MOST OF THE VARIABLES WILL HAVE TO BE */
/* INITIALIZED IN THE NO_SAVE DO LOOP. ELECTRIC FIELD WITHOUT */
/* SPACE CHARGES IN THE FORM OF KK/R IS CALCULATED. IF DATA IS */
/* SAVED, THEN N AND INNER AND OUTER CONDUCTORS ARE ASSUMED TO */
/* BE THE SAME. */

```

```

/*****
IF SAVE = 'NO' THEN
NO_SAVE: DO;
    ALLOCATE R(O:N), J_E(O:N), E(O:N), ELE_CHG_D(O:N),
        P_I_CHG_D(O:N), N_I_CHG_D(O:N), J_N_I(O:N), J_P_I(O:N),
        ALPHA(O:N), ETA(O:N), PHOTO_ELEMENT(O:N), CURRENT(O:N);
    R(O) = R_INNER;
    SUM2 = 0;
    X = 0;
    Y = N;
    DO K = 1 TO N-1;
        R(K) = R(K-1) + DELTA_R;
        SUM2 = SUM2 + 1./R(K);
        E(K) = KK/R(K);
        IF E(K) >= 30400 THEN X = K;
        ELSE IF E(K) >= 19000 THEN Y = K;
    END;
    E(O) = KK/R(O);
    R(N) = R(N-1) + DELTA_R;
    E(N) = KK/R(N);
/*****
/***** THE FOLLOWING DO LOOP INPUT DATA FROM PREVIOUS RUNS SO AS TO */
/***** CONTINUE THE ITERATION PROCESS IF DESIRED. */
/***** IF CARD_IN = 'YES' THEN */
DO;
    GET LIST ((ELE_CHG_D(K) DO K = 0 TO N));
    GET LIST ((P_I_CHG_D(K) DO K = 0 TO N));
    GET LIST ((N_I_CHG_D(K) DO K = 0 TO N));
END;
/*****
/***** THE FOLLOWING SECTION CALCULATES THE GEOMETRIC FACTOR. */
/***** IF (CASE = 1) & (R_OLD = R_INNER) THEN FREE G;
/***** DO;

```

POS-0217

POS-0218

POS-0219

POS-0220

POS-0221

POS-0222

POS-0223

POS-0224

POS-0225

POS-0226

POS-0227

POS-0228

POS-0229

POS-0230

POS-0231

POS-0232

POS-0233

POS-0234

POS-0235

POS-0236

POS-0237

POS-0238

POS-0239

POS-0240

POS-0241

POS-0242

POS-0243

POS-0244

POS-0245

POS-0246

POS-0247

POS-0248

POS-0249

POS-0250

POS-0251

POS-0252

POS-0253
 POS-0254
 POS-0255
 POS-0256
 POS-0257
 POS-0258
 POS-0259
 POS-0260
 POS-0261
 POS-0262
 POS-0263
 POS-0264
 POS-0265
 POS-0266
 POS-0267
 POS-0268
 POS-0269
 POS-0270
 POS-0271
 POS-0272
 POS-0273
 POS-0274
 POS-0275
 POS-0276
 POS-0277
 POS-0278
 POS-0279
 POS-0280
 POS-0281
 POS-0282
 POS-0283
 POS-0284
 POS-0285
 POS-0286
 POS-0287
 POS-0288

```

ALLOCATE G(O:N);
R_OUT = 10;
DO K = 0 TO N;
  TEMP = (R(O)**2 - SQRT( (R(K)**2 - R(O)**2) *
    (R_OUT**2 - R(O)**2) ) ) / R_OUT / R(K);
  ANGLE = PI/2 - ATAN(TEMP/SQRT(1-TEMP**2));
  G(K) = (ANGLE/2 + ATAN( (R_OUT+R(K)) * TAN(ANGLE/2)
    / (R_OUT-R(K)) ) ) / PI;
END;
END;
END NO_SAVE;

/*****
/* THE ELECTRON CURRENT DENSITY DISTRIBUTION IS INITIALIZED IF */
/* PREVIOUS DATA IS AVAILABLE . PHOTOIONIZATION TERM CAN BE */
/* CALCULATED IF THE ELECTRON CURRENT DENSITY IS KNOWN. */
/*****
IF SAVE = 'YES' | CARD_IN = 'YES' THEN
DO;
  CALL E_FIELD;
  DO K = 0 TO Y;
    J_E(K) = -(5.E6+329*E(K))*ELE_CHG_D(K);
  END;
  DO K = Y+1 TO N;
    J_E(K) = -592 * E(K) * ELE_CHG_D(K);
  END;
END;

/*****
/* THE ITERATION PROCESS IS PERFORMED WITHIN THE II DO LOOP. */
/* TO GUARD AGAINST THE UNSTABLE CASE, THE MAXIMUM NUMBER OF */
/* ITERATIONS ALLOWED IS M. HOWEVER IF THE TOTAL CURRENT STOPPED */
/* INCREASING AND THE DIFFERENCE BETWEEN PRESENT AND PREVIOUS */
/* TOTAL CURRENT IS WITHIN .5 PERCENT OF THE PRESENT TOTAL */
/* CURRENT, AND THE OVERSHUT PARAMETER( OVER) IS SET AT 1, THEN */

```

```

/* THE ITERATION PROCESS STOPS. THE OVERSHUT PARAMETER IS TO */
/* INCREASE THE GROWTH RATE. IF THE TOTAL CURRENT REACHED THE */
/* ESTIMATED TOTAL CURRENT, THE OVERSHUT PARAMETER IS SET TO 1. */
/* WHEN OVER IS NOT 1, THE PROGRAM IS ACTUALLY SOLVING A */
/* DIFFERENT PROBLEM. */
/* ***** */
11: DO I = 1 TO M WHILE ((I_DIFF>0 | I_DIFF<-.005) | OVER=1);
    IF TOTAL_CUR(I-1) >= EST THEN OVER =1;
    ALLOCATE ALPHA2(0:N), ETA2(0:N), PHOTO_ELE2(0:N);
    J_N_I(N) =0;
    J_E(N) = ENTERJE;
/* ***** */
/* ALPHA AND ETA ARE CALCULATED. T=1 IS FOR THE CASE E/P>=40 IN */
/* THE CALCULATION OF ALPHA. */
/* ***** */
T=1;
DO K = 0 TO N;
  IF K=X THEN T=2;
  E0 = E(K);
  ALPHA(K) = AA(T)*EXP(-BB(T)/E0);
  IF K <= Y THEN
    ETA(K) =(1.203E-8*E0 - .000567*E0 + 10.12)*MOD_ETA;
  ELSE ETA(K) = (1.545E-4*E0 + .866)*MOD_ETA;
END;
/* ***** */
/* ALPHA2 AND ETA2 ARE FOR THE VALUES OF ALPHA AND ETA HALF WAY */
/* BETWEEN THE GRID POINTS. THIS IS NECESSARY FOR RUNGE-KUTTA */
/* INTEGRATION. */
/* ***** */
T=1;
DO K = 2 TO N-1;
  IF K=X THEN T=2;
  E0 = (-E(K-2)-E(K+1)+9*(E(K-1)+E(K)))/16;
  ALPHA2(K) = AA(T) * EXP(-BB(T)/E0);
  IF K <= Y THEN
    ETA2(K)=(1.203E-8*E0 - .000567*E0 + 10.12)*MOD_ETA;

```

```

POS-0289
POS-0290
POS-0291
POS-0292
POS-0293
POS-0294
POS-0295
POS-0296
POS-0297
POS-0298
POS-0299
POS-0300
POS-0301
POS-0302
POS-0303
POS-0304
POS-0305 -157
POS-0306
POS-0307
POS-0308
POS-0309
POS-0310
POS-0311
POS-0312
POS-0313
POS-0314
POS-0315
POS-0316
POS-0317
POS-0318
POS-0319
POS-0320
POS-0321
POS-0322
POS-0323
POS-0324

```

PUS-0325
 PUS-0326
 PUS-0327
 PUS-0328
 PUS-0329
 PUS-0330
 PUS-0331
 PUS-0332
 PUS-0333
 PUS-0334
 PUS-0335
 PUS-0336
 PUS-0337
 PUS-0338
 PUS-0339
 PUS-0340
 PUS-0341
 PUS-0342
 PUS-0343
 PUS-0344
 PUS-0345
 PUS-0346
 PUS-0347
 PUS-0348
 PUS-0349
 PUS-0350
 PUS-0351
 PUS-0352
 PUS-0353
 PUS-0354
 PUS-0355
 PUS-0356
 PUS-0357
 PUS-0358
 PUS-0359
 PUS-0360

```

ELSE ETA2(K) = (1.545E-4*EO + .866)*MOD_ETA;
END;
EO = (5*E(N) + E(N-3) + 15*E(N-1) - 5* E(N-2) ) / 16;
ALPHA2(N) = AA(I) * EXP (-BB(I)/EO);
IF EO >= 19000 THEN
ETA2 (N) = (1.203E-8*EO*EO -.000567*EO + 10.12)*MOD_ETA;
ELSE ETA2(N) = (1.545E-4*EO + .866)*MOD_ETA;
EO = (5*E(O) + E(3) + E(1) * 15 - 5*E(2)) / 16;
IF EO >= 30400 THEN T=1;
ELSE T=2;
ALPHA2(1) = AA(I) * EXP( -BB(I)/EO);
IF EO >= 19000 THEN
ETA2 (1) = (1.203E-8*EC*EO -.000567*EO + 10.12)*MOD_ETA;
ELSE ETA2(1) = (1.545E-4*EO + .866)*MOD_ETA;

```

```

/*****
/* IF THERE IS NO PREVIOUS DATA USED IN THE FIRST ITERATION, */
/* PHOTOIONIZATION IS ASSUMED NOT TO BE PRESENT SINCE ELECTRON */
/* CHARGE DENSITY IS NOT KNOWN. */
/*****
IF I = 1 & SAVE = 'NO' & CARD_IN = 'NO' THEN

```

```

DO;
PHOTO_ELE(*) = 0;
PHOTO_ELE2(*) = 0;
P_I_CHG_D(*) = 0;
N_I_CHG_D(*) = 0;
END;

```

```

/*****
/* CALCULATE PHOTOIONIZATION TERM. */
/*****

```

```

ELSE DO;
PHOTO_ELE(O), PHOTO_ELE2(O) = 0;
TEMP = PHOTOMU * EFF* CVER;
ABS_MU = PHOTOMU * 1.8;
KU = ALPHA(O) * R(O) * J_E(O) * EXP( ABS_MU * R(O) ) / 8;

```

POS-0361
 POS-0362
 POS-0363
 POS-0364
 POS-0365
 POS-0366
 POS-0367
 POS-0368
 POS-0369
 POS-0370
 POS-0371
 POS-0372
 POS-0373
 POS-0374
 POS-0375
 POS-0376
 POS-0377
 POS-0378
 POS-0379
 POS-0380
 POS-0381
 POS-0382
 POS-0383
 POS-0384
 POS-0385
 POS-0386
 POS-0387
 POS-0388
 POS-0389
 POS-0390
 POS-0391
 POS-0392
 POS-0393
 POS-0394
 POS-0395
 POS-0396

```

INT=0;
DO K = 1 TO N;
  TEMP1 = (R(K)+R(K-1))/2;
  K1 = ALPHA2 (K) *(J_E(K)+J_E(K-1) ) * TEMP1 *
    (G(K)+G(K-1)) * EXP(ABS_MU*TEMP1)/16;
  INT = INT + KO +K1;
  PHOTO_ELE2(K) = INT * TEMP*EXP(-ABS_MU*TEMP1);
  KO = ALPHA(K) * R(K)*J_E(K)*G(K)*EXP(ABS_MU*R(K))/4;
  INT = INT + KO +K1;
  PHOTO_ELE(K) = INT * TEMP * EXP (-ABS_MU * R(K));
END;
END;

/*****
/* RUNGE-KUTTA METHOD IS USED FOR INTEGRATION BECAUSE IT IS SELF */
/* STARTING AND GENERALLY RELIABLE METHOD. HOWEVER, IT IS */
/* PROBABLY MORE EXPENSIVE THAN SOME OTHER METHODS. THE */
/* PROCESSES INCLUDED ARE ELECTRON AVALANCHE, ATTACHMENT, COSMIC */
/* RADIATION, PHOTOIONIZATION, AND RECOMBINATION. */
/*****
ALLOCATE KP(O:N), KN(O:N);
R_JE = ENTERJE * R(N);
TEMP1=0;
DO K = N TO 1 BY -1;
  KON = ETA(K)*R_JE + TEMP1;
  KOP = ALPHA(K)*R_JE + PHOTO_ELE(K) + COSMIC*R(K) +
    TEMP1;
  TEMP = DELTA_R *(KOP-KON)/2 + R_JE;
  TEMP2=RECOMB*(P_I_CHG_D(K)+P_I_CHG_D(K-1))*(R(K)+R(K-1))*
    (N_I_CHG_D(K) + N_I_CHG_D(K-1))/8/1.602E-19;
  KIN = TEMP * ETA2(K) + TEMP2;
  KIP = TEMP*ALPHA2(K) + PHOTO_ELE2(K) + TEMP2 +
    COSMIC*(R(K)+R(K-1))/2;
  TEMP = DELTA_R *(KIP-KIN)/2 + R_JE;
  K2N = TEMP * ETA2(K) + TEMP2;
  K2P = TEMP*ALPHA2(K) + PHOTO_ELE2(K) + TEMP2 +
  
```

PUS-0397
 PUS-0398
 PUS-0399
 PUS-0400
 PUS-0401
 PUS-0402
 PUS-0403
 PUS-0404
 PUS-0405
 PUS-0406
 PUS-0407
 PUS-0408
 PUS-0409
 PUS-0410
 PUS-0411
 PUS-0412
 PUS-0413
 PUS-0414
 PUS-0415
 PUS-0416
 PUS-0417
 PUS-0418
 PUS-0419
 PUS-0420
 PUS-0421
 PUS-0422
 PUS-0423
 PUS-0424
 PUS-0425
 PUS-0426
 PUS-0427
 PUS-0428
 PUS-0429
 PUS-0430
 PUS-0431
 PUS-0432

```

    COSMIC*(R(K)+R(K-1))/2;
    TEMP = DELTA_R * (K2P-K2N) + R_JE;
    TEMPI = RECOMB * P_I_CHG_D(K-1) * N_I_CHG_D(K-1)
      * R(K-1)/1.602E-19;
    K3N = TEMP * ETA(K-1) + TEMPI;
    K3P = TEMP*ALPHA(K-1) + PHOTO_ELE(K-1) + TEMPI +
      COSMIC *R(K-1);
    KP(K) =(KOP+ 2*KIP + 2 *K2P + K3P)*DELTA_R/6;
    KN(K)=(KON+2*KIN+2*K2N+K3N)*DELTA_R /6;
    R_JE = R_JE + KP(K) - KN(K);
  END;
  FREE ALPHA2, ETA2, PHOTO_ELE2;

  /*****/
  /* KP AND KN ARE THE NET GAIN IN POSITIVE AND NEGATIVE CURRENT */
  /* DENSITIES RESPECTIVELY BETWEEN TWO GRID POINTS. THE CURRENT */
  /* DENSITIES ARE THEN CALCULATED FROM THEM DIRECTLY. */
  /*****/
  R_J_N=0;
  R_JE = ENTERJE * R(N);
  DO K = N-1 TO 0 BY -1;
    R_JE = R_JE + KP(K+1) - KN(K+1);
    J_E(K) = R_JE/R(K);
    R_J_N = R_J_N + KN(K+1);
    J_N_I(K) = R_J_N/R(K);
  END;
  K_J_P = 0;
  J_P_I(0) =0;
  DO K = 1 TO N;
    K_J_P = R_J_P + KP(K);
    J_P_I(K) = R_J_P/R(K);
  END;
  FREE KP, KN;

  /*****/
  /* THE ELECTRON, POSITIVE AND NEGATIVE CHARGE DENSITIES, AND THE */
  /*****/

```



```

/* TOTAL CURRENT IS CALCULATED.
/*****
DO K = 0 TO Y;
  ELE_CHG_D(K) = -J_E(K)/(5.E6 + 329*E(K));
END;
DO K = Y+1 TO N;
  ELE_CHG_D(K) = -J_E(K)/592/E(K);
END;
DO K = 0 TO N;
  N_I_CHG_D(K) = -J_N_I(K)/MOB_N_I/E(K);
  P_I_CHG_D(K) = J_P_I(K)/MOB_P_I/E(K);
  CURRENT(K) = (J_E(K) + J_P_I(K) + J_N_I(K)) *2*PI * R(K);
END;
I_DIFF = (CURRENT(0)-TOTAL_CUR(I-1))/CURRENT(0);
TOTAL_CUR(I) = CURRENT(0);
/*****
/* A NEW SET OF CHARGE DENSITIES IS NOW KNOWN. SO A NEW ELECTRIC
/* DISTRIBUTION IS CALCULATED, AND THE PROCESS REPEATS.
/*****
CALL E_FIELD;
/*****
/* THE DATA IS OUTPUTED IF THE PROCESS IS ALREADY WITHIN A
/* SPECIFIED (OUT_NUM) POINT OF PRINTING OR WHEN THE DIFFERENCE
/* BETWEEN ITERATIONS IS VERY SMALL.
/*****
IF I>(M-OUT_NUM) | ( (I_DIFF<.00001)&(1_DIFF>-.0055) ) THEN
  CALL OUT;
END I;
/*****
/* OCCASIONALLY MORE ITERATIONS ARE NEEDED FOR CONVERGENCE THAN
/* THE SPECIFIED. YET ONE DOES NOT WANT TO WASTE THE PRESENT
/* EFFORT. SO ELECTRON, POSITIVE ION AND NEGATIVE ION CHARGE
/* DENSITIES ARE OUTPUTED ON CARDS IF ITERATION DID NOT CONVERGE
*/

```

POS-0433
 POS-0434
 POS-0435
 POS-0436
 POS-0437
 POS-0438
 POS-0439
 POS-0440
 POS-0441
 POS-0442
 POS-0443
 POS-0444
 POS-0445
 POS-0446
 POS-0447
 POS-0448
 POS-0449
 POS-0450
 POS-0451
 POS-0452
 POS-0453
 POS-0454
 POS-0455
 POS-0456
 POS-0457
 POS-0458
 POS-0459
 POS-0460
 POS-0461
 POS-0462
 POS-0463
 POS-0464
 POS-0465
 POS-0466
 POS-0467
 POS-0468

```

/* AND IF INPUT SPECIFICALLY NOTED CARD_OUT=0 YES. */
/*****Q*****
IF CARD_OUT = 0 YES THEN *****
IF I>M THEN *****
DO;
PUT FILE (PUNCH) EDIT (( ELE_CHG_D(K) DO K = 0 TO N))
(COLUMN(2), (5)(E(13,5), X(1) ));
PUT FILE (PUNCH) EDIT (( P_I_CHG_D(K) DO K = 0 TO N))
(COLUMN(2), (5)(E(13,5), X(1) ));
PUT FILE (PUNCH) EDIT (( N_I_CHG_D(K) DO K = 0 TO N))
(COLUMN(2), (5)(E(13,5), X(1) ));
END;

R_OLD = R_INNER;
GET LIST (N, SAVE, CARD_IN, CARD_OUT);
IF SAVE = 0 NO THEN FREE R, J_E, E, ELE_CHG_D, N_I_CHG_D,
P_I_CHG_D, J_N_I, J_P_I, ALPHA, ETA, PHOTO_ELE, CURRENT;
/*****
/* THE CURRENT IN TERMS OF ITERATIONS ARE OUTPUTTED SO THAT THE */
/* RATE OF CONVERGENCE IS KNOWN. ALSO ADDITIONAL INPUT */
/* PARAMETERS ARE PRINTED FOR REFERENCE. */
/*****
DO J = 1 TO I-1 BY 3;
PUT LIST (I=J, J, CURRENT=TOTAL_CUR(J))
, I=J+1, CURRENT=TOTAL_CUR(J+1))
, I=J+2, CURRENT=TOTAL_CUR(J+2) ) SKIP;
END;
PUT LIST (A(1)=A(1), B(1)=B(1), A(2)=A(2), B(2)=B(2) ) SKIP(2);
PUT LIST ( THE INITIAL SOURCE ARE PAIRS CHARGED
, PAIRS PRODUCED BY COSMIC RADIATION PER CC PER
, SEC, AND ELECTRON CURRENT DENSITY OF
ENTERJ, AMPS PER CM**2 AT THE OUTER RADIUS.)SKIP;
FREE TOTAL_CUR;
END CC;

```

POS-0469
POS-0470
POS-0471
POS-0472
POS-0473
POS-0474
POS-0475
POS-0476
POS-0477
POS-0478
POS-0479
POS-0480
POS-0481
POS-0482
POS-0483
POS-0484
POS-0485
POS-0486
POS-0487
POS-0488
POS-0489
POS-0490
POS-0491
POS-0492
POS-0493
POS-0494
POS-0495
POS-0496
POS-0497
POS-0498
POS-0499
POS-0500
POS-0501
POS-0502
POS-0503
POS-0504

STOPP: END SS:

PUS-0505

Appendix 5

Program Listing for Negative Corona

To use the negative corona program, the input data is in the same order as positive corona case from 1 to 24. The ENTERJE now should be a quantity less than or equal to zero. In addition, two more parameters are needed.

25. PHOTO_E - This is the number of electrons emitted at the cathode per photon arrived, γ_p .

26. ION_B - This is the number of electrons emitted at the cathode per positive ion arrived, γ_1 .

```

SS: PROCEDURE OPTIONS (MAIN);
/*****
/* THIS PROGRAM CALCULATES THE STEADY STATE CHARGE DENSITY
/* FOR NEGATIVE CORONA WHEN THE SOURCE IS ELECTRON CURRENT
/* DENSITY AT THE INNER BOUNDARY, PHOTO EMISSION, ION BOMBARDMENT
/* AT THE CATHODE, AND OR PHOTOIONIZATION IN THE INTERIOR.
/* PREVIOUS RESULTS WILL BE USED IF ANY. OVERSHUT PARAMETER IS
/* USED FOR FASTER CONVERGENCE. RUNGE-KUTTA METHOD IS USED FOR
/* THE INTEGRATION.
*****/
DECLARE (R_INNER, /* RADIUS OF INNER CYLINDER
OVER, /* ADJUSTED OVERSHUT PARAMETER.
R_OLD, /* INNER RADIUS
MOD_ETA, /* FACTOR BY WHICH ETA IS CHANGED
DELTA_R) FIXED (7,4),
(N, /* ACTUAL NUMBER OF DIVISIONS.
INCR, /* OUTPUT INCREMENT.
OUT_NUM, /* # OF TIMES OUTPUT WILL BE PRINTED
X, /* GRID PT. E/P=40
Y, /* GRID PT. E/P=25
I, J, K, CASE, M, T) FIXED(15,0) BINARY,
(SAVE, /* SAVING PREVIOUS DATA?
CARD_IN, /* ANY INPUT DATA
CARD_OUT) /* OUTPUT DATA ON CARDS
CHARACTER(3),
(SUM1, SUM2,
PAIRS, /* ELECTRON/ION PAIRS/CC BY COSMIC RAY
COSMIC, /* PAIRS*1.602E-19
RECOMB, /* RECOMBINATION COEFFICIENT
A(2),B(2),AA(2),BB(2), /* USED IN ALPHA
EO, /* VALUE OF E
TEMP, TEMP1, TEMP2, /* PHOTO EMISSION COEFFICIENT
PHOTO_E, /* ION BOMBARDMENT COEFFICIENT
IUN_B, INT1, INT2, INT3,

```

NEG-0001
 NEG-0002
 NEG-0003
 NEG-0004
 NEG-0005
 NEG-0006
 NEG-0007
 NEG-0008
 NEG-0009
 NEG-0010
 NEG-0011
 NEG-0012
 NEG-0013
 NEG-0014
 NEG-0015
 NEG-0016
 NEG-0017
 NEG-0018
 NEG-0019
 NEG-0020
 NEG-0021
 NEG-0022
 NEG-0023
 NEG-0024
 NEG-0025
 NEG-0026
 NEG-0027
 NEG-0028
 NEG-0029
 NEG-0030
 NEG-0031
 NEG-0032
 NEG-0033
 NEG-0034
 NEG-0035
 NEG-0036

```

VOLT,          /* VOLTAGE APPLIED BETWEEN CYLINDERS          NEG-0037
ENTERJE,      /* DIFFERENT BOUNDARY CONDITIONS             NEG-0038
R_JE,         /* R(K) * J_E(K)                             NEG-0039
EST,          /* ESTIMATE OF FINAL TOTAL CURRENT.         NEG-0040
R_J_N,        /* R * J_N_I                                  NEG-0041
R_J_P,        /* R * J_P_I                                  NEG-0042
KK1, KK2, KK3, /* KK/R(0) IS E(0) FOR NO SPACE CHG        NEG-0043
K0, K1, K2, K3, /* MOBILITY OF NEGATIVE IONS               NEG-0044
K0P, K1P, K2P, K3P, /* MOBILITY OF POSITIVE IONS              NEG-0045
K0N, K1N, K2N, K3N, /* PHOTON IONIZATION COEFFICIENT          NEG-0046
KK,           /* PHOTON ABSORPTION COEFFICIENT *1.86    NEG-0047
MOB_N_I,      /* NUMBER OF PHOTONS CREATED PER ELECTRON  NEG-0048
MOB_P_I,      /* CREATED                                  NEG-0049
PHOTOMU,     /* CONSTANT                                NEG-0050
ABS_MU,      /* CHANGE OF TOTAL I BETWEEN ITERATIONS   NEG-0051
EFF,         /* FOR CALCULATING GEOMETRIC FACTOR      NEG-0052
PI,          /* EPSILON) BINARY FLOAT,                 NEG-0053
OLD_CHG, NEW_CHG, /* THE SIZE OF THE FOLLOWING ARRAYS IS NOT FIXED. THEY WILL BE NEG-0054
I_DIFF,      /* ALLOCATED WHEN N IS KNOWN.             NEG-0055
R_OUT, ANGLE, /* R(0) FIXED (8,5) CONTROLLED,          NEG-0056
EPSILON)     /* (CHARGE(*), /* TOTAL CHARGE WITHIN A CERTAIN RADIUS.  NEG-0057
/*          /* J_P_I(*), /* POSITIVE ION CURRENT DENSITY          NEG-0058
/*          /* J_N_I(*), /* NEGATIVE ION CURRENT DENSITY          NEG-0059
/*          /* J_E(*), /* ELECTRON CURRENT DENSITY          NEG-0060
/*          /* E(*), /* ELECTRIC FIELD          NEG-0061
/*          /* CURRENT(*), /* TOTAL CURRENT.          NEG-0062
/*          /* VOLTAGE(*), /* VOLTAGE AS DEFINED FROM R(0)          NEG-0063
/*          /* ALPHA(*), /* NUMBER OF ELECTRONS CREATED /CM          NEG-0064
/*          /* ETA(*), /* NUMBER OF ELECTRONS ATTACHED/CM          NEG-0065

```

NEG-0073
 NEG-0074
 NEG-0075
 NEG-0076
 NEG-0077
 NEG-0078
 NEG-0079
 NEG-0080
 NEG-0081
 NEG-0082
 NEG-0083
 NEG-0084
 NEG-0085
 NEG-0086
 NEG-0087
 NEG-0088
 NEG-0089
 NEG-0090
 NEG-0091
 NEG-0092
 NEG-0093
 NEG-0094
 NEG-0095
 NEG-0096
 NEG-0097
 NEG-0098
 NEG-0099
 NEG-0100
 NEG-0101
 NEG-0102
 NEG-0103
 NEG-0104
 NEG-0105
 NEG-0106
 NEG-0107
 NEG-0108

```

ALPHA2(*), ETA2(*),
PHOTO_ELE(*), /* SOURCE DUE TO PHOTOIONIZATION
PHOTO_ELE2(*),
G(*), /* GEOMETRIC FACTOR
G1(*), /* GEOMETRIC FACTOR FOR EXTERIOR
TOTAL_CUR(*), /* VALUE OF SUM OF ALL THE CURRENT.
KP(*), /* KOP+2*K1P+2*K2P+K3P
KN(*), /* KON+2*K1N+2*K2N+K3N
P_I_CHG_D(*), /* POSITIVE ION CHARGE DENSITY
N_I_CHG_D(*), /* NEGATIVE ION CHARGE DENSITY
ELE_CHG_D(*), /* ELECTRON CHARGE DENSITY
BINARY FLOAT CONTROLLED;

/*****
/* THE PROCEDURE E_FIELD CALCULATES THE ELECTRIC FIELD WHEN THE
/* VOLTAGE AND CHARGE DENSITIES ARE KNOWN BETWEEN THE TWO
/* ELECTRODES. SUM2 IS CALCULATED IN THE NO_SAVE DO LOOP OF THE
/* MAIN PROCEDURE.
*****/
E_FIELD: PROCEDURE;
  ALLOCATE CHARGE (0:N);
  VOLT = -KK * LOG(R(N)/R(0));
  SUM1 = 0;
  CHARGE(0) = 0;
  OLD_CHG = R(0) * DELTA_R * (ELE_CHG_D(0) + N_I_CHG_D(0) +
    P_I_CHG_D(0) )/2;
  DO J = 1 TO N;
    NEW_CHG = R(J) * DELTA_R * ( ELE_CHG_D(J) +
      N_I_CHG_D(J) + P_I_CHG_D(J) ) /2;
    CHARGE(J) = (OLD_CHG+ NEW_CHG) + CHARGE(J-1);
    OLD_CHG = NEW_CHG;
    SUM1 = SUM1 + CHARGE(J) / R(J);
  END;
  SUM1 = SUM1 - CHARGE (N) /2/R(N);
  E(0) = (VOLT /DELTA_R-SUM1/EPSILCN) /
    (R(0) * (SUM2 + .5 /R(N) ) + .5);
  
```

NEG-0109
 NEG-0110
 NEG-0111
 NEG-0112
 NEG-0113
 NEG-0114
 NEG-0115
 NEG-0116
 NEG-0117
 NEG-0118
 NEG-0119
 NEG-0120
 NEG-0121
 NEG-0122
 NEG-0123
 NEG-0124
 NEG-0125
 NEG-0126
 NEG-0127
 NEG-0128
 NEG-0129
 NEG-0130
 NEG-0131
 NEG-0132
 NEG-0133
 NEG-0134
 NEG-0135
 NEG-0136
 NEG-0137
 NEG-0138
 NEG-0139
 NEG-0140
 NEG-0141
 NEG-0142
 NEG-0143
 NEG-0144

```

X = 0;
Y = N;
DO J = 1 TO N;
  E(J) = ( CHARGE(J) / EPSILON + R(0)*E(0) ) / R(J);
  IF -E(J) >= 30400 THEN X=J;
  ELSE IF -E(J) >= 19000 THEN Y =J;
END;
FREE CHARGE;
END E_FIELD;

/*****/
/* THE PROCEDURE OUT IS CALLED WHEN OUTPUT IS DESIRED. */
/* THE FIRST DO LOOP CALCULATE THE VOLTAGE AS A FUNCTION OF */
/* POSITION ONCE THE ELECTRIC FIELD DISTRIBUTION IS KNOWN. IT */
/* PROVIDES A CHECK ON THE ACCURACY OF THE ELECTRIC FIELD. */
/*****/
OUT: PROCEDURE;
  ALLOCATE VOLTAGE(0:N);
  VOLTAGE (N) =0;
  DO J = N-1 TO 0 BY -1;
    VOLTAGE(J) = VOLTAGE(J+1) + E(J) * DELTA_R;
  END;

/*****/
/* NOW OUTPUT THE VALUES ASSOCIATED WITH INPUT DATA. */
/*****/
PUT LIST ('CASE',ICASE, ' ', III, 'TH. ITERATION. ',
  ' ', DELTA_R = ' ', DELTA_R, ' ', OVERSHUT = ' ');
OVER, RECOMBINATION = ' ', RECUMB) PAGE;
PUT LIST ('PHOTO_MU = ' ', PHOTO_MU, ' ', EFF = ' ', EFF, ' ',
  ' ', PHOTO_EMISSION = ' ', PHOTO_EI, ' ', ION BOMBARDMENT ',
  ' ', COEFFICIENT = ' ', ION_B) SKIP;
PUT LIST ('MOB_P_I = ' ', MOB_P_I, ' ', MOB_N_I = ' ', MOB_N_I
  ' ', VELOCITY OF ELECTRON IS 4.5E5 * E/P, ' ',
  ' ', FOR E/P < 25. IT IS 2.5E5 * E/P + 5.E6 FOR ' ',
  ' ', E/P >= 25. ') SKIP;
  
```



```

NEG-0145
NEG-0146
NEG-0147
NEG-0148
NEG-0149
NEG-0150
NEG-0151
NEG-0152
NEG-0153
NEG-0154
NEG-0155
NEG-0156
NEG-0157
NEG-0158
NEG-0159
NEG-0160
NEG-0161
NEG-0162
NEG-0163
NEG-0164
NEG-0165
NEG-0166
NEG-0167
NEG-0168
NEG-0169
NEG-0170
NEG-0171
NEG-0172
NEG-0173
NEG-0174
NEG-0175
NEG-0176
NEG-0177
NEG-0178
NEG-0179
NEG-0180

PUT LIST ('AT R =',IR(0),'CM J_N_1 = 0. ',I)
'VOLTAGE = ',VOLT,'E = ',IKK/R(0),'
' (WHEN FREE OF SPACE CHARGES) ')SKIP;

PUT LIST ('AT R =',IR(N),'CM J_P_1 = 0. ',I)
'VOLTAGE = 0. MOD_ETA =',MOD_ETA)SKIP;
/*****
/* THE NEXT 3 PUT EDIT STATEMENTS PRINT OUT THE HEADINGS FOR THE */
/* LIST OF DATA. */
/*****
PUT EDIT ('RADIUS', 'E FIELD', 'VOLTAGE ', 'POSITIVE',
'NEGATIVE', 'ELECTRON', 'POSITIVE', 'NEGATIVE',
'ELECTRON', 'TOTAL', 'ALPHA', 'ETA', 'PHOTO_ELE')
( A(6), X(1), A(7), X(2), A(9), X(3), A(8), X(3),
A(8), X(3), A(8), X(2), A(8), X(4), A(8), X(4),
A(8), X(3), A(5), X(4), A(5), X(4), A(3), X(4), A(9))
SKIP(2);

PUT EDIT ('ION CHARGE', 'ION CHARGE', 'CHARGE',
'ION CURRENT', 'ION CURRENT', 'CURRENT', 'CURRENT')
( X(28), A(10), X(1), A(10), X(1), A(6), X(4),
A(11), X(1), A(11), X(1), A(7), X(4), A(7)) SKIP;

PUT EDIT ('DENSITY', 'DENSITY', 'DENSITY', 'DENSITY',
'DENSITY', 'DENSITY')
( X(28), A(7), X(4), A(7), X(4), A(7), X(3),
A(7), X(5), A(7), X(5), A(7), X(6)) SKIP;
/*****
/* THIS SECTION ACTUALLY OUTPUT THE DATA . ONLY ONE OUT OF A */
/* SPECIFIED NUMBER OF GRID POINTS IS ACTUALLY PRINTED TO SAVE */
/* PRINTING COST. THE VARIABLE INCR TAKES CARE OF THE SPECIFIED */
/* NUMBER. */
/*****
DU J=0 TO N BY INCR;
PUT EDIT (R(J), E(J), VOLTAGE(J), P_I_CHG_D(J),
N_I_CHG_D(J), ELE_CHG_D(J), J_P_I(J), J_N_I(J),
J_E(J), CURRENT(J), ALPHA(J), ETA(J), PHOTO_ELE(J))
( F(6,4), E(11,4), E(10,3), X(1), E(10,3), X(1),
E(10,3), X(1), E(10,3), E(11,4), E(11,4),

```

NEG-0181
NEG-0182
NEG-0183
NEG-0184
NEG-0185
NEG-0186
NEG-0187
NEG-0188
NEG-0189
NEG-0190
NEG-0191
NEG-0192
NEG-0193
NEG-0194
NEG-0195
NEG-0196
NEG-0197
NEG-0198
NEG-0199
NEG-0200
NEG-0201
NEG-0202
NEG-0203
NEG-0204
NEG-0205
NEG-0206
NEG-0207
NEG-0208
NEG-0209
NEG-0210
NEG-0211
NEG-0212
NEG-0213
NEG-0214
NEG-0215
NEG-0216

```
      E(11,4), E(11,4), E(9,2), E(9,2), E(9,2))SKIP;  
END;  
FREE VOLTAGE;  
END OUT;  
/*****  
/* DATA ARE INPUTED AND VALUES INITIALIZED IN THE NEXT SECTION */  
/* BEFORE THE II DO LOOP. */  
/*****  
EPSILON= 8.854E-14; /* COULOMB /VOLTS /CM */  
PI = 3.14159;  
CASE = 0;  
GET LIST (N, SAVE, CARD_IN, CARD_OUT);  
R_ULU = -1;  
/*****  
/* THE CONDITION THAT THE PRGRAM WILL CONTINUE IS THAT THE VALUE */  
/* OF N INPUTED IS GREATER THAN ZERO. THE MAIN PORTION OF */  
/* THE PROGRAM IS LOCATED IN THE CC DO LOOP. */  
/*****  
CC: DO WHILE (N>0);  
CASE = CASE +1;  
GET LIST (R_INNER, DELTA_R, INCR, M, OUT_NUM, EO, ENTERJE,  
MOB_P_1, MOB_N_1, A(1), B(1), A(2), B(2), PHOTOMU,  
EFF, MOD_ETEA, OVER, EST, RECOMB, PAIRS, PHOTO_E,  
IUN_B);  
ALLOCATE TOTAL_CUR(0:M);  
TOTAL_CUR(*) = 0;  
TOTAL_CUR(0) = 1;  
KK =EO*R_INNER;  
I_DIFF = 10;  
COSMIC = PAIRS * 1.602E-19;  
AA(1) = A(1)*760;  
AA(2) = A(2)*760;  
BB(1) = B(1)*760;  
BB(2) = B(2)*760;  
/*****
```

```

/* IF NO DATA IS SAVED, MOST OF THE VARIABLES WILL HAVE TO BE */
/* INITIALIZED IN THE NO_SAVE DO LOOP.  ELECTRIC FIELD WITHOUT */
/* SPACE CHARGES IN THE FORM OF KK/R IS CALCULATED.  IF DATA IS */
/* SAVED, THEN N AND INNER AND OUTER CONDUCTORS ARE ASSUMED TO */
/* BE THE SAME. */
/***** */

```

```

IF SAVE = 'NO' THEN

```

```

NO_SAVE: DO:

```

```

    ALLOCATE R(O:N), J_E(O:N), E(O:N), ELE_CHG_D(O:N),
    P_I_CHG_D(O:N), N_I_CHG_D(O:N), J_A_I(O:N), J_P_I(O:N),
    ALPHA(O:N), ETA(O:N), PHOTO_ELE(O:N), CURRENT(O:N);

```

```

    J_P_I(O) = 0;

```

```

    R(O) = R_INNER;

```

```

    SUM2 = 0;

```

```

    X = 0;

```

```

    Y = N;

```

```

    DO K = 1 TO N-1;

```

```

        R(K) = R(K-1) + DELTA_R;

```

```

        SUM2 = SUM2 + 1./R(K);

```

```

        E(K) = -KK/R(K);

```

```

        IF -E(J) >= 30400 THEN X=K;

```

```

        ELSE IF -E(K) >= 19000 THEN Y = K;

```

```

    END;

```

```

    E(O) = -KK/R(O);

```

```

    R(N) = R(N-1) + DELTA_R;

```

```

    E(N) = -KK/R(N);

```

```

/***** */
/* THE FOLLOWING DO LOOP INPUT DATA FROM PREVIOUS RUNS SO AS TO */
/* CONTINUE THE ITERATION PRCESS IF DESIRED. */
/***** */

```

```

IF CARD_IN = 'YES' THEN

```

```

DO:

```

```

    GET LIST ((ELE_CHG_D(K) DO K = 0 TO N));

```

```

    GET LIST ((P_I_CHG_D(K) DO K = 0 TO N));

```

```

    GET LIST ((N_I_CHG_D(K) DO K = 0 TO N));

```

```

    J_P_I(O) = P_I_CHG_D(O) * E(O) + MUB_P_I;

```

```

NEG-0217
NEG-0218
NEG-0219
NEG-0220
NEG-0221
NEG-0222
NEG-0223
NEG-0224
NEG-0225
NEG-0226
NEG-0227
NEG-0228
NEG-0229
NEG-0230
NEG-0231
NEG-0232
NEG-0233
NEG-0234
NEG-0235
NEG-0236
NEG-0237
NEG-0238
NEG-0239
NEG-0240
NEG-0241
NEG-0242
NEG-0243
NEG-0244
NEG-0245
NEG-0246
NEG-0247
NEG-0248
NEG-0249
NEG-0250
NEG-0251
NEG-0252

```

```

NEG-0253
NEG-0254
NEG-0255
NEG-0256
NEG-0257
NEG-0258
NEG-0259
NEG-0260
NEG-0261
NEG-0262
NEG-0263
NEG-0264
NEG-0265
NEG-0266
NEG-0267
NEG-0268
NEG-0269
NEG-0270
NEG-0271
NEG-0272
NEG-0273
NEG-0274
NEG-0275
NEG-0276
NEG-0277
NEG-0278
NEG-0279
NEG-0280
NEG-0281
NEG-0282
NEG-0283
NEG-0284
NEG-0285
NEG-0286
NEG-0287
NEG-0288

END;
/*****
/* THE FOLLOWING SECTION CALCULATES THE GEOMETRIC FACTOR.
*****/
IF (CASE  $\neq$  1) & (R_OLD  $\neq$  R_INNER) THEN FREE G, G1;
IF R_OLD  $\neq$  R_INNER THEN
DO;
  ALLOCATE G(0:N), G1(0:N);
  R_OUT = 10;
  DO K = 1 TO N;
    TEMP = (R(0)**2 - SQRT( (R(K)**2 - R(0)**2) *
      (R_OUT**2 - R(0)**2) ) )/R_OUT/R(K);
    ANGLE = PI/2 - ATAN(TEMP/SQRT(1 - TEMP**2));
    TEMPI = ATAN((R_OUT + R(K))*TAN(ANGLE/2)/(R_OUT - R(K)) );
    G(K) = (ANGLE/2 + TEMPI)/PI;
    TEMP = R(0)/R(K);
    ANGLE = PI/2 - ATAN(TEMP/SQRT(1 - TEMP**2));
    TEMPI = ATAN((R(K) + R(0))*TAN(ANGLE/2)/(R(K) - R(0)));
    G1(K) = (ANGLE/2 - TEMPI)/PI;
  END;
  G1(0) = -.5;
  G(0) = .5;
END;
END NO_SAVE;

/*****
/* THE ELECTRON CURRENT DENSITY DISTRIBUTION IS INITIALIZED IF
/* PREVIOUS DATA IS AVAILABLE. PHOTOIONIZATION TERM CAN BE
/* CALCULATED IF THE ELECTRON CURRENT DENSITY IS KNOWN.
*****/
IF SAVE = 'YES' | CARD_IN = 'YES' THEN
DU;
CALL E_FIELD;
DO K = 0 TO Y;
  J_E(K) = -(-5.E6 + 329 * E(K)) * ELE_CHG_D(K);
END;

```

```

DO K = Y+1 TO N;
  J_E(K) = -592 * E(K) * ELE_CHG_D(K);
END;
END;
0

```

```

/*****
/* THE ITERATION PROCESS IS PERFORMED WITHIN THE I1 DO LOOP.
/* TO GUARD AGAINST THE UNSTABLE CASE, THE MAXIMUM NUMBER OF
/* ITERATIONS ALLOWED IS M. HOWEVER IF THE TOTAL CURRENT STOPPED
/* INCREASING AND THE DIFFERENCE BETWEEN THE PRESENT AND PREVIOUS
/* TOTAL CURRENT IS WITHIN .5 PERCENT OF THE PRESENT TOTAL
/* CURRENT, AND THE OVSERSHUT PARAMETER( OVER) IS SET AT 1, THEN
/* THE ITERATION PROCESS STOPS. THE OVSERSHUT PARAMETER IS TO
/* INCREASE THE GROWTH RATE. IF THE TOTAL CURRENT REACHED THE
/* ESTIMATED TOTAL CURRENT, THE OVSERSHUT PARAMETER IS SET TO 1.
/* WHEN OVER IS NOT 1, THE PROGRAM IS ACTUALLY SOLVING A
/* DIFFERENT PROBLEM.
*****/
I1: DO I = 1 TO M WHILE ((I_DIFF>0 | I_DIFF<-.005) | OVER=1);
  IF TOTAL_CUR(I-1) <= EST THEN OVER = 1;
  ALLOCATE ALPHA2(0:N), ETA2(0:N), PHOTO_ELE2(0:N);
  J_N_I(I) = 0;
*****/
/* ALPHA AND ETA ARE CALCULATED. T=1 IS FOR THE CASE E/P>=40 IN
/* THE CALCULATION OF ALPHA.
*****/
T=1;
DO K = 0 TO N;
  IF K=X THEN T=2;
  EO = -E(K);
  ALPHA(K) = AA(T)*EXP(-BB(T)/EO);
  IF K <= Y THEN
    ETA(K) = (1.203E-8*EO*EC -.000567*EO + 10.12)*MOD_ETA;
  ELSE ETA(K) = MOD_ETA * (1.545E-4*EO+.866);
END;

```

-173-

NEG-0289
 NEG-0290
 NEG-0291
 NEG-0292
 NEG-0293
 NEG-0294
 NEG-0295
 NEG-0296
 NEG-0297
 NEG-0298
 NEG-0299
 NEG-0300
 NEG-0301
 NEG-0302
 NEG-0303
 NEG-0304
 NEG-0305
 NEG-0306
 NEG-0307
 NEG-0308
 NEG-0309
 NEG-0310
 NEG-0311
 NEG-0312
 NEG-0313
 NEG-0314
 NEG-0315
 NEG-0316
 NEG-0317
 NEG-0318
 NEG-0319
 NEG-0320
 NEG-0321
 NEG-0322
 NEG-0323
 NEG-0324

```

T=1;
/*****
/* ALPHA2 AND ETA2 ARE FOR THE VALUES OF ALPHA AND ETA HALF WAY
/* BETWEEN THE GRID POINTS. THIS IS NECESSARY FOR RUNGE-KUTTA
/* INTEGRATION.
/*****
DO K = 2 TO N-1;
  IF K=X THEN T=2;
  EO = -(-E(K-2)-E(K+1)+9*(E(K-1)+E(K)))/16;
  ALPHA2(K) = AA(T) * EXP(-BB(T)/EO);
  IF K <= Y THEN
    ETA2(K)=(1.203E-8*EC*EO -.000567*EO + 10.12)*MOD_ETA;
    ELSE ETA2(K) = MOD_ETA * (1.545E-4*EO +.866);
  END;
  EO = -(5*E(N) +E(N-3)+15*E(N-1)-5* E(N-2) )/16;
  ALPHA2(N) = AA(T) * EXP(-BB(T)/EO);
  IF EO>= 19760 THEN
    ETA2 (N) =(1.203E-8*EC*EO -.000567*EO + 10.12)*MOD_ETA;
    ELSE ETA2(N) = MOD_ETA * (1.545E-4*EO+.866);
  EO = -(5*E(0)+E(3)+E(1)*15-5*E(2))/16;
  IF EO >= 30400 THEN T=1;
    ELSE T=2;
  ALPHA2(1) = AA(T) * EXP(-BB(T)/EO);
  IF EO >= 19760 THEN
    ETA2 (1) =(1.203E-8*EC*EO -.000567*EO + 10.12)*MOD_ETA;
    ELSE ETA2(1) = MOD_ETA * (1.545E-4*EO+.866);
/*****
/* IF THERE IS NO PREVIOUS DATA USED IN THE FIRST ITERATION,
/* PHOTOIONIZATION IS ASSUMED NOT TO BE PRESENT SINCE ELECTRON
/* CHARGE DENSITY IS NOT KNOWN.
/*****
IF I =1 & SAVE ='NO ' & CARD_IN='NO ' THEN
DO;
  PHOTO_ELE(*) =0;
  PHOTO_ELE2(*) = 0;

```

NEG-0325
NEG-0326
NEG-0327
NEG-0328
NEG-0329
NEG-0330
NEG-0331
NEG-0332
NEG-0333
NEG-0334
NEG-0335
NEG-0336
NEG-0337
NEG-0338
NEG-0339
NEG-0340
NEG-0341
NEG-0342
NEG-0343
NEG-0344
NEG-0345
NEG-0346
NEG-0347
NEG-0348
NEG-0349
NEG-0350
NEG-0351
NEG-0352
NEG-0353
NEG-0354
NEG-0355
NEG-0356
NEG-0357
NEG-0358
NEG-0359
NEG-0360

```

N_I_CHG_D(*) = 0;
P_I_CHG_D(*) = 0;
END;

```

```

/*****
/* CALCULATE PHOTONIZATION TERM.
/*****

```

```

ELSE IF PHOTOMU  $\neq$  0 THEN
DO;

```

```

  PHOTU_ELE2(0) = 0;
  TEMP = PHOTOMU * EFF * CVER;
  ABS_MU = PHOTOMU * 1.8;
  INT1 = 0;
  INT2 = 0;
  INT3 = 0;
  K1 = ALPHA(N)*J_E(N)* EXP(-ABS_MU*(N))/8;
  K2 = R(N)*K1;
  K3 = G1(N)*K2;
  DO K = N-1 TO 0 BY -1;

```

```

    TEMP1 = (R(K)+R(K+1))/2;
    KK1 = ALPHA2(K+1) * (J_E(K) + J_E(K+1))
      * EXP(-ABS_MU*TEMP1)/8;

```

```

    KK2 = TEMP1*KK1;

```

```

    KK3 = (G1(K)+G1(K+1))*KK2/2;

```

```

    INT1 = INT1 + K1 + KK1;

```

```

    INT2 = INT2 + K2 + KK2;

```

```

    INT3 = INT3 + K3 + KK3;

```

```

    PHOTU_ELE2(K+1) = (INT3-.112*INT2+.93*TEMP1*INT1)
      * EXP(ABS_MU*TEMP1);

```

```

    K1 = ALPHA(K)*J_E(K)*EXP(-ABS_MU*(K))/4;

```

```

    K2 = R(K)*K1;

```

```

    K3 = G1(K)*K2;

```

```

    INT1 = INT1 + K1 + KK1;

```

```

    INT2 = INT2 + K2 + KK2;

```

```

    INT3 = INT3 + K3 + KK3;

```

```

    PHOTU_ELE(K) = (INT3-.112*INT2+.93*R(K)*INT1)

```

```

NEG-0361
NEG-0362
NEG-0363
NEG-0364
NEG-0365
NEG-0366
NEG-0367
NEG-0368
NEG-0369
NEG-0370
NEG-0371
NEG-0372
NEG-0373
NEG-0374
NEG-0375
NEG-0376
NEG-0377
NEG-0378
NEG-0379
NEG-0380
NEG-0381
NEG-0382
NEG-0383
NEG-0384
NEG-0385
NEG-0386
NEG-0387
NEG-0388
NEG-0389
NEG-0390
NEG-0391
NEG-0392
NEG-0393
NEG-0394
NEG-0395
NEG-0396

```

NEG-0397
 NEG-0398
 NEG-0399
 NEG-0400
 NEG-0401
 NEG-0402
 NEG-0403
 NEG-0404
 NEG-0405
 NEG-0406
 NEG-0407
 NEG-0408
 NEG-0409
 NEG-0410
 NEG-0411
 NEG-0412
 NEG-0413
 NEG-0414
 NEG-0415
 NEG-0416
 NEG-0417
 NEG-0418
 NEG-0419
 NEG-0420
 NEG-0421
 NEG-0422
 NEG-0423
 NEG-0424
 NEG-0425
 NEG-0426
 NEG-0427
 NEG-0428
 NEG-0429
 NEG-0430
 NEG-0431
 NEG-0432

```

    * EXP(ABS_MU*R(K));

END;
PHOTO_ELE(0) = TEMP * PHOTO_ELE(0)/2;
KO = ALPHA(0)*R(0)*J_E(0)*EXP(ABS_MU*R(0))/8;
INT1 = 0;
DO K = 1 TO N;
  TEMPI = (R(K)+R(K-1))/2;
  K1 = ALPHA2(K)*(J_E(K)+J_E(K-1))*TEMPI*
    (G(K)+G(K-1))*EXP(ABS_MU*TEMPI)/16;
  INT1 = INT1 +K0 + K1;
  PHOTO_ELE2(K) = TEMP * (PHOTO_ELE2(K) + INT1 *
    EXP(-ABS_MU*TEMPI));
  K0 = ALPHA(K)*R(K)*J_E(K)*G(K)*EXP(ABS_MU*K(K))/4;
  INT1 = INT1 +K0 + K1;
  PHOTO_ELE(K) = TEMP* (INT1*EXP(-ABS_MU*R(K)) +
    PHOTO_ELE(K));
END;
ELSE IF I=1 THEN PHOTO_ELE(*),PHOTO_ELE2(*) =0;
ALLOCATE KP(0:N), KN(0:N);
/*****
/* RUNGE-KUTTA METHOD IS USED FOR INTEGRATION BECAUSE IT IS SELF /*
/* STARTING AND GENERALLY RELIABLE METHCD. HOWEVER, IT IS /*
/* PRUBABLY MORE EXPENSIVE THAN SOME OTHER METHODS. THE /*
/* PROCESSES INCLUDED ARE ELECTRON AVALANCHE, ATTACHMENT, COSMIC /*
/* RADIATION, PHOTOIONIZATION, AND RECOMBINATION. /*
/*****
IF PHOTOMU =0 THEN R_JE = ENTERJE*R(0) + IUN_B*J_P_I(0);
ELSE
R_JE = ENTERJE * R(0) + IUN_B * J_P_I(0)
+ PHOTO_E*PHOTO_ELE(0)/PHOTOMU;
TEMPI=0;
DO K = 0 TO N-1;
  KON = ETA(K)*R_JE - TEMPI;
  KOP = ALPHA(K)*R_JE + PHOTO_ELE(K) - COSMIC*R(K) -

```


NEG-0433
 NEG-0434
 NEG-0435
 NEG-0436
 NEG-0437
 NEG-0438
 NEG-0439
 NEG-0440
 NEG-0441
 NEG-0442
 NEG-0443
 NEG-0444
 NEG-0445
 NEG-0446
 NEG-0447
 NEG-0448
 NEG-0449
 NEG-0450
 NEG-0451
 NEG-0452
 NEG-0453
 NEG-0454
 NEG-0455
 NEG-0456
 NEG-0457
 NEG-0458
 NEG-0459
 NEG-0460
 NEG-0461
 NEG-0462
 NEG-0463
 NEG-0464
 NEG-0465
 NEG-0466
 NEG-0467
 NEG-0468

```

TEMP1;
TEMP = DELTA_R *(KOP-KON)/2 + R_JE;
TEMP2=RECUMB*(P_I_CHG_D(K)+P_I_CHG_D(K+1))*(R(K)+R(K+1))*
(N_I_CHG_D(K) + N_I_CHG_D(K+1))/8/1.602E-19;
KIN = TEMP * ETA2(K+1) - TEMP2;
KIP = TEMP*ALPHA2(K+1) + PHOTO_ELE2(K+1) - TEMP2 -
COSMIC*(R(K)+R(K+1))/2;
TEMP = DELTA_R *(KIP-KIN)/2 + R_JE;
K2N = TEMP * ETA2(K+1) - TEMP2;
K2P = TEMP*ALPHA2(K+1) + PHOTO_ELE2(K+1) - TEMP2 -
COSMIC*(R(K)+R(K+1))/2;
TEMP = DELTA_R * (K2P-K2N) + R_JE;
TEMP1 = RECUMB * P_I_CHG_D(K+1) * N_I_CHG_D(K+1)
* R(K+1)/1.602E-19;
K3N = TEMP * ETA(K+1) - TEMP1;
K3P = TEMP*ALPHA(K+1) + PHOTO_ELE(K+1) - TEMP1 -
COSMIC*R(K+1);
KP(K) =(KOP+ 2*KIP + 2 *K2P + K3P)*DELTA_R/6;
KN(K)=(KON+2*KIN+2*K2N+K3N)*DELTA_R /6;
R_JE = R_JE + KP(K) - KN(K);
END;
FREE ALPHA2, ETA2, PHOTO_ELE2;
/*****
/* KP AND KN ARE THE NET GAIN IN POSITIVE AND NEGATIVE CURRENT */
/* DENSITIES RESPECTIVELY BETWEEN TWO GRID POINTS. THE CURRENT */
/* DENSITIES ARE THEN CALCULATED FROM THEM DIRECTLY. */
/*****
R_J_N=U;
IF PHOTOMU =0 THEN R_JE = ENTERJE*R(0) + ION_B*J_P_I(0);
ELSE
R_JE = ENTERJE * R(0) + ION_B * J_P_I(0)
+ PHOTO_E*PHOTO_ELE(0)/PHOTOMU/EFF;
J_E(0) = R_JE /R(0);
DO K = 1 TO N ;
R_JE = R_JE + KP(K-1) - KN(K-1);
  
```

7

NEG-0469
 NEG-0470
 NEG-0471
 NEG-0472
 NEG-0473
 NEG-0474
 NEG-0475
 NEG-0476
 NEG-0477
 NEG-0478
 NEG-0479
 NEG-0480
 NEG-0481
 NEG-0482
 NEG-0483
 NEG-0484,
 NEG-0485,
 NEG-0486,
 NEG-0487
 NEG-0488
 NEG-0489
 NEG-0490
 NEG-0491
 NEG-0492
 NEG-0493
 NEG-0494
 NEG-0495
 NEG-0496
 NEG-0497
 NEG-0498
 NEG-0499
 NEG-0500
 NEG-0501
 NEG-0502
 NEG-0503
 NEG-0504

```

J_E(K) = R_JE/R(K);
R_J_N = R_J_N + KN(K-1);
J_N_I(K) = R_J_N/R(K);
END;
R_J_P = 0;
J_P_I(N) = 0;
DO K = N-1 TO 0 BY -1;
  R_J_P = R_J_P + KP(K);
  J_P_I(K) = R_J_P/R(K);
END;
FREE KP, KN;

/*****
/* THE ELECTRON, POSITIVE AND NEGATIVE CHARGE DENSITIES, AND THE */
/* TOTAL CURRENT IS CALCULATED. */
/*****
DO K = 0 TO Y;
  ELE_CHG_D(K) = -J_E(K)/(-5.E6 + 329*E(K));
END;
DO K = Y+1 TO N;
  ELE_CHG_D(K) = -J_E(K)/592/E(K);
END;
DO K = 0 TO N;
  N_I_CHG_D(K) = -J_N_I(K)/MOB_N_I/E(K);
  P_I_CHG_D(K) = J_P_I(K)/MOB_P_I/E(K);
  CURRENT(K) = (J_E(K) + J_P_I(K) + J_N_I(K)) * 2*PI * R(K);
END;
I_DIFF = (CURRENT(0) - TOTAL_CUR(I-1))/CURRENT(0);
TOTAL_CUR(I) = CURRENT(0);

/*****
/* A NEW SET OF CHARGE DENSITIES IS NOW I.NOWN. SO A NEW ELECTRIC */
/* DISTRIBUTION IS CALCULATED, AND THE PROCESS REPEATS. */
/*****
CALL E_FIELD;
  
```

```

/*****
/* THE DATA IS OUTPUTED IF THE PROCESS IS ALREADY WITHIN A
/* SPECIFIED (OUT_NUM) POINT OF PRINTING OR WHEN THE DIFFERENCE
/* BETWEEN ITERATIONS IS VERY SMALL.
/*****
IF I>(M-OUT_NUM) | ( (I_DIFF<.00001)&(I_DIFF>-.0055) ) THEN
    CALL OUT;
END I;
/*****
/* OCCASIONALLY MORE ITERATIONS ARE NEEDED FOR CONVERGENCE THAN
/* THE SPECIFIED. YET ONE DOES NOT WANT TO WASTE THE PRESENT
/* EFFORT. SO ELECTRON, POSITIVE ION AND NEGATIVE ION CHARGE
/* DENSITIES ARE OUTPUTED ON CARDS IF ITERATION DID NOT CONVERGE
/* AND IF INPUT SPECIFICALLY NCTED CARD_OUT='YES'.
/*****
IF CARD_OUT ='YES' THEN
IF I>M THEN
DU;
    PUT FILE (PUNCH) EDIT ((ELE_CHG_D(K) DO K = 0 TO N)
    ( COLUMN(2), (5)(E(13,5), X(1) ));
    PUT FILE (PUNCH) EDIT ((P_I_CHG_D(K) DO K = 0 TO N)
    ( COLUMN(2), (5)(E(13,5), X(1) ));
    PUT FILE (PUNCH) EDIT ((N_I_CHG_D(K) DO K = 0 TO N)
    ( COLUMN(2), (5)(E(13,5), X(1) ));
END;
/*****
/* THE CURRENT IN TERMS OF ITERATIONS ARE CUTPUTED SO THAT THE
/* RATE OF CONVERGENCE IS KNOWN. ALSO ADDITIONAL INPUT
/* PARAMETERS ARE PRINTED FOR REFERENCE.
/*****
R_OLD = R_INNER;
GET LIST (N, SAVE, CARD_IN, CARD_OUT);
IF SAVE ='NO' THEN FREE R, J_E, E, ELE_CHG_D, N_I_CHG_D,
P_I_CHG_D, J_N_I, J_P_I, ALPHA, ETA, PHOTO_ELE, CURRENT;

```

NEG-0505
NEG-0506
NEG-0507
NEG-0508
NEG-0509
NEG-0510
NEG-0511
NEG-0512
NEG-0513
NEG-0514
NEG-0515
NEG-0516
NEG-0517
NEG-0518
NEG-0519
NEG-0520
NEG-0521
NEG-0522
NEG-0523
NEG-0524
NEG-0525
NEG-0526
NEG-0527
NEG-0528
NEG-0529
NEG-0530
NEG-0531
NEG-0532
NEG-0533
NEG-0534
NEG-0535
NEG-0536
NEG-0537
NEG-0538
NEG-0539
NEG-0540

NEG-0541
 NEG-0542
 NEG-0543
 NEG-0544
 NEG-0545
 NEG-0546
 NEG-0547
 NEG-0548
 NEG-0549
 NEG-0550
 NEG-0551
 NEG-0552
 NEG-0553
 NEG-0554

```

DO J = 1 TO I-1 BY 3:
  PUT LIST ('I='||J||' ' CURRENT='||TOTAL_CUR(J)||' )
  ' I='||J+1||' ' CURRENT='||TOTAL_CUR(J+1)||' )
  ' I='||J+2||' ' CURRENT='||TOTAL_CUR(J+2)||' ) SKIP;
END;
PUT LIST ('A(1) =||A(1)||' B(1) =||B(1)||' A(2) =||'
A(2)||' B(2) =||B(2)||' SKIP(2);
PUT LIST (' THE INITIAL SOURCE ARE '||PAIRS||' CHARGED' ||
' PAIRS PRODUCED BY COSMIC RADIATION PER CC PER' ||
' SEC, AND ELECTRON CURRENT DENSITY OF ' ||
ENTERJELL' AMPS PER CM**2 AT THE INNER RADIUS.' )SKIP;
FREE TOTAL_CUR;
END CC;
STOPP: END SS;
  
```

References

1. Boyd, H. A. & Tedford, D., J., "The Mechanism of Breakdown of Ambient Air in Long Uniform-field Gaps", Journal of Physics D: Applied Physics, 1971, Vol. 4, p1140.
2. Brown, Samborn C., Basic Data of Plasma Physics, 1966, The MIT Press, Cambridge, 1967.
3. Chatterton, P.A. & Craggs, J.D., "Attachment Coefficient Measurements in Carbon Dioxide, Carbon Monoxide, Air and Helium-Oxygen Mixtures", Proc. Phys. Soc., 1965, Vol. 85, p355.
4. Cobine, James D., Gaseous Conductors, Dover, New York, 1958.
5. Hagstrum, Homer D., "Auger Ejection of Electrons from Tungsten", Physical Review, Vol. 96, No. 2, 1954, p325.
6. Hagstrum, Homer D., "Theory of Auger Ejection of Electrons From Metals by Ions", Physical Review, Vol. 96, No. 2, 1954, p336.
7. Harrison, Melvin A. & Geballe, Ronald, "Simultaneous Measurement of Ionization and Attachment Coefficients", Physical Review, Vol. 91, No. 1, 1953, p1.
8. Huber, Elsa L., "Breakdown Processes in Nitrogen, Oxygen, and Mixtures", Physical Review, Vol. 97, No. 2, 1955, p267.
9. Kaminsky, Manfred, Atomic and Ionic Impact Phenomena on Metal Surfaces, Academic Press, New York, 1965.
10. Kuffel, E., "Electron Attachment Coefficients in Oxygen, Dry Air, Humid Air and Water Vapour", Proc. Phys. Soc., Vol. 74, p297.
11. Loeb, Leonard B., Basic Processes of Gaseous Electronics, Univ. of Calif. Press, Los Angeles, 1955.
12. Loeb, Leonard B., Electrical Coronas Their Basic Physical Mechanisms, Univ. of Calif. Press, Los Angeles, 1965.
13. Meek, J.M., and Craggs, J.D., Electrical Breakdown of Gases, Oxford Press, London, 1953.

14. Miller, Charles G. & Loeb, Leonard B., "Negative Coaxial Cylindrical Corona in Pure N_2 , O_2 , and Mixtures Thereof", Journal of Applied Physics, Vol. 22, No. 5, 1951, p614.
15. Miller, Charles G. & Loeb, Leonard B., "Positive Coaxial Cylindrical Corona Discharges in Pure N_2 , O_2 , and Mixtures Thereof", Journal of Applied Physics, Vol. 22, 1951, p495.
16. Nasser, Essam, Fundamentals of Gaseous Ionization and Plasma Electronics, Wiley-Interscience, New York, 1971.
17. Parker, James H. Jr., "Electron Ejection by Slow Positive Ions Incident on Flashed and Gas-Covered Metallic Surfaces", Physical Review, Vol. 93, No. 6, 1954, p1148.
18. Peek, F. W. Jr., Dielectric Phenomena in High-Voltage Engineering, McGraw-Hill, New York, 1929.
19. Baether, H., Electron Avalanches and Breakdown in Gases, Butterworths, Washington, 1964.
20. Ryzko, H., "Drift Velocity of Electrons and Ions in Dry and Humid Air and in Water Vapour", Proceedings of the Physical Society of London, Vol. 85, 1965, p1283.
21. Schneider, Herman M., "A Review of the Basic Properties of Corona Discharges", Report No. 34, Electric Power Systems Engineering Laboratory, MIT, Dec, 1971.
22. Takeishi, Y. and Hagstrum, H.D., "Auger-Type Electron Ejection from the (111) Face of Nickel by slow He^+ , Ne^+ , and Ar^+ Ions", Physical Review, Vol. 137, No. 2A, 1965, pA641.
23. Von Engel, A., Handbuck der Physik XXI, Springer-Verlag, Berlin, 1956.
24. Von Engel, A., Ionized Gases, Oxford University Press, London, 1965.
25. Waters, R. T., Richard, T.E.S., and Stark, W.B., "Measurements of Power-Frequency Corona Discharge on Smooth Line Conductors", Gas Discharge, IEE Conference Publication No. 70, p266.

26 Verney

26. Varney, Robert N., "Liberation of Electrons by Positive-Ion Impact on the Cathode of a Pulsed Townsend-Discharge Tube", Physical Review, vol. 93, No. 6, 1954, p.1156.